

การเพิ่มประสิทธิภาพการบำบัดน้ำเสียที่ปนเปื้อนอะนิลีน
ด้วยกระบวนการเฟนตันไฟฟ้า



นายเสริมพงศ์ สายเรียม

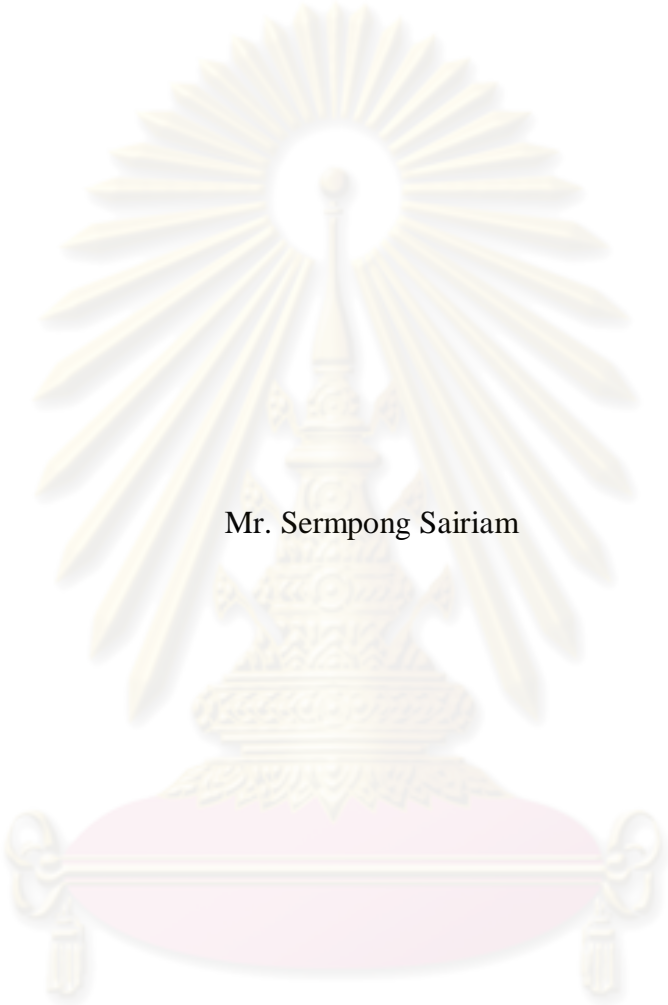
วิทยานิพนธ์นี้เป็นส่วนหนึ่งของการศึกษาตามหลักสูตรปริญญาวิทยาศาสตรมหาบัณฑิต
สาขาวิชาการจัดการสิ่งแวดล้อม (สหสาขาวิชา)

บัณฑิตวิทยาลัย จุฬาลงกรณ์มหาวิทยาลัย

ปีการศึกษา 2551

ลิขสิทธิ์ของจุฬาลงกรณ์มหาวิทยาลัย

ENHANCING TREATMENT EFFICIENCY OF WASTEWATER CONTAINING
ANILINE BY ELECTRO-FENTON PROCESS



Mr. Sermpong Sairiam

A Thesis Submitted in Partial Fulfillment of the Requirements
for the Degree of Master of Science Program in Environmental Management

(Interdisciplinary Program)

Graduate School

Chulalongkorn University

Academic Year 2008

Copyright of Chulalongkorn University

เสริมพงศ์ สายเยี่ยม : การเพิ่มประสิทธิภาพการบำบัดน้ำเสียที่ปนเปื้อนอะนิลีนด้วยกระบวนการเฟนตันไฟฟ้า. (ENHANCING TREATMENT EFFICIENCY OF WASTEWATER CONTAINING ANILINE BY ELECTRO-FENTON PROCESS) อ.ที่
 ปรึกษาวิทยานิพนธ์หลัก : รศ.ดร.จินต์ อโณทัย, อ.ที่ปรึกษาวิทยานิพนธ์ร่วม : PROF.
 MING-CHUN LU, Ph.D., 84 หน้า.

การย่อยสลายอะนิลีนด้วยกระบวนการเฟนตันไฟฟ้าในปฏิกรณ์ทรงกระบอกด้วย $\text{IrO}_2/\text{RuO}_2$ เคลือบด้วยไทเทเนียมเป็นขั้วบวกและสแตนเลสเป็นขั้วลบดำเนินการโดยอาศัยการออกแบบการทดลองในขั้นต้นเพื่อหาตัวแปร (ความเข้มข้นของไฮโดรเจนเปอร์ออกไซด์, เฟอร์รัส, พีเอช และกระแสไฟฟ้า) ที่สำคัญโดยใช้ Factorial Design ซึ่งพบว่าความเข้มข้นของไฮโดรเจนเปอร์ออกไซด์, เฟอร์รัส และพีเอชเป็นพารามิเตอร์ที่มีอิทธิพลต่อการย่อยสลายอะนิลีนและซีโอดี เมื่อนำผลการทดลองทั้งหมด 16 ชุดมาวิเคราะห์ผลโดยใช้เทคนิคพื้นที่ผิวผลตอบแบบ Box-Behnken Design พบว่าความเข้มข้นของไฮโดรเจนเปอร์ออกไซด์, เฟอร์รัส และพีเอชที่เหมาะสมต่อการย่อยสลายอะนิลีนและซีโอดีคือ 72 mM, 1.25 mM และ 2 ตามลำดับ โดยจะสามารถย่อยสลายอะนิลีนและซีโอดีได้ 100% และ 57.12% ซึ่งผลจากการทดลองจริงภายใต้สภาวะดังกล่าวให้ผลสอดคล้องกับที่คาดการณ์ไว้ การเติมไฮโดรเจนเปอร์ออกไซด์เป็นช่วงๆ มีประสิทธิภาพต่อการย่อยสลายอะนิลีนและซีโอดีในกระบวนการเฟนตันไฟฟ้ามากกว่าการเติมเพียงครั้งเดียว นอกจากนี้ยังพบว่ากระแสปล่อยกระแสไฟฟ้าในกระบวนการเฟนตันไฟฟ้าสามารถลดช่วงเวลาการจ่ายไฟฟ้าได้โดยประสิทธิภาพโดยรวมของกระบวนการไม่เปลี่ยนแปลง เป็นผลให้สามารถประหยัดพลังงานในการดำเนินการได้

ศูนย์วิทยทรัพยากร จุฬาลงกรณ์มหาวิทยาลัย

สาขาวิชาการจัดการสิ่งแวดล้อม.....
 ปีการศึกษา...2551.....

ลายมือชื่อนิสิต เสริมพงศ์ สายเยี่ยม
 ลายมือชื่อ อ.ที่ปรึกษาวิทยานิพนธ์หลัก
 ลายมือชื่อ อ.ที่ปรึกษาวิทยานิพนธ์ร่วม

Ming-Chun Lu

508 75529 20 : MAJOR ENVIRONMENTAL MANAGEMENT

KEYWORDS : ANILINE / ELECTRO-FENTON PROCESS / ADVANCED
OXIDATION PROCESSES

SERMPONG SAIRIAM: ENHANCING TREATMENT EFFICIENCY OF
WASTEWATER CONTAINING ANILINE BY ELECTRO-FENTON
PROCESS. ADVISOR : ASSOC. PROF. JIN ANOTAI, Ph.D., CO-
ADVISOR : PROF. MING-CHUN LU, Ph.D., 84 pp.

Aniline degradation was investigated using a cylindrical reactor with IrO₂/RuO₂ coated titanium metal anodes and stainless steel cathodes. A systematic experimental design was used as an initial screening process to determine the significant parameter (Fe²⁺, H₂O₂, pH and current) on aniline and COD removals. Results show that Fe²⁺, H₂O₂ and pH were the main factors affecting on the process performance. The Box-Behnken design was used to specify the optimum conditions from 16 experimental data. The optimized conditions for aniline and COD removals were 1.79 mM, 72 mM and 2 for Fe²⁺, H₂O₂, and pH, respectively. Under these conditions, aniline and COD removals were estimated to be 100 and 57.12%, respectively. The experiment performed under these optimum conditions provided the data which agreed very well with these estimations. In addition, the stepwise or continuous addition of H₂O₂ was more effective than the addition of H₂O₂ in a single step. Furthermore, the delay in electrical current supply for electro-Fenton process provides a possibility in reducing power consumption while maintaining the system performance.

Field of Study : Environmental Management

Academic Year : 2008

Student's Signature Sermpong Sairiam

Advisor's Signature Jin Anotai

Co-Advisor's Signature Ming-Chun Lu

ACKNOWLEDGEMENTS

I would like to express my sincere thanks to my advisor Assoc. Prof. Dr. Jin Anotai and my Co-advisor Prof. Dr. Ming-Chun Lu for their invaluable advice, guidance, support, and encouragement throughout the course of this study. Their comments and suggestions are very valuable and also broaden my perspective in the practical applications.

Special thanks go to the committee members, Asst. Prof. Dr. Manaskorn Rachakornkij, Asst. Prof. Dr. Khemarath Osathaphan, and Associate Prof. Duangrat Inthorn for their helpful and valuable comments that significantly enhanced the quality of this work. I should also like to thank the Department of Environmental Resources Management, Chia Nan University of Pharmacy and Science in Tainan of Taiwan and the Department of Environment engineering, King Mongkut's University of Technology Thonburi in Bangkok of Thailand for providing the worth opportunity for me to do my great research.

I also thank to wonderful friends, Thai and Taiwanese student, who took care and helped me while staying at Chia Nan University of Pharmacy and Science, Tainan in Taiwan and others who have shared experiences throughout my studying period and made my research much more enjoyable and my lovely friends at National Center of Excellence for Environmental and Hazardous Waste Management, Chulalongkorn University, Thailand. Very special thanks to my family for love and encouraging.

Finally I would like to thank the National Center of Excellence for Environmental and Hazardous Waste Management, Chulalongkorn University for its financial support.



ศูนย์วิทยทรัพยากร
จุฬาลงกรณ์มหาวิทยาลัย

CONTENTS

	Page
ABSTRACT (THAI).....	iv
ABSTRACT (ENGLISH).....	v
ACKNOWLEDGEMENTS.....	vi
CONTENTS.....	vii
LIST OF TABLES.....	ix
LIST OF FIGURES.....	x
CHAPTER I	
INTRODUCTION.....	1
1.1 Rational.....	1
1.2 Objectives.....	1
1.3 Hypothesis.....	2
1.4 Scope of Investigation.....	2
1.5 Obtained Results.....	2
CHAPTER II THEORETICAL BACKGROUND AND LITERATURE	
REVIEWS.....	3
2.1 Aniline.....	3
2.1.1 Physical and Chemical Properties.....	3
2.1.2 Health Effects and Toxicity.....	3
2.1.3 Environmental Impact.....	3
2.1.4 Production and Use of Aniline.....	4
2.1.5 Environmental Fate.....	4
2.2 Advanced Oxidation Process (AOPs).....	5
2.2.1 Fenton Process.....	6
2.2.2 Photo-Fenton Process.....	6
2.2.3 Electro-Fenton Process.....	7
2.3 Response Surface Methodology (RSM).....	8
2.3.1 Two-level Factorial Design.....	9
2.3.2 Box-Behnken Design.....	9
2.4 Literature Reviews.....	9
2.4.1 Biological Treatment of Aniline.....	9
2.4.2 Degradation of Aniline by AOPs.....	10
2.4.3 Affecting Factors in Electro-Fenton Process.....	11
2.4.4 Electro-Fenton Process for Treatment Various Chemicals.....	13
2.4.5 Application of Response Surface Method (RSM).....	14
CHAPTER III METHODOLOGY.....	
3.1 Chemical Substances.....	15
3.2 Analytical Methods.....	15
3.2.1 Analysis of Aniline.....	15
3.2.2 Analysis of ferrous.....	15
3.2.3 Analysis of Hydrogen Peroxide.....	15
3.2.4 Analysis of COD.....	15
3.2.5 Other Measurements.....	15
3.3 Reactor Setup and Electrodes.....	16

	Page
3.4 Experimental Procedures.....	17
3.4.1 Fenton Experiment.....	17
3.4.2 Electro-Fenton Experiment.....	17
3.5 Strategy of Experiment.....	17
3.5.1 Phase 1: Screening Experiment.....	17
3.5.2 Phase 2: Box-Behnken Design.....	22
3.5.3 Phase 3: Increasing Efficiency of Aniline Removal by Electro-Fenton.....	23
CHAPTER IV RESULTS AND DISCUSSION.....	24
4.1 Control Experiments.....	24
4.2 Screening Experiments.....	25
4.3 Box-Behnken Design.....	29
4.3.1 Aniline Removal.....	30
4.3.1.1 Interactive Effect of Fe ²⁺ and H ₂ O ₂	31
4.3.1.2 Interactive Effect of Fe ²⁺ and pH.....	31
4.3.1.3 Interactive Effect of pH and H ₂ O ₂	31
4.3.2 COD Removal.....	33
4.3.2.1 Interactive Effect of Fe ²⁺ and H ₂ O ₂	34
4.3.2.2 Interactive Effect of Fe ²⁺ and pH.....	34
4.3.2.3 Interactive Effect of pH and H ₂ O ₂	34
4.3.3 Process Optimization.....	35
4.3.4 Comparison of Fenton and Electro-Fenton Process.....	38
4.4 Improvement of Aniline Removal by Electro-Fenton Process.....	40
4.4.1 Effect of H ₂ O ₂ Addition Pattern on Electro-Fenton Process.....	40
4.4.2 Effect of Current-Supply Delay on Electro-Fenton Process.....	42
4.5 Pathway of aniline degradation.....	46
4.6 Economic Considerations.....	49
CHAPTER V CONCLUSIONS.....	50
5.1 Conclusions.....	50
5.2 Future Works.....	51
REFERENCES.....	52
APPENDICES.....	59
APPENDIX A Analytical Method and Analytical Method for Hydrogen Peroxide (H ₂ O ₂).....	60
APPENDIX B Experimental Figures.....	64
APPENDIX C Experimental Data.....	66
BIOGRAPHY.....	84

LIST OF TABLES

Table		Page
2.1	Physical and chemical properties of aniline.....	4
2.2	Oxidation power of selected oxidized species.....	5
3.1	The levels of variable in two-level factorial design experiment.....	21
3.2	Design matrix of two-level factorial design experiment.....	21
3.3	Levels of variable Box-Behnken design experiment.....	22
3.4	Experimental scenarios from box-Behnken design.....	22
3.5	Scenarios for effect of H ₂ O ₂ stepwise addition on the aniline removal by electro-Fenton process at the optimum condition.....	23
3.6	Scenarios for effect of current supply delay on the aniline removal by electro-Fenton process at the optimum condition.....	23
4.1	Result of design matrix of two-level factorial design experiment.....	25
4.2	ANOVA test for aniline removal by two-level factorial.....	29
4.3	ANOVA test for COD removal by two-level factorial.....	29
4.4	Experimental design matrix proposed by Box-Behnken and responses on aniline and COD removal.....	30
4.5	ANOVA test for aniline removal by Box-Behnken design.....	33
4.6	ANOVA test for COD removal by Box-Behnken design.....	35
4.7	Results of optimum operational conditions for 10 mM of aniline and COD removal.....	37
4.8	Efficiency and rate constant of aniline removal at 10 mM of aniline and current 2 A by electro-Fenton.....	37
4.9	COD removal efficiency versus number of feeding at 10 mM of aniline, 1.25 mM of Fe ²⁺ , 72 mM of H ₂ O ₂ , pH 2 and current 2 A.....	42



 ศูนย์วิทยทรัพยากร
 จุฬาลงกรณ์มหาวิทยาลัย

LIST OF FIGURES

Figure		Page
2.1	Chemical structure of aniline.....	3
2.2	Schematic presentation of the electrocatalytic production of •OH radicals by the electro-Fenton process.....	8
3.1	Schematic diagram of electro-Fenton system.....	16
3.2	Flow chart for Fenton experiment.....	18
3.3	Flow chart for electro-Fenton experiment.....	19
3.4	RSM procedures to optimize the electro-Fenton process.....	20
4.1	Aniline and COD removal in control experiments with 10 mM of aniline, 1.79 mM of Fe ²⁺ , 72 mM of H ₂ O ₂ , current 2 A and at pH 2...	24
4.2	Standardized effect and half-normal probability plot of aniline removal.....	26
4.3	Standardized effect and half-normal probability plot of COD removal.....	26
4.4	Average effect of the significant factors.....	27
4.5	3D response surface plot for aniline and COD removal.....	32
4.6	Normal probability plot of residual for aniline removal.....	34
4.7	Normal probability plot of residual for COD removal.....	36
4.8	Aniline and COD removal by electro-Fenton process at the optimum condition.....	37
4.9	Comparison of aniline and COD removal by electrolysis, Fenton and electro-Fenton process at the optimum condition.....	39
4.10	Fe ²⁺ remaining in the experiments by Fenton and electro-Fenton processes at 2 A for 10 mM of aniline at pH 2, 1.79 mM of Fe ²⁺ and 72 mM of H ₂ O ₂	40
4.11	Effects of H ₂ O ₂ of stepwise addition during electro-Fenton process at 10 mM of aniline, 1.25 mM of Fe ²⁺ , 72 mM of H ₂ O ₂ , pH 2 and current 2 A.....	41
4.12	Profile of Fe ²⁺ of H ₂ O ₂ stepwise addition during electro-Fenton process at 10 mM of aniline, 1.25 mM of Fe ²⁺ , 72 mM of H ₂ O ₂ , pH 2 and current 2 A.....	42
4.13	Profile of H ₂ O ₂ of H ₂ O ₂ stepwise addition during electro-Fenton process at 10 mM of aniline, 1.25 mM of Fe ²⁺ , 72 mM of H ₂ O ₂ , pH 2 and current 2 A.....	43
4.14	Effects of electrical discharging time at 10 mM of aniline, 1.25 mM of Fe ²⁺ , 72 mM of H ₂ O ₂ , pH 2 and current 2 A.....	44
4.15	Profile of Fe ²⁺ and H ₂ O ₂ on effects of electrical discharging time at 10 mM of aniline, 1.25 mM of Fe ²⁺ , 72 mM of H ₂ O ₂ , pH 2 and current 2 A.....	45
4.16	Aniline, COD and TOC removal by electro-Fenton process at the optimum condition.....	46
4.17	The degradation pathway of aniline by radical oxidation.....	47
4.18	Formation of oxalic and maleic acids in electro-Fenton process at the optimum condition.....	48
4.19	Formation of nitrobenzene in electro-Fenton process at the optimum condition.....	48

CHAPTER I

INTRODUCTION

1.1 Rational

Advanced oxidation processes (AOPs) are regarded as the most effective approaches for wastewater treatment containing with organic pollutants (Liou et al., 2004). AOPs can generate the hydroxyl radicals which are very powerful oxidants, (Mazellier et al., 2004; Wu et al., 2006). These radicals can be produced by different ways such as hydrogen peroxide/ultraviolet irradiation ($\text{H}_2\text{O}_2/\text{UV}$), hydrogen peroxide/ozone ($\text{H}_2\text{O}_2/\text{O}_3$), ozone/ultraviolet irradiation (O_3/UV), TiO_2 -catalyzed UV oxidation, and also the combination of H_2O_2 with ferrous ions (Fenton reagent). Fenton process has been found effectively decompose a wide range of refractory synthetics or natural organic compounds (Badawy et al., 2006; Liou and Lu, 2008). It has been widely used for treatment of highly contaminated wastewater (Argun et al., 2008).

Fenton process, ferrous ion reacts with hydrogen peroxide to produce hydroxyl radicals, which combine with organic compounds resulting in oxidation, reduction or combination reaction (Liou et al., 2004). Despite the high oxidative efficiency of Fenton's reagent, a large amount of sludge will be produced during the process, especially when the high strength wastewater is treated (Losito et al., 2008; Wang et al., 2008). There is a development of new advanced electrochemical oxidation process, namely electro-Fenton process, for detoxification of organic wastewater without the sludge disadvantage (Losito et al., 2008). This method is based on electrocatalytic generation of Fenton's reagent to produce hydroxyl radicals in the electrolytic cell and ferrous regenerated via the reduction of ferric ion on the cathode (Zhang et al., 2006).

Aniline was chosen as a target compound in this study. Aniline is a widely distributed pollutant in the environment resulting from industrial manufacture and use, but it can also be released as a result of the partial biodegradation of xenobiotic compounds including certain azo dyes and herbicides (e.g. acylanilides, phenylureas and phenylcarbamates) (Liu et al., 2002; O'Neill et al., 2000). Since aniline is toxic and carcinogenic to living organism (Zhuang et al., 2007). Aniline is considered to be an increasing threat both to the environment and to human health. Thus, the fate of aniline in the environment should be concerned.

This research study intended to investigate the efficiency of aniline removal using electro-Fenton process.

1.2 Objectives

The objectives of this study are described as follows:

- To investigate and compare the treatability of aniline wastewater by Fenton and electro-Fenton processes.
- To determine the optimum condition of aniline removal using response surface methodology.
- To optimize the process and investigate the factors such as Fe^{2+} , H_2O_2 , pH and electric current that influence the removal efficiency by electro-Fenton process.
- To determine the hydrogen peroxide stepwise addition and current delay on aniline removal by electro-Fenton process.

1.3 Hypothesis

Electric current can enhance the efficiency of Fenton process on aniline.

1.4 Scope of Investigation

1. Using synthetic wastewater and working at room condition.
2. Operating in a batch mode.
3. Anodes and cathodes of the electro-Fenton reactors were titanium metals coated with $\text{IrO}_2/\text{RuO}_2$ and stainless steel, respectively.
4. Using response surface methodology for the experimental design and optimization by Design-Expert[®] 7.0 (trial version).

1.5 Obtained Results

1. Effectiveness of aniline wastewater treatment by Fenton and electro-Fenton processes.
2. The optimum condition for aniline wastewater removal by using response surface methodology with electro-Fenton process.



ศูนย์วิทยทรัพยากร
จุฬาลงกรณ์มหาวิทยาลัย

CHAPTER II

THEORETICAL BACKGROUND AND LITERATURE REVIEWS

2.1 Aniline

2.1.1 Physical and Chemical Properties

Aniline is a clear to slightly yellow liquid with a characteristic odor. It does not readily evaporate at room temperature. Aniline is slightly soluble in water and mixed readily with the most organic solvent. The formula of aniline is C_6H_7N . It is an organic chemical compound, specifically an aryl amine, consists of a phenyl group attached to an amino group. The chemical structure of aniline is shown in Fig. 2.1. Information regarding the physical and chemical properties of aniline is located in Table 2.1.

2.1.2 Health Effects and Toxicity

Acute Effect

Acute inhalation exposure to high levels of aniline in humans has resulted in adverse effects on lung, such as upper respiratory tract irritation and congestion. Aniline has been classified as very toxic in humans, with a probable oral dose in humans at 50 to 500 mg/kg for a 150-lb person. Aniline is considered to have high acute toxicity based on short-term animal tests such as the LC_{50} test in rats.

Chronic Effect (Noncancer)

The major effects from chronic (long-term) inhalation exposure to aniline in humans is the formation of methemoglobin, which can cause cyanosis (interference with the oxygen-carrying capacity of the blood). Aniline is severely irritating to mucous membranes and affects the eyes, skin, and upper respiratory tract. Significant amounts of aniline can be absorbed through the skin. Animal studies have reported a dose-related decrease in red blood cell count, hemoglobin levels, and hematocrit. The RfC for aniline is 0.001 mg/m^3 based on spleen toxicity in rats.

Cancer Risk

Tumors of the spleen and body cavity were induced in two strains of rats in separate dietary studies. This information of aniline was used by U.S. EPA as a basis for classifying aniline as a B2, a probable human carcinogen.

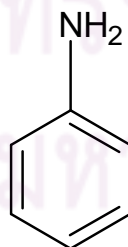


Figure 2.1 Chemical structure of aniline.

Table 2.1 Physical and chemical properties of aniline (U.S. EPA, 1994)

Property	Information
Chemical name	aniline
Synonym (s)	aminobenzene; aminophen; phenylamine; benzeneamine
Formula	C ₆ H ₇ N
Molecular weight	93.12 g/mol
Physical state	liquid
Melting point	6.15 °C
Boiling point	184.4 °C at 1 atm
Vapor density (Air = 1)	3.22
Water solubility at 20 °C	34 g/L
at 25 °C	35 g/L
Vapor pressure at 20 °C	0.3 mmHg
at 25 °C	0.67 mmHg
Henry's law constant at 25 °C	1.9×10 ⁻⁶ atm m ³ /mole
Density at 20 °C	1.022 g/cm ³
Flash point (closed cup)	76 °C

2.1.3 Environmental Impact

Aniline in air will be broken down rapidly by other chemicals and by sunlight. It will be broken down within a few days. Aniline in water can stick to sediment and particulate matter or evaporate to the air. Most of it will be broken down by bacteria and other microorganisms. Aniline will partially absorb on to the soil. Small amounts may evaporate into air or pass through the soil to groundwater. Most of the aniline in soil will be broken down by bacteria and other microorganisms. Aniline does not accumulate in the food chain.

The aniline industry has completed aquatic toxicity studies in response to the U.S.EPA request for testing. These tests show that aniline is highly toxic to aquatic life. Reported LC₅₀ values for daphnids are less than 1 mg/L. Reported chronic values for daphnids are less than 0.1 mg/L.

2.1.4 Production and Use of Aniline

Isocyanates derived from aniline are used to produce urethanes. The production of methyl diphenyl diisocyanate, an intermediate for the production of urethanes, is the largest end use for aniline. Other principal applications of aniline include production of rubber accelerators and antioxidants to vulcanize rubber; the manufacture of intermediates for herbicides and other pesticides, especially fungicides; and the manufacture of dyes and pigments, especially azo dyes. Aniline is also used to produce medicinal and pharmaceutical products, resins, varnishes, perfumes, shoe blacks, photographic chemicals (hydroquinone), explosives, petroleum refining chemicals, diphenylamine, and phenolics

2.1.5 Environmental Fate

Aniline is released into the environment primarily from industrial uses. The largest sources of aniline release are from its primary uses as a chemical intermediate in the production of polymers, pesticides, pharmaceuticals and dyes. The chemical has been detected, but not quantified, in ground water in a shallow aquifer known to be contaminated by coal-tar wastes. Aniline has been found in industrial wastewater and leachates from disposal sites. Aniline in solution adsorbs strongly to colloidal organic matter, which effectively increases its solubility and movement into

groundwater. It is also moderately adsorbed to organic material in the soil (pKa of 4.596). It will slowly volatilize from soil and surface water (vapor pressure 0.67 mm Hg at 25 °C) and is subject to biodegradation. Although rapidly degraded in the atmosphere, aniline can be deposited in the soil by wet and dry deposition, and by adsorption on aerosol particles.

2.2 Advanced Oxidation Processes (AOPs)

Advanced Oxidation processes (AOPs) are an attractive for treatment of contaminated grounds, surface, and wastewaters containing hardly biodegradable anthropogenic substances. These technologies generate hydroxyl radical ($\bullet\text{OH}$) which is a highly reactive oxidant ($E^\circ = 2.8 \text{ V}$ versus SHE) (Farre et al., 2006; Guinea et al., 2008; Pera-Titus et al., 2004). These methods are attractive because of the possibility of the mineralizing the target compounds (Zoh and Stenstrom, 2002). The main interesting of $\bullet\text{OH}$ radicals are also characterized by a non selectivity of attack which is a useful attribute for an oxidant used in wastewater treatment and to solve pollution problems. $\bullet\text{OH}$ is the second strongest oxidant after fluorine as shown in Table 2.2.

Methods based on chemical and photolytic catalysis have been included in a group of new technologies denominated. AOPs generated highly degrading $\bullet\text{OH}$ radicals. As $\bullet\text{OH}$ radicals are so reactive and unstable, they must be produced continuously. These radicals are produced by several methods such as hydrogen peroxide/ultraviolet irradiation ($\text{H}_2\text{O}_2/\text{UV}$), hydrogen peroxide/ozone ($\text{H}_2\text{O}_2/\text{O}_3$), ozone/ultraviolet irradiation (O_3/UV), TiO_2 -catalyzed UV oxidation, and also the combination of H_2O_2 with ferrous ions (Fenton reagent).

Table 2.2 Oxidation power of selected oxidizing species (Beltran et al., 1998)

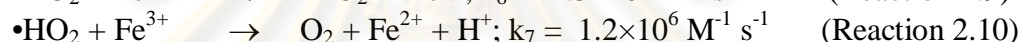
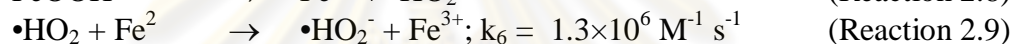
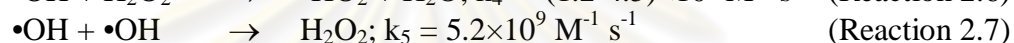
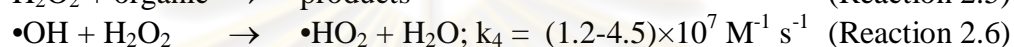
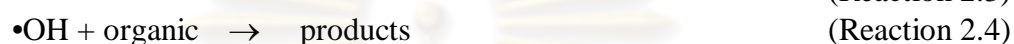
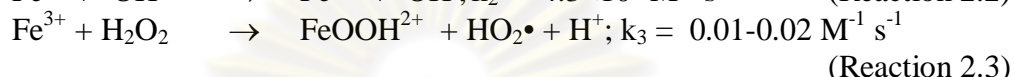
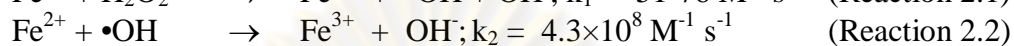
Oxidation species	Oxidation power (V)
Fluorine (F_2)	3.03
Hydroxyl radical ($\bullet\text{OH}$)	2.80
Atomic oxygen	2.42
Ozone (O_3)	2.07
Hydrogen peroxide (H_2O_2)	1.77
Permanganate (KMnO_4)	1.67
Hypobromous acid (HBrO)	1.59
Chlorine dioxide (ClO_2)	1.50
Hypochlorous acid (HClO)	1.49
Hypoiodous acid	1.45
Chlorine (Cl_2)	1.36
Bromide (Br_2)	1.09
Iodine (I_2)	0.54

2.2.1 Fenton Process

Fenton process is known to be very effective in the removal of many hazardous organic pollutants from water based on an electron transfer between H_2O_2 and iron. The reactivity of this process was first observed in 1894 by its inventor H.J.H. Fenton, its utility was not recognized until the 1930s when a mechanism based on hydroxyl radicals was proposed. The main advantage is the complete destruction of contaminants to harmless compounds, e.g. CO_2 , water and inorganic salts. The

Fenton reaction causes the dissociation of the oxidant and the formation of highly reactive $\bullet\text{OH}$ that attack and destroy the organic pollutants.

The reaction mechanism can be described by means of the following reactions: the generation of hydroxyl radicals ($\bullet\text{OH}$) between H_2O_2 and Fe^{2+} (Reaction 2.1), the degradation of organic substance by the $\bullet\text{OH}$ (Reaction 8). In the mean time, some reversed reactions and side reactions (Reactions 2.2, 2.3, 2.5, and 2.6) also occur (Kang et al., 2002; Kang and Hwang, 2000; Neyens and Baeyens, 2003; Oturan et al., 2001).



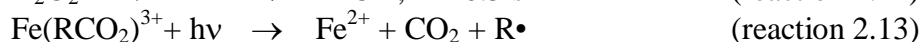
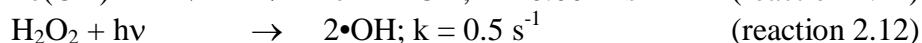
The reaction rate in reaction 2.3 is much slower than that of reaction 2.1 meaning that Fe^{2+} is consumed quickly, but reproduced slowly. Thereby, the oxidation rate of organic compounds is fast when large amount of Fe^{2+} is present because large amount of $\bullet\text{OH}$ is produced (Behnajady et al., 2007). Numerous competing reactions which involve Fe^{2+} , Fe^{3+} , H_2O_2 , $\bullet\text{OH}$, hydroperoxyl radicals ($\bullet\text{HO}_2$) and radicals derived from the substrate, may also be involved. $\bullet\text{OH}$ radicals may be scavenged by reacting with Fe^{2+} or H_2O_2 as seen in reactions 2.2 and 2.6. Fe^{3+} formed through reactions 2.1 and 2.2 can react with H_2O_2 following a radical mechanism that involves $\bullet\text{OH}$ and $\bullet\text{HO}_2$ with regeneration of Fe^{2+} as shown in reactions 2.3, 2.8, 2.9 and 2.10 (Lucas and Peres, 2006).

The Fenton reaction also has several important advantages such as short reaction time among all advanced oxidation processes, iron and H_2O_2 are cheap and non-toxic, and the process is easily to run and control (Argun et al., 2008).

However, in Fenton process, a large amount of sludge will be produced during the neutralization process, especially when the high strength wastewater is treated (Oturan et al., 2001; Qiang et al., 2003; Zhang et al., 2007). To solve this problem, the Fenton reaction efficiency can be enhanced in the presence of UV irradiation and electrochemical as commonly called photo-Fenton and electro-Fenton process, respectively.

2.2.2 Photo-Fenton Process

The iron product in reaction 5 can be photoreduced to regenerate Fe^{2+} and producing more $\bullet\text{OH}$ radicals as shown in reaction 15. UV light can accelerate the mineralization process through the following possible pathways: (i) the enhancement of Fe^{2+} regeneration from the additional photo-reduction of Fe^{3+} species; (ii) the photolysis of H_2O_2 ; (iii) the photolysis of complex of Fe^{3+} with some oxidation products such as oxalic acid (reaction 2.13) (Huang et al., 2008; Segura et al., 2008; Silva et al., 2007)



A slow reaction of reaction 2.11 will occur only when no complexing ligand is present. As complexing ligands exist in a photo-Fenton process, reaction 16 should be considered. Fe^{3+} complexes of oligocarboxylic acids that absorb the UV-vis range are photolyzed through the metal charge transfer reaction 2.13.

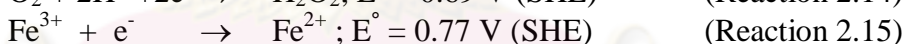
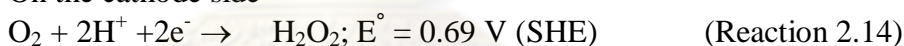
The main disadvantage of the photo-Fenton process, high energy consumption of electrical lamps, might be overcome by solar irradiation. Although some studies have been reported on solar photo-Fenton process for the degradation of hazardous materials in water, the data on the solar photo-Fenton process are still very rare (Sun et al., 2008).

2.2.3 Electro-Fenton Process

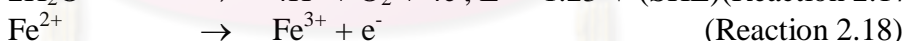
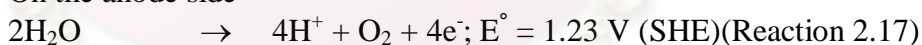
The application of electrochemical method in Fenton process, named electro-Fenton process, could be generally divided into four categories (Khataee et al., 2009; Ting et al., 2009; Zhang et al., 2006). In the first one, H_2O_2 is externally applied while a sacrificial iron anode is used as Fe^{2+} source. In the second category, Fe^{2+} ion and H_2O_2 are electro-generated using a sacrificial anode and cathode via the two-electro reduction of sparged oxygen, respectively. In the third category, Fe^{2+} ion is externally applied, and both of H_2O_2 and Fe^{2+} are concurrently generated at cathode, but primarily focusing on H_2O_2 generation on mercury pool, carbon felt, reticulated vitreous carbon, graphite, activated carbon fiber, stainless steel plate or carbon-PTFE cathode. In the fourth category, Fenton's reagent is utilized to produce $\bullet\text{OH}$ radicals in the electrolytic cell, and Fe^{2+} ion is regenerated via the reduction of Fe^{3+} ion or ferric hydroxide sludge on the cathode

Fenton reaction involves several sequential reactions as shown in reaction 2.1-2.10. The well known Fenton's reaction (reaction 2.1) constitutes a source of $\bullet\text{OH}$ radicals production by chemical means. The H_2O_2 and Fe^{2+} ions are simultaneously generated on the working electrode at a potential of -0.5 V (SCE), according to the following electrochemical reactions:

On the cathode side



On the anode side



Fenton's reaction (reaction 2.1) takes place then in homogeneous medium leading to the formation of $\bullet\text{OH}$ radicals.

The anodic reaction is the oxidation of water to molecular oxygen (reaction 2.17) which is used for optimal production of H_2O_2 (reaction 2.14) necessary for Fenton's reaction. Figure 2.2 shows two catalytic cycles taking place during this process. Electrochemical reactions 2.14 and 2.15 can take place when the aqueous solution is maintained under oxygen saturation by bubbling compressed air.

The electro-Fenton process can be considered very efficient and much cleaner techniques than chemical ones for improving the quality of water resources and eliminating organic compounds in water.

In this study, a novel electro-Fenton process, in which Fenton's reagent was utilized to produce $\bullet\text{OH}$ in the electrolytic cell and Fe^{2+} ion is regenerated via the reduction of Fe^{3+} ion on the cathode was investigated.

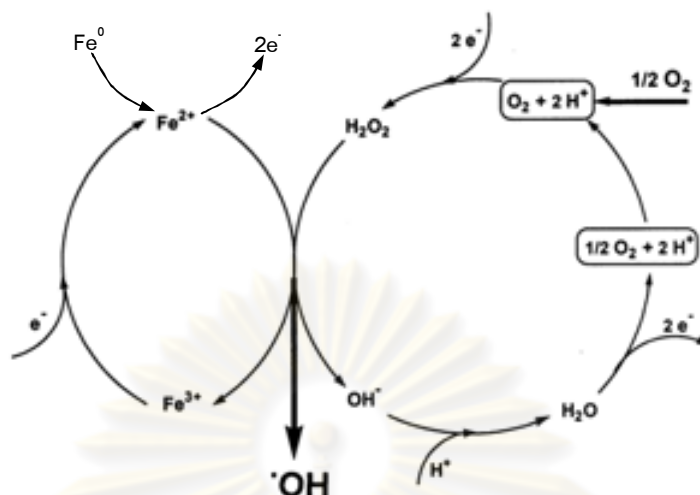


Figure 2.2 Schematic presentation of the electrocatalytic production of $\bullet\text{OH}$ radicals by the electro-Fenton process (Oturán et al., 2001).

2.3 Response Surface Methodology (RSM)

Experimental process optimization should be based on statistical design tools. In the design and statistical evaluation of experiments, response surface methodology (RSM) can be used for process optimization and prediction of interaction between process variables, reducing the number of experiment and thus the time and associated cost spent for conducting these experiments (Cojocaru and Zakrzewska-Trznadel, 2007; Khayet et al., 2008; Rahulan et al., 2009). RSM has already proven to be a reliable statistical tool in the investigation of chemical treatment processes (Myers and Montgomery, 2002). RSM consist of a group of mathematical and statistical techniques that are based on the fit of empirical models to the experimental data obtained in relation to experimental design (Bezerra et al., 2008; Celebi et al., 2008).

Some stages in the application of RSM as an optimization technique are as follows (Bezerra et al., 2008):

- The selection of independent studies and the delimitation of the experimental region, according to the objective of the study and the experience of the researcher.
- The choice of the experimental design and carry out the experiments according to the selected experimental matrix.
- The mathematic-statistical treatment of the obtained experimental data through the fit of a polynomial function.
- The evaluation of the model's fitness.
- The verification of the necessity and possibility of performing a displacement in direction to the optimal region.
- Obtained the optimum values for each studied variable.

Experimental designs for first-order models, e.g. factorial designs, can be used when the data set does not present curvature. However, to approximate a response function to experimental data that cannot be described by linear functions, experimental designs for quadratic response surfaces should be used, such as Box-

Behnken, central composite, and Doehlert designs (Bezerra et al., 2008; Ferreira et al., 2007).

2.3.1 Two-level Factorial Design

Although the choice of an experimental design ultimately depends on the objectives of the experiment and the number of factors to be investigated, initial experimental planning is paramount. Screening techniques such as factorial designs allow the experimenter to select which factors are significant and at what levels. The most general (two-level design) is a full factorial design (Hanrahan and Lu, 2006).

The two-level factorial design requires only two runs per factor study, e.g., low and high levels this statistics-based method involves simultaneous adjustment of experimental factors at only two levels, assuming linearity in the factor effects (Zhang et al., 2009). The effect of a factor can be estimated at several levels of the other factors, yielding conclusions that are valid over a range of experimental conditions. Even though two-level factorial design is unable to explore fully a wide range in the factor space, it can indicate major trends.

The number of experiments (N) required for the development of two-level factorial design is defined as (Prakash et al., 2009):

$$N = 2^k \quad \text{reaction 2.19}$$

where k is number of factors each with high and low value

2.3.1 Box-Behnken Design

The most common and efficient design used in response surface modeling is Box-Behnken design. It has three levels per factor, but avoids the corners of the spaces, and fills in the combinations of center and extreme levels in which the optimal conditions for an experiment are found (Tavares et al., 2009). Conversely, they are not indicated for situations in which the responses at the extremes are required, that is, at the vertices of the cube (Ferreira et al., 2007). Compared to the central composite design method, Box-Behnken design technique is considered as the most suitable for evaluating quadratic response surfaces particularly in cases when prediction of response at the extreme level is not the goal of the model. Another advantage of Box-Behnken design is that it does not contain combinations of for which all factors are simultaneously at their highest or lowest levels (Ferreira et al., 2007).

The number of experiments (N) required for the development of Box-Behnken design is defined as (Ferreira et al., 2007):

$$N = 2k(k-1) + C_0 \quad \text{reaction 2.20}$$

where k is number of factors;

C_0 is the number of center points

2.4 Literature Reviews

2.4.1 Biological Treatment of Aniline

Aniline wastewater containing highly concentrated organic nitrogenous and aromatic structure is less biodegradation and very toxic to microorganism (Chen et al., 2007). The productions of derivatives of aniline are difficult to be degraded and inhibit the biodegradation of other chemicals. Moreover, ammonia is one of the hydrolysis products during the biodegradation, which makes the water more toxic and leads to inhibitory effect. Several investigations have reported that anaerobic digesters used for the treatment of animal wastes and some industrial streams often encountered very high ammonia production.

Several authors have studied bacteria that are able to degrade aniline and some catabolic pathways for degradation of aniline by bacteria elucidated (Liu et

al., 2002). Recently much effort has been devoted to isolate organisms that can degrade aniline. Most of organisms discovered were members of aerobic organisms such as *Nocardia*, *Pseudomonas diminuta*, *Frateruia*, *Rhodococcus erythropolis* AN-13, *Rhizopus* (Aoki et al., 1983; Liu et al., 2002; O'Neill et al., 2000; Zhuang et al., 2007). Apart from aerobic organisms, the anaerobic bacteria, *Desulfobacterium aniline*, was also found capable of degrading aniline (Liu et al., 2002).

However, the disadvantages of the biological treatment are taking longer time than other treatment options and do not totally remove all contaminants or complete degradation (Vidali, 2001). In addition, this biological treatment needs to have environmental conditions appropriate for biodegradation such as temperature, nutrients, and bioavailability (Boopathy, 2000; Oh and Kim, 1998; Romantschuk et al., 2000).

2.4.2 Degradation of Aniline by AOPs

There are many methods to remove this chemical such as TiO_2 photocatalysis, ozonation, Fenton processes. The photocatalytic degradation of organic environmental pollutants in the presence of semiconductor such as TiO_2 or ZnO , or Fe_2O_3 has been used for treatment. One of reasons for this is that photocatalysis may completely mineralize a variety of aliphatic and aromatic compounds under suitable conditions (Son et al., 2004). Irradiation of UV light of an aniline wastewater in the presence of TiO_2 suspension, could be degraded aniline quickly and the solution pH decreased as the reaction proceeds (Wenhua et al., 2000). Solar light was also can be studied for aniline removal. Increase of the surface area of the catalyst bed enhances the solar photocatalysis (Karunakaran et al., 2005). There were many factors influencing the photocatalysis such as aniline concentration, air flow rate, solvent, and electron donors.

Ozonation is an effective way to reduce aniline in aqueous solution. Ozone may attack on the pollutants via two different reaction pathways, i.e. directly or indirectly (Sarasa et al., 2002; Shang et al., 2007). The molecule of ozone can remain as O_3 or it can be decomposed by a variety of mechanisms producing $\bullet\text{OH}$ which is a stronger oxidizing agent than molecule ozone itself (Sarasa et al., 2002). The practical use of ozonation is limited by its high energy demand. Several techniques have been taken to improve by combination with others such as UV light, H_2O_2 and Fe^{2+} , and photocatalysis with TiO_2 (Sauleda and Brillas, 2001). When the solution presence of catalytic Fe^{2+} , aniline was quickly degraded by $\bullet\text{OH}$ produced (Sauleda and Brillas, 2001). The combination of ozonation and photocatalysis with TiO_2 increased aniline degradation and ozonation pretreatment followed by photocatalysis increase TOC removal in comparison to either ozonation or photocatalysis working separately (Sánchez et al., 1998). The addition of activated carbon to the ozonation process could also improve the removal of aniline when compared to the single ozonation (Faria et al., 2007).

Aniline mineralization was studied by various Fenton processes such as ordinary Fenton, electro-Fenton, and photoelectron-Fenton processes. Fenton's reagent, in which H_2O_2 is decomposed into $\bullet\text{OH}$ and hydroxide ion in the presence of Fe^{2+} ions, has been widely applied in the treatment of hazardous organics. It is one process for generating $\bullet\text{OH}$ (Huang et al., 1993). The presence of electric current (electro-Fenton) could improve both aniline removal efficiency and the rate of Fenton process due to the rapid electrochemical regeneration of Fe^{2+} (Anotai et al., 2006). The electrochemical experiment performed in the presence of electro-Fenton and UV irradiation led to a quickly aniline mineralization (Brillas et al., 1998). Almost complete mineralization of aniline was achieved using photoelectron-Fenton process

because of an increase in Fe^{2+} concentration in solution due to UVA irradiation and direct photodecomposition of intermediates (Brillas et al., 1998). In addition, the use of goethite as an iron dosage source represented a more effective mineralization electro-Fenton treatment that avoided the use of light irradiation to achieve an exhaustive mineralization (Sánchez-Sánchez et al., 2007). For the photo-Fenton process, the degradation of aniline was facilitated by light irradiation ($\lambda > 370$ nm) of an aqueous solution resulting in significant enhancement in aniline removal (Fukushima et al., 2000). Higher current density significantly decreased the required treatment period (Anotai et al., 2006; Sánchez-Sánchez et al., 2007). A decrease in the TOC removal efficiency rate was obtained as the solution pH decreased. The optimum pH was 3 for goethite catalyzed electro-Fenton process (Anotai et al., 2006; Sánchez-Sánchez et al., 2007). Increasing both of Fe^{2+} and H_2O_2 raised the removal efficiency of aniline (Anotai et al., 2006).

2.4.3 Affecting Factors in Electro-Fenton Process

Electrode Materials

Pt anode has been successfully used to degrade herbicides and pesticides because of its stability and excellent transmission of electrons (Brillas et al., 1998; Oturan, 2000). However, Pt anode is hardly used in practical wastewater treatment because of its high cost. Therefore, iron (Fe) anode is widely used, especially in the practical wastewater treatment. Pt and Fe are the main anode materials in electro-Fenton process. Besides, new materials, for instance, boron-doped diamond (BDD) electrode have emerged (Flox et al., 2006). However, BDD electrode is more expensive than Pt.

For cathode, the graphite cathode is widely applied as the working electrode (cathode), and Pt as the anode to treat wastewater containing p-nitrophenol (Oturan et al., 2000), pentachlorophenol (Oturan et al., 2001), biosphenol A (Gözmen et al., 2003). Carbon-polytetrafluoroethylene (Carbon-PTFE) was used as a typical composite cathode in the electro-Fenton process, for instance, aniline (Brillas et al., 1998). Activated carbon fiber (ACF) is a new material with string ability of adsorption and feasibility in the electro-Fenton process (Wang et al., 2005).

In the recent years, some researchers studied on the electrochemical oxidation and they have mainly focused in the used of other anodic materials such as titanium coated with $\text{RuO}_2/\text{IrO}_2$ (DSA). DSA as anode to remove 4-nitrophenol (Zhang et al., 2007), aniline (Anotai et al., 2006), 2,6-dimethylaniline (Ting et al., 2009), benzene sulfonic acid (Ting et al., 2008).

Dissolved Oxygen

In some types of electro-Fenton process, H_2O_2 is generated from oxygen reduction. The efficiency of aeration is not only important for the generation of H_2O_2 , but also the cost. There are generally two approaches to improve the production of H_2O_2 . One is to select a cathode with large surface area, and the other is to enhance the aeration efficiency. Oxygen is introduced into the system mainly by aeration. The gas diffusion electrode was also proved effective even using air as the oxygen source with a significant decrease of operating cost (Pozzo et al., 2005). So far, there is no special discussion about the different of the several types of electrodes. However, the gas diffusion electrode has shown obvious advantages, and the composite electrodes with high efficiency and low cost are promising.

Operation Parameters

It has been proved that the Fenton's reaction is a chain reaction. Various factors were found to have significant impacts on the electro-Fenton performance.

pH

pH is one of the most important factors for the electro-Fenton process. It has been confirmed that the optimum value of pH is 2-4. In addition, when the pH increases, the iron ions especially the Fe^{3+} precipitate. Therefore, the amount of catalyst of Fenton's reaction decreases. When pH is lower than 2, H_2O_2 cannot be effectively decomposed to $\bullet\text{OH}$ by Fe^{2+} . This can be explained that in lower pH, the scavenging effect of the $\bullet\text{OH}$ by H^+ is severe to form an oxonium ion such as H_3O_2^+ ; result in reducing the generation of $\bullet\text{OH}$ (Sun et al., 2008). H_3O_2^+ is electrophilic leading to the decreasing rate of reaction between H_2O_2 and Fe^{2+} . The optimum pH for removal aniline and 2,6 dimethylaniline was 2 (Anotai et al., 2006; Ting et al., 2009). At the pH above 3 the composition rate of synthetic dyes decreased because the oxidation potential of $\bullet\text{OH}$ and also the dissolved fraction of iron species decrease with increasing pH (Panizza and Cerisola, 2009).

In fact, the optimum pH indicates a disadvantage of electro-Fenton process because the pH of most water is not within the optimal range. There are two ways to decrease the pH of wastewater. One is to add acid, and then other is to mix the target wastewater with some acidic wastewater. Some researchers investigated the wastewater treatment at neutral pH and the organics can also be removed successfully. But, in that case, the wastewater is treated mainly by coagulation rather than by degradation of $\bullet\text{OH}$

Applied Voltage and Current

These two operation parameters are related directly to the cost of electro-Fenton process. With the increase of voltage or current applied, the degradation of substrate increases at the beginning, and then tends to be stable because of the side reaction and polarization. Increasing the current density increased the production rate of Fe^{2+} (Ting et al., 2009) and H_2O_2 (Wang et al., 2008) on the cathode leading to the generation of higher amount of $\bullet\text{OH}$ radicals from Fenton's reaction. In the electro-Fenton process, the current density is always low. This is the other disadvantage of the electro-Fenton process, because higher current density means larger reaction rate. Some researchers found that increased of electrical current would lower COD removal efficiency because at higher current the competitive electrode reactions such as the discharge of oxygen at the anode via reaction 2.17 and the evolution hydrogen at the cathode would become pronounced (Zhang et al., 2007).

Distance Between Electrodes

The decrease of the distance between the electrodes leads to a decrease of the ohmic drop through the electrolyte and then an equivalent decrease of the cell voltage and energy consumption (Fockedey and Lierde, 2002). It can be concluded that the closer the electrode are, the better the performance. However, it is necessary to keep appropriate distance between the electrodes for installation and avoidance of short circuit between anode and cathode.

Ratio of Fe^{2+} and H_2O_2

Ratio of Fe^{2+} and H_2O_2 is a very important operational parameter of electro-Fenton process. Although Fe^{2+} can react with H_2O_2 to generate $\bullet\text{OH}$ and greater $\bullet\text{OH}$ radicals could be generated with increasing Fe^{2+} concentration. Fe^{2+} and H_2O_2 cannot be excessive unilaterally because of the occurrence of undesired side reactions (reaction 2.2 and 2.6). In reaction 2.6, the $\bullet\text{HO}_2$ is also an oxidant, but has an oxidation potential much less than $\bullet\text{OH}$. COD removal efficiency increased with the increasing Fe^{2+} to H_2O_2 molar ratio (Zhang et al., 2007). The removal efficiency of color should increase with the amount of added Fe^{2+} but the exceed of added Fe^{2+} would decrease efficiency because of complexes of Fe^{2+} and Fe^{3+} (Wang et

al., 2008). Increasing the H_2O_2 concentration from 10 to 25 mM increased the removal efficiency, 46% of 2,6-dimethylaniline but increase from 25 to 30 mM decrease in removal efficiency, 35% (Ting et al., 2009).

Supporting Electrolyte

Sodium sulfate is generally used as the supporting electrolyte, such electrolyte improves the solution conductivity, and accelerates the electro-Fenton reaction. Therefore, supporting electrolyte is necessary, especially in the solution without enough conductivity. The inert support electrolyte (NaClO_4) affects the total potential drop of the electrolyzer, but does not affect the net generation rate of H_2O_2 (Qiang et al., 2002). NaCl is the electrolyte that was studied to increase on Cr(IV) removal. In the study of Ölmez, 2009, complete Cr(VI) removal could be achieved in less than 90 min application times with the electrolyte concentrations higher than 20mM (Ölmez, 2009).

2.4.4 Electro-Fenton Process for Treatment Various Chemicals

The electro-Fenton process is widely used to treat non-biodegradable or refractory organic compounds such as dye, herbicide, pesticide, and landfill leachate.

Azo Dyes

Azo dyes are widespread environmental pollutants related to many important industries such as textile, printing, and cosmetic manufacturing. There are many azo dyes being treated by the electro-Fenton treatment such as methyl red, acid red 14, indigo carmine, orange II, reactive black B etc (Daneshvar et al., 2008; Flox et al., 2006; Huang et al., 2008; Wang et al., 2005; Zhou et al., 2007). An increase in applied current could enhance the production of electrogenerated H_2O_2 . The acceleration in degradation with increasing the applied current could be explained by the higher production of $\bullet\text{OH}$ (Flox et al., 2006; Wang et al., 2005). The suitable Fe^{2+} concentration was an important prerequisite in the electro-Fenton process. An excess of ferrous ion would consume the strong oxidant of hydroxyl radical, which led to the dye removal decreased (Wang et al., 2005; Zhou et al., 2007). Increasing cathode surface area, accumulation of H_2O_2 increased and so will led to an increase in the dye decoloration (Daneshvar et al., 2008). The solution pH not only affected the production of hydrogen peroxide, but also controlled the existence species of ferrous catalyst, which showed a better performance for methyl red degradation at pH 3 (Zhou et al., 2007). When the solution pH further increased, the formation of hydroxyl-complexes of iron occurred. Therefore, the formation of this ferric hydroxide complexes led to the deactivation of a ferrous catalyst, which in turn caused the oxidation efficiency dramatically decreased (Zhou et al., 2007).

Landfill Leachate

Landfill leachate contains organic and inorganic pollutants in high concentrations. COD removal efficiency increased with the increasing current, but further increase of current would reduce the removal efficiency (Atmaca, 2009; Zhang et al., 2006). As the initial concentration of H_2O_2 in the electro-Fenton reactor increased, the COD removal also increased considerably (Atmaca, 2009; Lin and Chang, 2000; Zhang et al., 2006). The optimum pH also affected on the removal of COD in the leachate. COD removal efficiency increased with increasing pH. If the initial pH was higher than 3, the removal efficiency was found to decrease (Atmaca, 2009). COD removal efficiency increased with the increase of ferrous dosage at the fixed hydrogen peroxide dose, but further increase of ferrous ion would reduce the removal efficiency (Zhang et al., 2006).

Herbicide and Pesticide

There were many herbicides and pesticides which have been treated by the electro-Fenton process, e.g. 2,4,5-trichlorophenoxyacetic acid, picloram, 2-(2,4-dichlorophenoxy)-propionic acid, 3,6-dichloro-2-methoxybenzoic acid, 4-chloro-2-methylphenol, phenyl-urea herbicides (Boye et al., 2003; Brillas et al., 2003; Brillas et al., 2007; Irmak et al., 2006; Losito et al., 2008; Ozcan et al., 2008). The degradation rates increased with increasing applied current (Boye et al., 2003; Brillas et al., 2007; Ozcan et al., 2008). The pH optimum were in the range of 3-4 (Boye et al., 2003; Brillas et al., 2003). In addition, it was found that the degradation increased with increasing Fe^{2+} (Irmak et al., 2006). During this degradation, the $\bullet\text{OH}$ radicals contributed to breaking down the aromatic ring and removing the toxicity of the herbicide and pesticide solutions. The degradation of herbicide chlortoluron in aqueous medium by electro-Fenton process using a carbon felt cathode and a platinum anode was studied (Abdessalem et al., 2008). In this study, electro-Fenton process seemed to be a clean and efficient technique for the degradation of herbicides in water because oxidative degradation of chlortoluron by $\bullet\text{OH}$ led to the formation of carboxylic acids such as oxalic, glyoxilic, malonic and acetic acids. Although the ozone oxidation technology is a commonly process for degrading non-biodegradation organic compounds in drinking water treatment plant, some pesticides such as atrazine, were refractory to ozone, while they could be degraded efficiently by electro-Fenton process (Ventura et al., 2002).

2.4.5 Application of Response Surface Method (RSM)

RSM has been applied in numerous studies in many fields, including biotechnology, food processing, pharmacy, biochemical engineering, chemical, metallurgical industry, and environmental application (Hanrahan and Lu, 2006; Rahulan et al., 2009).

Güven et al. (2008) optimized the electrochemical treatment conditions by using response surface methodology (RSM). The applied voltage was kept in the range where electrolyte concentration was minimized. The waste concentration and COD removal percent were maximized at 25°C and optimum conditions were estimated through RSM as 11.29V applied voltage, 100% waste concentration (containing 40 g/L lactose) and 19.87 g/L electrolyte concentration to achieve 29.27% COD removal (Güven et al., 2008). Secular et al. (2008) used RSM together with central composite design were used to find the significance of factors at different levels of photocatalytic decolorization (Secula et al., 2008). Central composite design was also used for the optimization of the electrocoagulation process and to evaluate the effects and interactions of process variables: applied electric current, electrolyte concentration and application time on the removal of Cr(VI) and got the second-order polynomial equation (Ölmez, 2009). For biotechnology, RSM has been used to optimize the critical parameters responsible for higher Cd^{2+} removal by a unicellular cyanobacterium *Synechocystis pevalekii* based on a three-level Box–Behnken factorial design (Khattar and Shailza, 2009). The result showed that this RSM technique not only providing the optimum point but also being simple, efficient, time and material saving.

CHAPTER III

METHODOLOGY

3.1 Chemical Substances

Aniline (99.5%), Ferrous sulfate heptahydrate ($\text{FeSO}_4 \cdot 7\text{H}_2\text{O}$), hydrogen peroxide (H_2O_2 , 35%), perchloric acid (HClO_4 , 70-72%), sodium hydroxide (NaOH , 99%), and all other chemical substances are analytical reagent grade (MERCK). Aqueous solutions used for oxidation reaction were prepared by using deionized (DI) water from a Millipore system with a resistivity of $18.2 \text{ M}\Omega \text{ cm}^{-1}$. All preparations and experiments were conducted at room condition.

3.2 Analytical Methods

3.2.1 Analysis of Aniline

Aniline was analyzed by HP 4890 gas chromatography (GC) with a flame ionization detector and HP-5 column (0.53 mm inside diameter, and 15 m long). The analytical method of aniline by GC was shown at Appendix A. Before the analysis, all supernatants were diluted 10 times by 0.1 N NaOH , and then the solutions were filtered with TOYO 0.45 μm mixed cellulose ester filters to separate iron sludge from the solution before injecting to the GC.

3.2.2 Analysis of Ferrous

The sample was added with 1, 10-phenanthroline agent by 1, 10-phenanthroline method, according to the Standard Methods (APHA, 1992). Then, the DI water is added to make up the volume to 50 ml before analyzing by the Genesis 20UV-VIS spectrophotometer. The DI water mixed with sample without phenanthroline is used as a blank for every sample.

3.2.3 Analysis of Hydrogen Peroxide

The sample was added with potassium titanium (IV) oxalate agent following the potassium titanium (IV) oxalate method (Eisenberg, 1943; Liu et al., 2007; Sellers, 1980) as shown in Appendix A. Then, the DI water is added to make up the volume to 100 ml before analyzing by the Genesis 20UV-VIS spectrophotometer.

3.2.4 Analysis of COD

COD was determined using a closed-reflux titrimetric method based on Standard Methods (APHA, 1992).

3.2.5 Other Measurements

Analysis of total organic carbon (TOC) was performed in an elemental liquiTOC analyzer with high temperature catalytic oxidation mode coupled with non-dispersive infrared (NDIR) detector. The carrier gas was air zero with a flow rate of 200 ml/min. Calibration of the analyzer was achieved with potassium hydrogen phthalate (99.5%, Merck) and sodium carbonate (secondary reference material, Merck) as the standards for total carbon (TOC) and inorganic carbon (IC), respectively. The difference between total carbon and IC gives TOC data of the sample.

Anions concentration were determined by Ion Chromatography (IC) Dionex DX-120 Ion Chromatograph with the operating flow rate of 1.0 ml/min and equipped with Reagent-FreeTM Controller with RFICTM EGC II KOH (RFC-30), Autosampler Thermo Finnigan SpectraSYSTEM model AS1000 with 20 μl injection volume, Guard column IonPac[®] AG-11 (4 \times 50 mm), analytical column IonPac[®] AS-11 (4 \times 250 mm), column temperature stabilizer model CTS-10 controlled at 30 $^\circ\text{C}$, suppressor ASRS[®]-ULTRA II 4-mm with conductivity detector with gradient 0.1

mM at KOH 0-4 min, 0.1 – 18 mM KOH at 4-22 min, 18 mM KOH at 22-26 min, 0.1 mM at KOH 26-30 min.

For the total iron and soluble iron, the samples were digested by nitric acid and diluted by DI water. The soluble iron were filtered with TOYO 0.45 μm mixed cellulose ester filters before. Then, both mixtures were analyzed using a PerkinElmer Atomic Absorption Spectrometer (AAs) model AAnalyst 200 with hollow cathode lamps Fe 248.33 nm, Slit 1.8/1.35 and used acetylene gas.

The solution pH is measured by a Suntex Digital pH/mV meter (TS-1).

3.3 Reactor Setup and Electrodes

Figure 3.1 shows the schematic experiment setup of this study. The cylindrical reactor (radius: 6.5 cm and height: 35 cm) was operated in this study. The total volume of the reactor was 3.5 liters. The anode used was titanium net coated with $\text{RuO}_2/\text{IrO}_2$ (DSA), and the cathode was made of stainless steel. The double electrode cell had a DSA anode with an inside diameter of 7 cm, and the cathodes were stainless steel walls with 2 and 13 cm of inside diameter. The anode and cathodes were connected with a DC power supply (Topward 33010D). pH meter and recirculated pump were also connected.

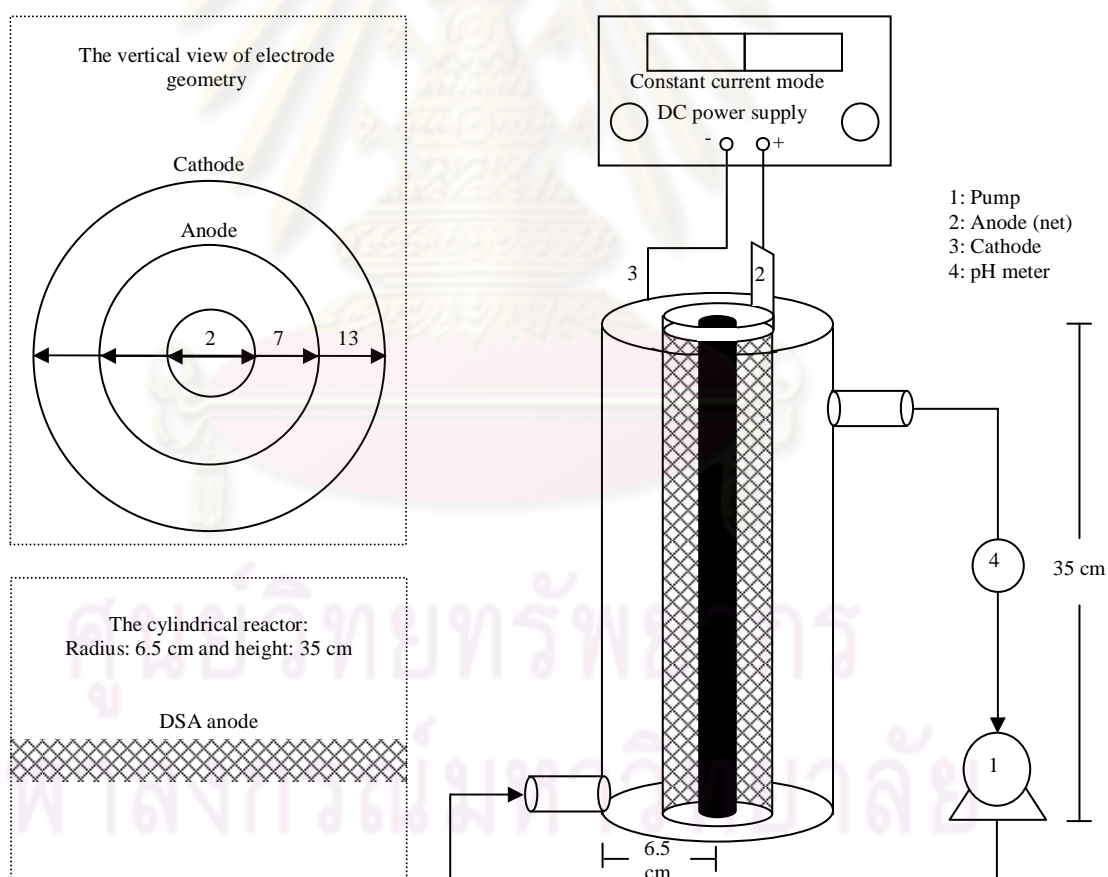


Figure 3.1 Schematic diagram of electro-Fenton system.

3.4 Experimental Procedures

3.4.1 Fenton Experiment

As shown in Figure 3.2, pH of the aniline solution was adjusted to the desired value by the addition of HClO_4 . After that, ferrous ion was added into the solution. The solution pH will be rechecked prior to the addition of H_2O_2 solution. The H_2O_2 was supplied into the solution and was simultaneously started. The sample of 1 ml was taken at 0, 1, 2, 5, 10, 20, 40, 60, 80, 100 and 120 minutes and was immediately injected into a tube. The Fenton reaction could not occur at $\text{pH} > 10$; therefore, the Fenton reaction was stopped instantly by adding 9 ml of 0.01N NaOH to the solution after sampling. The sample was then filtered with 0.45 μm filter to remove precipitation before analysis. The experiment was terminated in 2 hours. Sample was analyzed for COD, H_2O_2 residual, Fe^{2+} and aniline concentration.

3.4.2 Electro-Fenton Experiment

In this experiment, an electrical supply unit which consisted of a stainless steel cathode, a titanium net coated with $\text{RuO}_2/\text{IrO}_2$ (DSA), and a regulator DC power supply were installed additionally in the reactor. Most procedures were similar to those of typical Fenton reaction; however, in this experiment, the electrical current was delivered through out the experiment period as shown in Figure 3.1.

3.5 Strategy of Experimentation

The use of model to describe the effects of parameters involving in electro-Fenton experiment allows to identify the influencing parameters in a simple and systematic way and to predict the results of the experiment with different parameter combinations. Thus, the response surface methodology (RSM) enables to obtain an overview of the processing and relationship between parameters (variables) and influence (responses).

In this research, main experimental works can be divided into 3 phases as follows:

- Phase 1. Use two-level factorial design as a screening tool to identify the key factors (including interactions) from less significant-impact factors.
- Phase 2. Use Box-Behnken design to contract the experimental scenarios which could not lead to the optimization of aniline removal by electro-Fenton process.
- Phase 3. Study the H_2O_2 stepwise addition and current supply delay in the electro-Fenton process to improve system performance.

The overview to optimize the process parameters by RSM and enhance the efficiency for electro-Fenton process is shown in Figure 3.4

3.5.1 Phase 1: Screening Experiment

Design Expert Software 7.0 was used for the experimental design throughout this screening process study. The process was in accordance with two-level of factorial design. The main purpose of this part was to find the suitable key parameters that affecting in the removal of aniline and COD in electro-Fenton process. A total 16 sets of experiments (2^4 factorial design) were carried out at low and high levels for each factor; i.e., H_2O_2 (X_1 ; 44 and 100 mM), Fe^{2+} (X_2 ; 0.72 and 1.79 mM), current (X_3 ; 2 and 5 ampere) and pH (X_4 ; 2 and 3.5).

Table 3.1 shows the levels with coded of the four major factors tested in two-level factorial design experiment. The notations of (-1) and (+1) illustrated the low and high level of two-level factorial design experiment, respectively.

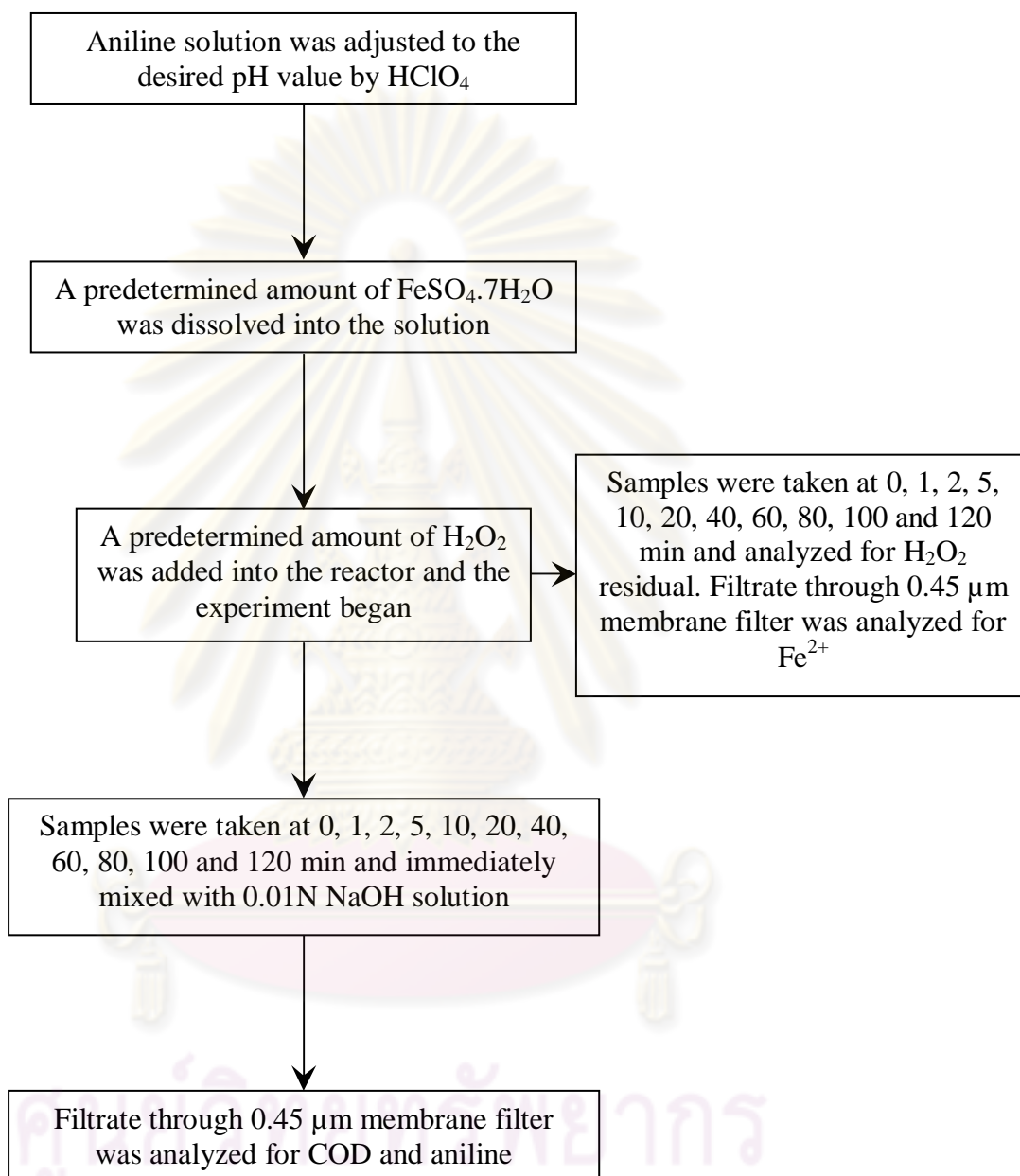


Figure 3.2 Flow chart for Fenton experiment

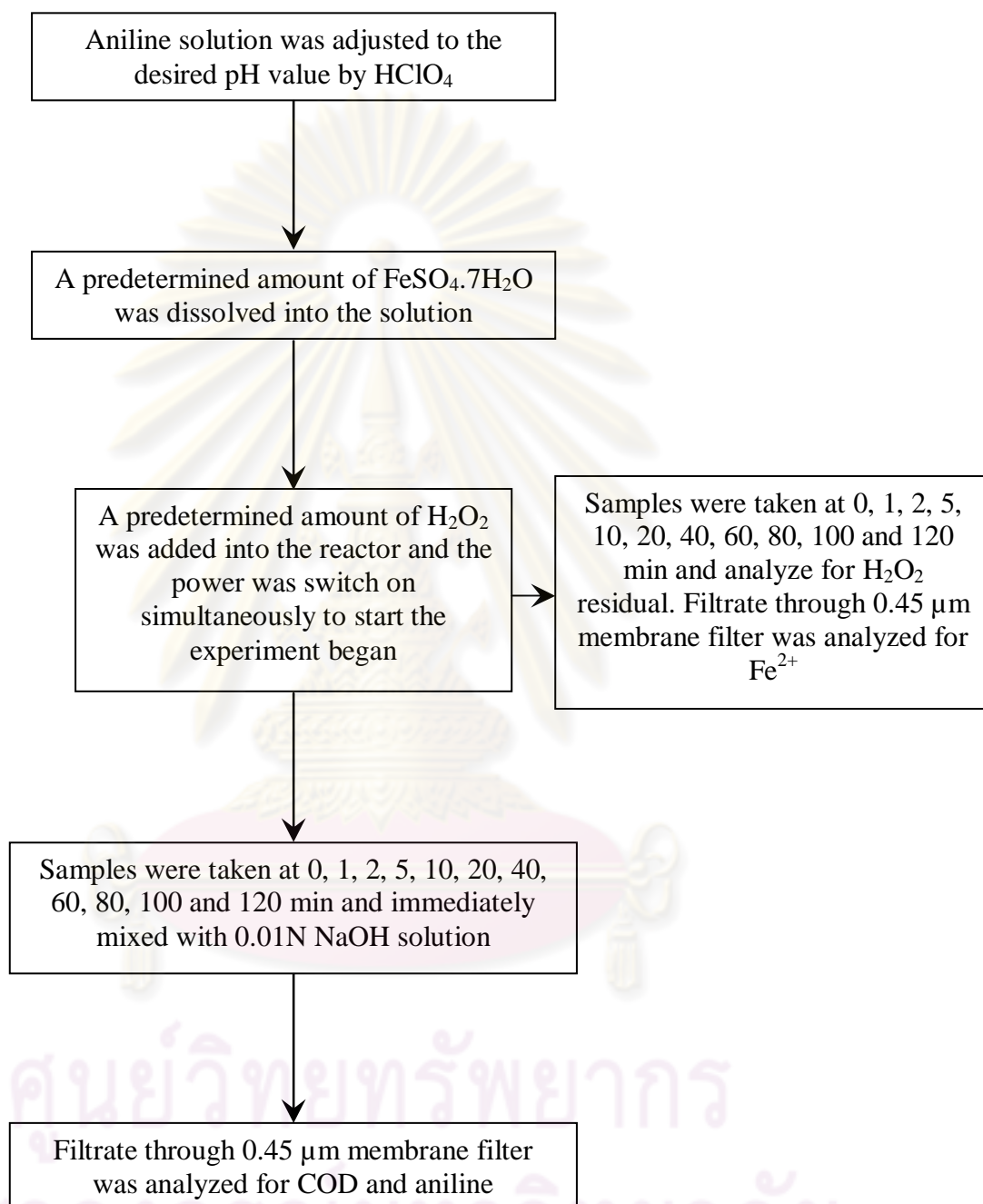


Figure 3.3 Flow chart for electro-Fenton experiment.

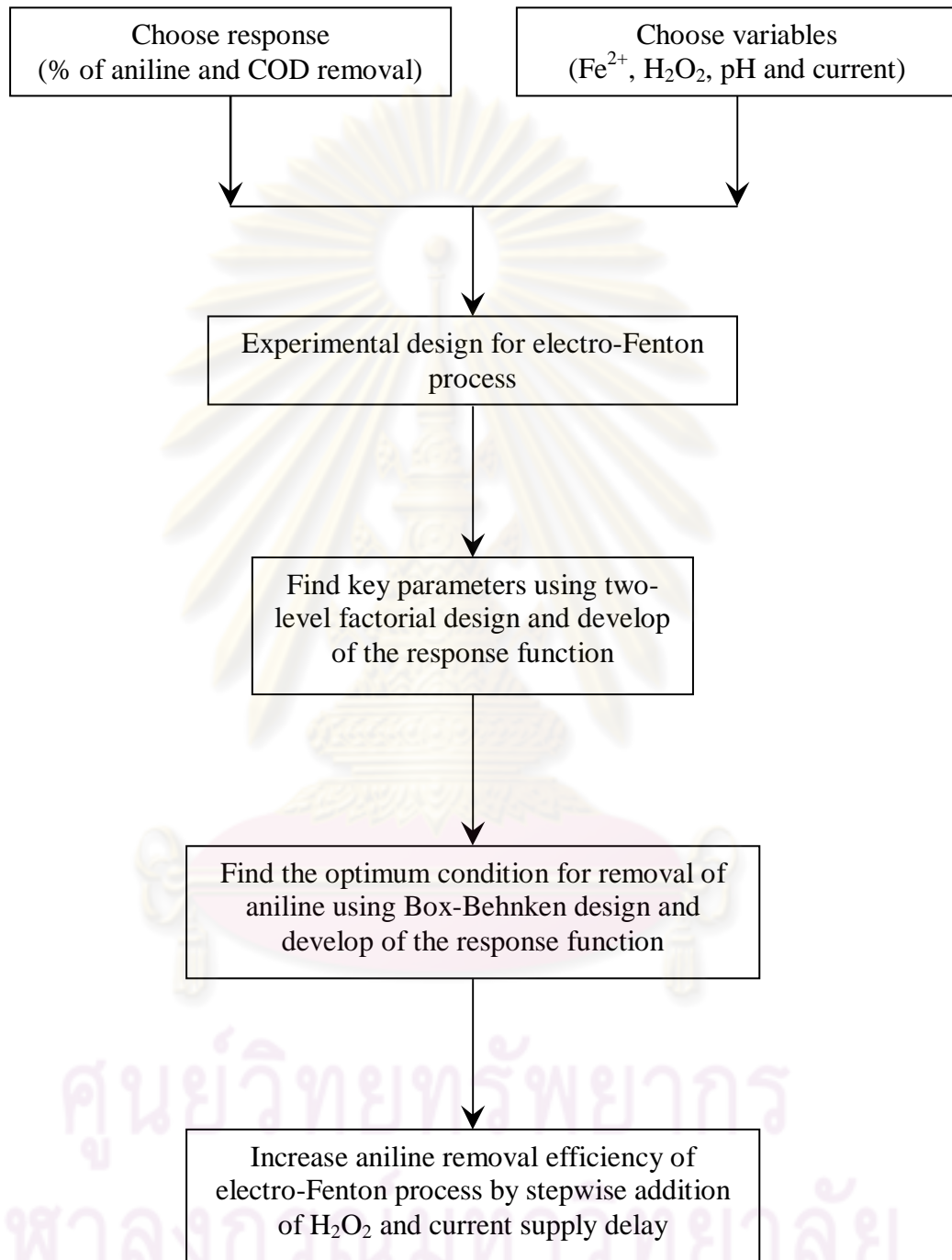


Figure 3.4 RSM procedures to optimize the electro-Fenton process.

Table 3.1 The levels of variable in two-level factorial design experiment

Variable	Symbol	Coded variable level	
		Low -1	High +1
H ₂ O ₂ (mM)	X ₁	44	100
Fe ²⁺ (mM)	X ₂	0.72	1.79
Current (A)	X ₃	2	5
pH	X ₄	2	3.5

At first, 16 (2⁴) runs of two-level factorial design experiment was performed randomly. The responses of the process were evaluated by the removal efficiency of aniline and COD. Table 3.2 shows a design matrix for the experiment.

Table 3.2 Design matrix of two-level factorial design experiment

Run	Factors			
	H ₂ O ₂ (mM)	Fe ²⁺ (mM)	Current (A)	pH
1	-1	+1	-1	+1
2	-1	+1	+1	+1
3	+1	+1	-1	-1
4	-1	-1	+1	-1
5	+1	-1	-1	+1
6	-1	-1	+1	+1
7	+1	+1	+1	+1
8	-1	-1	-1	+1
9	+1	+1	-1	+1
10	+1	+1	+1	-1
11	-1	+1	+1	-1
12	+1	-1	-1	-1
13	+1	-1	+1	-1
14	+1	-1	+1	+1
15	-1	+1	-1	-1
16	-1	-1	-1	-1

จุฬาลงกรณ์มหาวิทยาลัย

3.5.2 Phase 2: Box-Behnken Design

The two level of factorial design was further continued with the RSM developed based on the Box-Behnken design using aniline and COD removals as the responses while significant key parameters from preliminary screening process were chosen as variables. The Box-Behnken was conducted with a 12 runs of combination variables at 3 levels and 5 replicated runs at the center point. The low, center and high levels of each variable are designed with coded as -1, 0, +1, respectively, as shown in the Table 3.3 and the design of experiment of Box-Behnken design is shown in Table 3.4.

Table 3.3 Levels of variable Box-Behnken design experiment

Variable	Symbol	Coded variable level		
		Low	Center	High
		-1	0	+1
H ₂ O ₂ (mM)	X ₁	44	72	100
Fe ²⁺ (mM)	X ₂	0.72	1.25	1.79
pH	X ₃	2	2.75	3.5

Table 3.4 Experimental scenarios from box-Behnken design

Run	H ₂ O ₂ (mM), X ₁	Fe ²⁺ (mM), X ₂	pH, X ₃
1	+1	-1	0
2	0	+1	+1
3	-1	0	-1
4	-1	0	+1
5	0	0	0
6	0	0	0
7	-1	+1	0
8	+1	+1	0
9	+1	0	-1
10	0	-1	+1
11	0	0	0
12	0	0	0
13	0	+1	-1
14	0	0	0
15	0	-1	-1
16	-1	-1	0
17	+1	0	+1

3.5.3 Phase 3: Increasing Efficiency of Aniline Removal by Electro-Fenton

In this phase, the obtained optimum condition from Box-Behnken design was further tested for possible improvement by H₂O₂ stepwise addition and current supply delay as shown in Tables 3.5 and 3.6, respectively.

Table 3.5 Scenarios for effect of H₂O₂ stepwise addition on the aniline removal by electro-Fenton process at the optimum condition.

Number of Feedings	Add the H ₂ O ₂ at time (min)
1	0
2	0 and 60
3	0, 30 and 60
Continuous	0 to 60

Table 3.6 Scenarios for effect of current supply delay on the aniline removal by electro-Fenton process at the optimum condition.

Run	Time at which the current applied (min)	Ordinary Fenton reaction time (min)	Current discharge time (min)
1	After 20	20	100
2	After 40	40	80
3	After 60	60	60
4	After 80	80	40

ศูนย์วิทยทรัพยากร
จุฬาลงกรณ์มหาวิทยาลัย

CHAPTER IV

RESULTS AND DISCUSSION

4.1 Control Experiments

The results of control study were summarized in Figure 4.1. It was found that aniline and COD could not be removed significantly during the experimental period of 120 minutes without Fenton reaction. All scenarios still have 92% of aniline and COD remaining after 120 minutes. Therefore, it can be concluded that the aniline and COD degradations observed in next parts were solely due to $\bullet\text{OH}$ radicals oxidation.

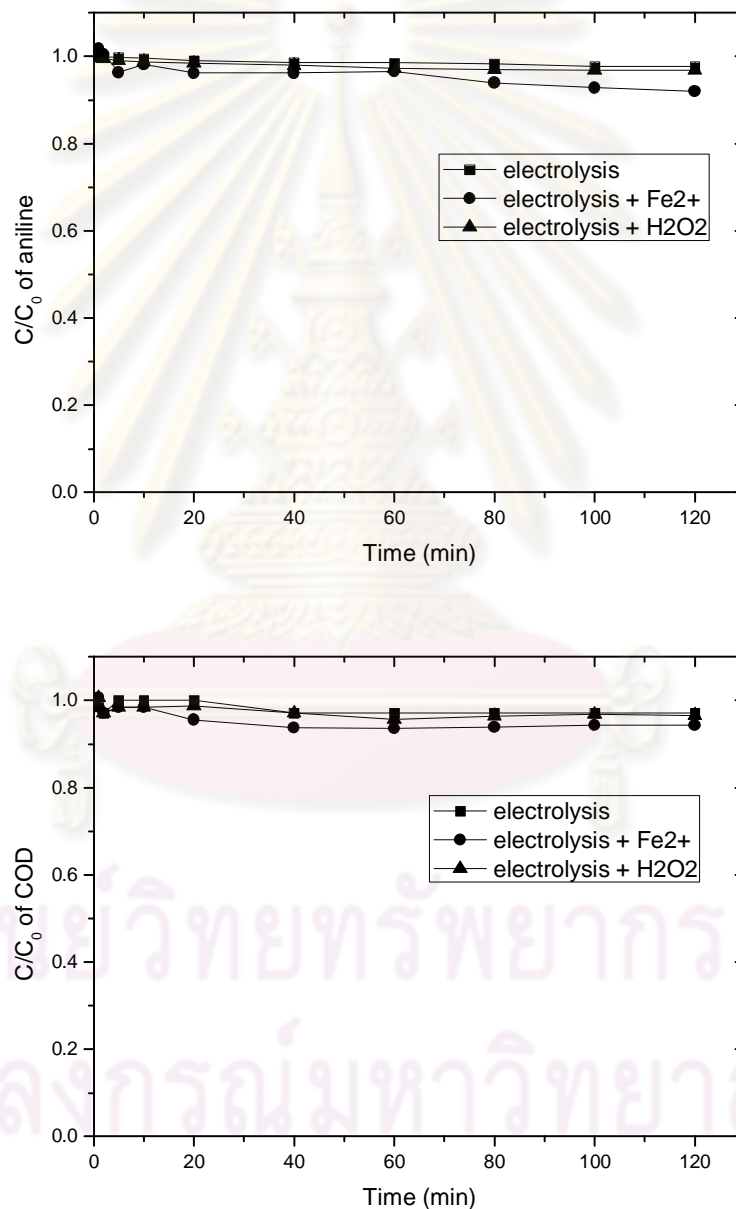


Figure 4.1 Aniline and COD removal in control experiments with 10 mM of aniline, 1.79 mM of Fe^{2+} , 72 mM of H_2O_2 , current 2 A and at pH 2.

4.2 Screening Experiments

Analysis of the experimental data by a complete 2^4 factorial design was systematically conducted as an initial screening process by examining the effects and interactions of H_2O_2 , Fe^{2+} , current and pH on aniline and COD removals as summarized in Table 4.1. The removals of aniline from two-level factorial design experiment were between 63.83% and 100% and removals of COD were between 34.97% and 69.29%. In order to screen several vital significant factors from those insignificant, a half-normal plot to the absolute value from low to high was constructed as shown in Figure 4.2. Significances of effects and interactions of factors on a response were further diagnosed and compared, graphically illustrated in the half normal plot, where the results of dominating effects that are likely to represent the important and influential factor were found consistent with the applying the analysis of variance (ANOVA) analysis results. Figure 4.2 shows the plots of the effects versus their assigned half-normal probability for aniline removal. A line was drawn to find the group of near zero effect which should locate near the straight line, whereas significant factors should apart from the line. Significant factors were labeled on the plots, which were found as follows: H_2O_2 (X_1), Fe^{2+} (X_2), and pH (X_3) whereas current (X_4) was insignificant factor. In contrast, H_2O_2 was only one significant factor on COD removal as shown in Figure 4.3. Moreover, the significance of interactions between factors on the response can be considered using interaction analysis graph of Figure 4.4.

Table 4.1 Result of design matrix of two-level factorial design experiment.

Run	Factors				Response	
	H_2O_2 (mM)	Fe^{2+} (mM)	Current (A)	pH	Aniline removal (%)	COD removal (%)
1	-1	+1	-1	+1	94.93	38.12
2	-1	+1	+1	+1	95.27	38.93
3	+1	+1	-1	-1	97.56	66.91
4	-1	-1	+1	-1	63.83	34.97
5	-1	-1	-1	+1	97.07	47.11
6	-1	-1	+1	+1	88.88	49.91
7	+1	+1	+1	+1	100	68.82
8	-1	-1	-1	+1	87.49	51.11
9	+1	+1	-1	+1	100	65.66
10	+1	+1	+1	-1	100	69.29
11	-1	+1	+1	-1	89.83	43.29
12	+1	-1	-1	-1	94.18	53.27
13	+1	-1	+1	-1	95.42	48.92
14	+1	-1	+1	+1	98.06	56.23
15	-1	+1	-1	-1	90.86	46.49
16	-1	-1	-1	-1	72.58	39.71

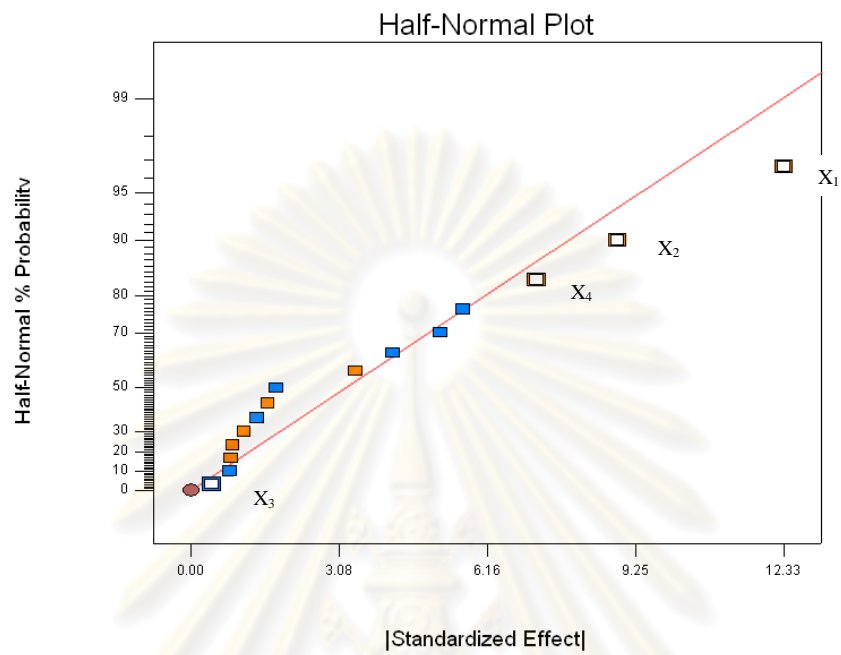


Figure 4.2 Standardized effect and half-normal probability plot of aniline removal.

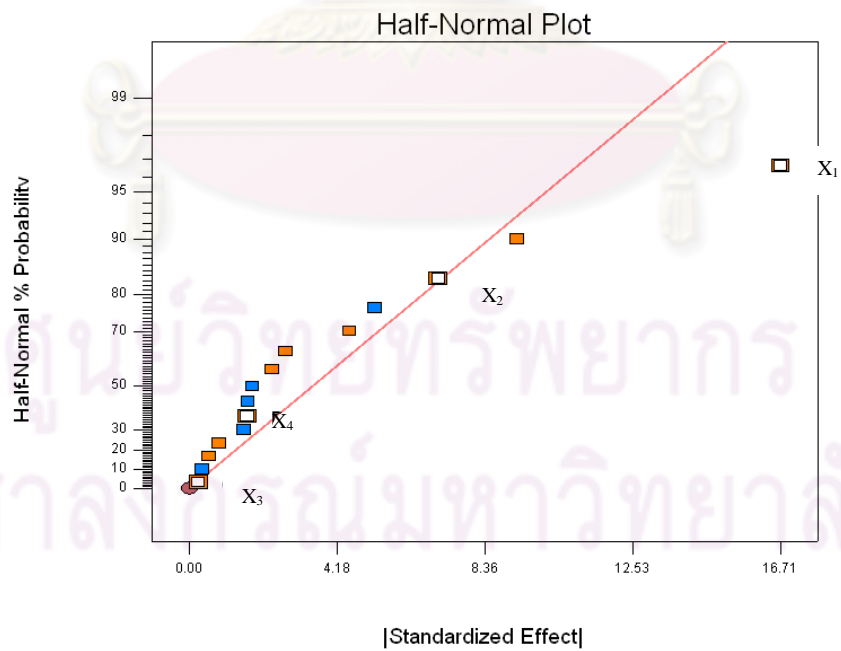


Figure 4.3 Standardized effect and half-normal probability plot of COD removal.

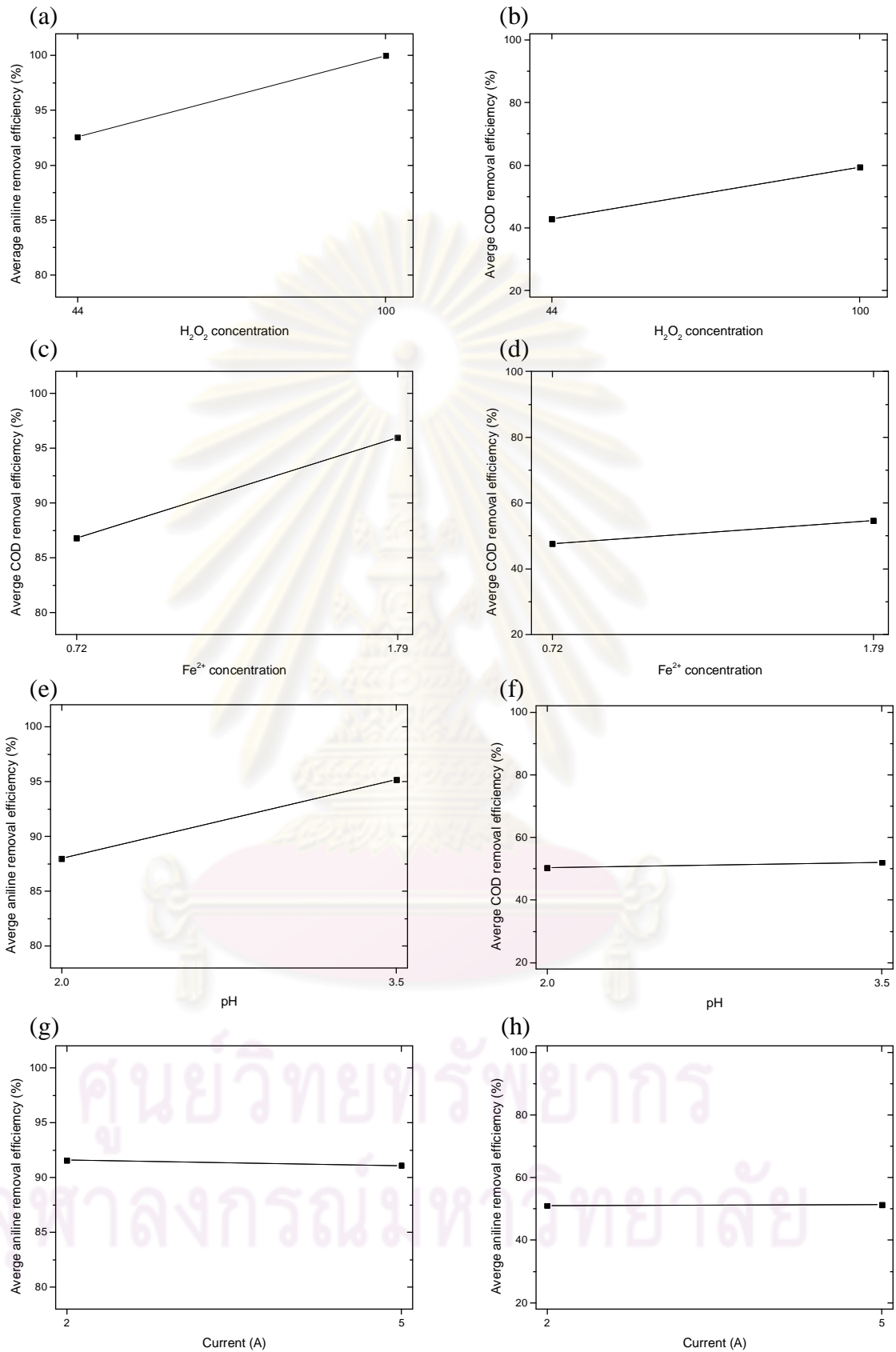


Figure 4.4 Average effect of the significant factors.

Removal efficiencies of aniline and COD were improved as the concentration of H_2O_2 increased from the minimal level to the maximum level as shown in Figure 4.4 (a) and (b). Increasing the concentration of Fe^{2+} from 0.72 to 1.79 mM also provide the positive effects on aniline and COD removals as shown in Figure 4.4 (c) and (d). Aniline and COD removals increased with increasing both initial H_2O_2 and Fe^{2+} concentrations due to increasing both $\bullet\text{OH}$ radicals production according to reaction 2.1 (Ay et al., 2009) and regeneration of Fe^{2+} that could simultaneously react with H_2O_2 to produce $\bullet\text{OH}$ radicals as shown in reaction 2.15. Some reseachers found that further increase in Fe^{2+} did not bring about further improvement in aniline and COD removal as excess of Fe^{2+} would consume $\bullet\text{OH}$ according to reaction 2.2 (Brillas et al., 2007; Panizza and Cerisola, 2001; Zhou et al., 2008). Increasing pH from 2 to 3.5 had a positive effect on aniline removal; in contrast, had only minor effects on the COD removal as shown in Figure 4.4 (e) and (f). This was evident from the results of Run 3 and Run 9 as shown in Table 4.1 which demonstrated the outstanding aniline removal of 97.56 and 100% and COD removal of 66.91 and 65.66%, respectively.

On the other hand, increasing the current from the minimal to maximal value appeared to have only minor effects on the aniline and COD removal as shown in Figure 4.4 (g) and (h) plotted by using the results from Run 1 and Run 2 from Table 4.1 which demonstrated outstanding aniline removal (94.93 and 95.27%, respectively) and COD removal (38.12 and 38.93%, respectively). As a result, for energy saving purpose, the low current was used in the next part. These comparable outcomes might be due to higher current led to the competitive electrode reactions such as the discharge of oxygen at the anode via reaction 2.17 and evolution of hydrogen at the cathode would be pronounced (Zhang et al., 2007).

Statistical testing of the model was performed with F-test to obtain the mathematical relationship between response and process variables. Tables 4.2 and 4.3 show the results of ANOVA for removal of aniline and COD, respectively. For aniline removal, the F-value equaled to 7.84 implying that estimation of the model was significant. Value of "p" equaled to 0.0031 which was less than 0.05 indicating that the model terms were significant. For COD removal, the model of F-value equaled to 5.85 implying that estimated of the model was significant as well. Value of "p" equaled to 0.0089 which was also less than 0.05 indicating that the model terms were significant. Values of "Prob > F" less than 0.0500 indicated model terms were significant for the removal aniline and COD. The ANOVA analysis indicated that H_2O_2 , Fe^{2+} and pH were significant and played important roles in the removal of aniline as summarized in Table 4.2. In other hand, H_2O_2 was the only significant parameter and played an important role on removal of COD as summarized in Table 4.3.

Table 4.2 ANOVA test for aniline removal by two-level factorial.

Source	Sum of squares	df	Mean square	F-value	p-value Prob > F	
Model	1129.32	4	282.33	7.84	0.0031	significant
X ₁ -H ₂ O ₂	607.87	1	607.87	16.88	0.0017	
X ₂ -Fe ²⁺	314.53	1	314.53	8.73	0.0131	
X ₃ -Current	0.71	1	0.71	0.020	0.8906	
X ₄ -pH	206.21	1	206.21	5.72	0.0357	
Residual	396.23	11	36.02			
Cor Total	1525.56	15				

Table 4.3 ANOVA test for COD removal by two-level factorial.

Source	Sum of squares	df	Mean square	F-value	p-value Prob > F	
Model	1325.73	4	331.43	5.85	0.0089	significant
X ₁ -H ₂ O ₂	1116.90	1	1116.90	19.72	0.0010	
X ₂ -Fe ²⁺	197.96	1	197.96	3.50	0.0883	
X ₃ -Current	0.25	1	0.25	4.327×10 ⁻³	0.9487	
X ₄ -pH	10.63	1	10.63	0.19	0.6732	
Residual	622.87	11	56.62			
Cor Total	1948.60	15				

4.3 Box-Behnken Design

The three significant variables, i.e., H₂O₂, Fe²⁺ and pH, obtained from the two level of factorial design were further optimized using the Box-Behnken design. Complete 17 runs of the experimental design matrix proposed by the Box-Behnken program and the observed responses in terms of aniline and COD removals were given in Table 4.4. The removal efficiencies of aniline and COD varied between 87.51-100% and 35.81-63.77%, respectively. Based on these results, the empirical relationships between the aniline and COD removals and the independent variables can be estimated by cubic and quadratic polynomials, respectively, in term of coded factors, as shown in the following equations:

$$\begin{aligned} \text{Aniline removal} = & +95.80 + 3.19X_1 + 3.52X_2 - 2.43X_3 + 0.72 X_1X_2 \\ & + 0.095 X_1X_3 - 0.98 X_2X_3 - 0.93X_1^2 - 1.84X_2^2 \\ & - 0.89X_3^2 - 1.84X_1^2X_2 + 5.17X_1^2X_3 + 1.38 X_1X_2^2 \\ & (R^2 = 0.99) \end{aligned} \quad (\text{equation 4.1})$$

$$\begin{aligned} \text{COD removal} = & +51.81 + 10.82X_1 + 2.06X_2 + 0.42X_3 + 4.48X_1X_2 \\ & - 0.29X_1X_3 - 1.26 X_2X_3 - 2.96X_1^2 + 0.015X_2^2 \\ & + 2.40X_3^2 \\ & (R^2 = 0.94) \end{aligned} \quad (\text{equation 4.2})$$

Considering on the coefficients in reactions 4.1 and 4.2, it can be said that the aniline removal decreased with the pH (X₃) whereas increased with H₂O₂ (X₁), Fe²⁺

(X_2) concentrations. The Fe^{2+} concentration had a more profound effect on aniline removal as compared to H_2O_2 concentration. COD removal increased with H_2O_2 , Fe^{2+} and pH with a more profound effect with the H_2O_2 concentration. Both value of R^2 is close to 1.0, which is very high and has advocated a high correlation value. This means that regression model provides an excellence explanation of the relationship between the independent variables (factors) and the response (aniline and COD removal).

4.3.1 Aniline Removal

H_2O_2 had a positive effect on aniline removal as shown in Figure 4.5. Aniline removal increased with increasing the H_2O_2 concentration upto 72 mM but decreased afterward due to the hydroxyl scavenging effect of H_2O_2 as shown in reaction 2.6. Effect of Fe^{2+} on aniline removal is shown in Figure 4.5. Aniline removal increased with increasing Fe^{2+} upto 100%. However, high Fe^{2+} concentration could also scavenge $\bullet OH$ yielding lower level of oxidation. pH was one of the most important factors and had a negative effect on aniline removal as shown in Figure 4.5.

Table 4.4 Experimental design matrix proposed by Box-Behnken and responses on aniline and COD removal.

Run	Actual and coded level of variables			Response	
	H_2O_2 (mM), X_1	Fe^{2+} (mM), X_2	pH, X_3	Aniline removal (%)	COD removal (%)
1	+1	-1	0	95.21	52.95
2	0	+1	+1	93.18	57.02
3	-1	0	-1	88.16	38.84
4	-1	0	+1	93.44	39.35
5	0	0	0	96.99	53.75
6	0	0	0	95.03	55.24
7	-1	+1	0	89.42	35.81
8	+1	+1	0	100	63.77
9	+1	0	-1	94.34	63.73
10	0	-1	+1	88.1	53.17
11	0	0	0	95.38	46.43
12	0	0	0	95.42	55.43
13	0	+1	-1	100	55.12
14	0	0	0	95.67	56.78
15	0	-1	-1	91.01	48.89
16	-1	-1	0	87.51	42.93
17	+1	0	+1	100	63.06

The interactive effects of two independent variables with another variable being fixed on the removal of aniline by electro-Fenton process were shown in the 3D surface plot (Figure 4.5) as described below.

4.3.1.1 Interactive Effect of Fe^{2+} and H_2O_2

To investigate the combined effect of Fe^{2+} and H_2O_2 , the RSM was used and results were shown in the form of three-dimensional (3D) surface plots. Figure 4.5 (a) showed that, as Fe^{2+} increased from 0.72 mM to 1.79 mM, aniline removal also increased. The increase on aniline removal was also observed as the H_2O_2 concentration increased from 44 to 72 mM, however, the efficiency decreased afterward. Aniline removal increased with increasing Fe^{2+} concentration from 0.72 to 1.70 mM. This is due to the fact that Fe^{2+} plays a very important role in initiating the decomposition of H_2O_2 to generate the $\bullet\text{OH}$ in the Fenton process. However, adverse effects were observed when excess dose of H_2O_2 was applied resulting in a decrease in aniline removal efficiency due to the $\bullet\text{OH}$ scavenging effect of H_2O_2 and recombination of the $\bullet\text{OH}$ following reactions 2.6 and 2.7 (Arslan-Alaton et al., 2009; Ay et al., 2009).

4.3.1.2 Interactive Effect of Fe^{2+} and pH

Figure 4.5 (c) showed the effect of Fe^{2+} concentration and pH on aniline removal under predefined conditions given by Design Expert program. The 3D surface plot showed that the maximum aniline removal occurred at the pH 2 and Fe^{2+} concentration was 1.79 mM, which was in accordance with the model. The removal of aniline increased with decreasing pH which might be due to the oxidation potential of $\bullet\text{OH}$ and also the solubility of iron species decreased with increasing pH (Panizza and Cerisola, 2009). As the pH increased, Fe^{3+} started to precipitate out in the form of amorphous $\text{Fe}(\text{OH})_{3(s)}$. The formation of $\text{Fe}(\text{OH})_{3(s)}$ not only decreased the dissolved Fe^{3+} concentration, but also inhibited Fe^{2+} regeneration by partially coating the electrode surface (Panizza and Cerisola, 2009; Sun et al., 2008). Fe^{2+} concentration of 1.79 mM and pH 2 were found to be the optimum conditions for aniline and COD removals.

4.3.1.3 Interactive Effect of pH and H_2O_2

Effect of pH and H_2O_2 has been analysed as shown in Figure 4.5 (e). Aniline removal efficiency increased almost linearly with an increase of H_2O_2 concentration. The 3D surface plot showed that, at pH 3.5, increasing H_2O_2 concentration from 44 to 100 mM could promote the aniline removal. In contrast, at pH 2, increasing H_2O_2 concentration from 44 to 72 mM could also increase the aniline removal; however, after increased H_2O_2 upto 100 mM, aniline removal decreased. In this study, the optimum of aniline removal was obtained at 72 mM of H_2O_2 at pH 2. H_2O_2 would be catalyzed by ferrous ion to produce hydroxyl radicals through reaction 2.1, and greater hydroxyl radicals could be generated with increasing concentrations of Fe^{2+} and H_2O_2 .

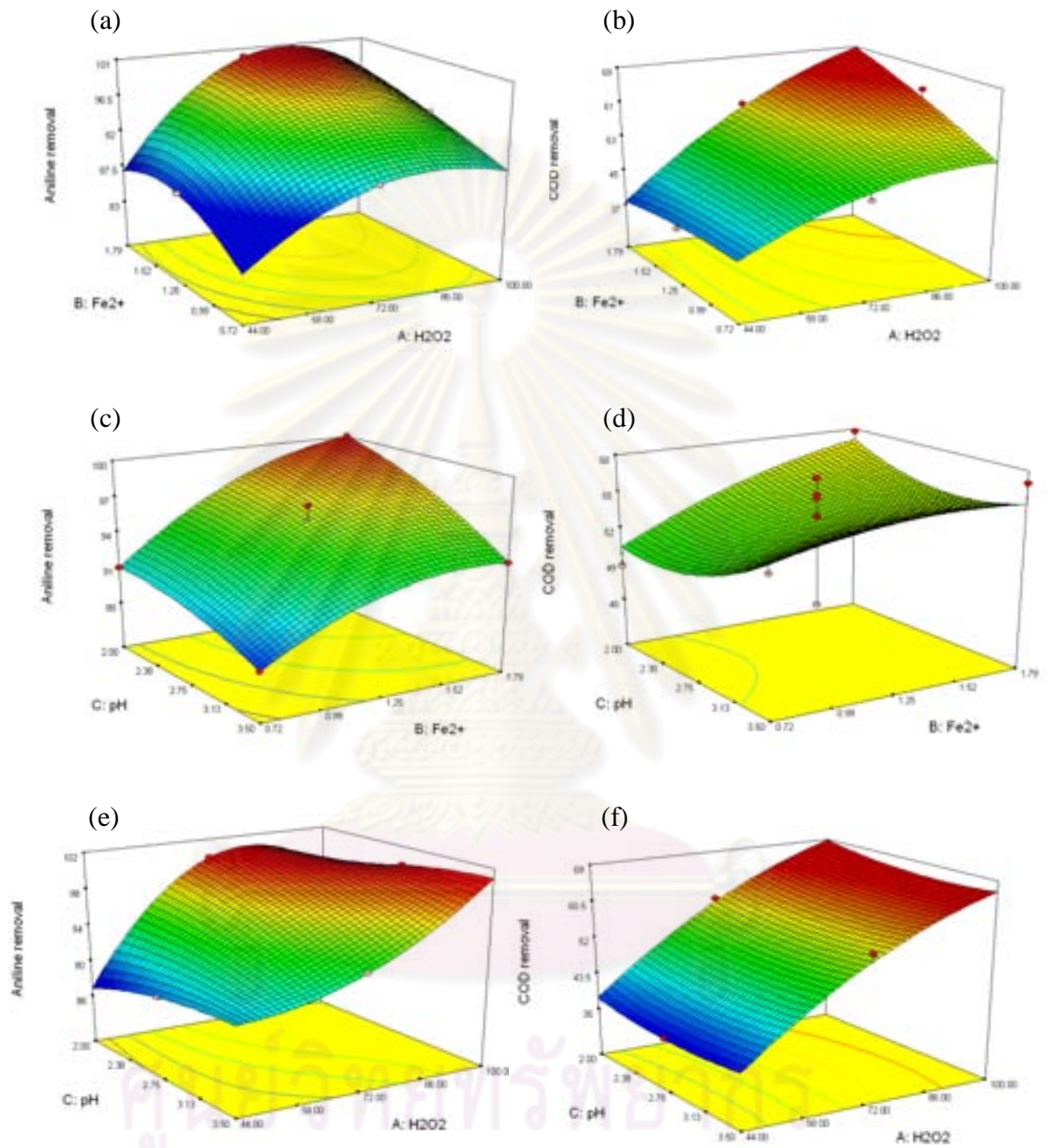


Figure 4.5 3D response surface plot for aniline and COD removal.

A statistical testing using F-test for ANOVA was also conducted for each response and found that the predictability of the model was at 95% confidence level ($P < 0.05$). From this ANOVA result as shown in Table 4.5, the model of F-value equaled to 38.62 implying that estimation of the model was significant. Value of "p" equaled to 0.0015 which was less than 0.05 indicated that the model terms were significant. Furthermore, the coefficient of determination " R^2 " of the model was reasonably close to 1 (0.99), implying that about of 99% of the variability in the data could be explained by the model. It was further shown that the main effect of H_2O_2 (X_1), Fe^{2+} (X_2), pH (X_3) and the two level interactions of X_1^2 , X_2^2 , $X_1^2X_2$ and $X_1^2X_3$ showed significant model terms (factors) which indicated the importance of these variables on the aniline removal by electro-Fenton process. Other model terms were relatively less significant influencing aniline removal as their confidence level were less than 95% ($P > 0.05$). Analysis on normal probability plot of the residual as shown in Figure 4.6 depicted nearly a straight line residual distribution denoting that the errors were evenly distributed and therefore supported the adequacy of the least square fit.

4.3.2 COD Removal

COD could not be completely removed under the studied conditions due to intermediate formation during the degradation of aniline. The effects of Fe^{2+} and H_2O_2 on COD removal are shown in Figure 4.5. Increasing Fe^{2+} and H_2O_2 concentrations greatly improved the COD removal. The results show that the Fenton's reagent was the most important factor affecting on the COD removal. From reaction 2.1, the generation of $\bullet OH$ from Fe^{2+} and H_2O_2 would increase as the Fenton's reagent increased.

The interactive effects of two independent variables on the removal of COD by electro-Fenton process were shown in Figure 4.5 as described below.

Table 4.5 ANOVA test for aniline removal by Box-Behnken design.

Source	Sum of Squares	df	Mean Square	F Value	p-value Prob > F	
Model	265.89	12	22.16	38.62	0.0015	significant
X_1 - H_2O_2	40.58	1	40.58	70.73	0.0011	
X_2 - Fe^{2+}	49.49	1	49.49	86.27	0.0007	
X_3 -pH	23.67	1	23.67	41.26	0.0030	
X_1X_2	2.07	1	2.07	3.61	0.1301	
X_1X_3	0.036	1	0.036	0.063	0.8143	
X_2X_3	3.82	1	3.82	6.66	0.2024	
X_1^2	3.23	1	3.23	5.62	0.0263	
X_2^2	13.46	1	13.46	23.46	0.0006	
X_3^2	2.96	1	2.96	5.15	0.0609	
$X_1^2X_2$	6.79	1	6.79	11.84	0.0263	
$X_1^2X_3$	53.41	1	53.41	93.10	0.0006	
$X_1X_2^2$	3.84	1	3.84	6.69	0.0609	
Pure Error		4	0.57			
Cor Total		16	R^2		0.99	

4.3.2.1 Interactive Effect of Fe^{2+} and H_2O_2

Figure 4.5 (b) presented the 3D surface plot representing an estimate of COD removal as a function of Fe^{2+} and H_2O_2 concentration. As can be understood from Figure 4.5 (b) that increasing the initial H_2O_2 concentration had a positive effect on COD removal at all selected initial Fe^{2+} concentration. In contrast, Fe^{2+} affected very little on COD removal. In addition, the maximum COD removal was occurred at the H_2O_2 and Fe^{2+} concentrations of 100 and 1.79 mM, respectively, which in accordance with the prediction from the model. At 0.72 mM of Fe^{2+} , COD removal was lower than at 1.79 mM of Fe^{2+} because of the scavenging effect of the excess H_2O_2 and the recombination of the $\bullet\text{OH}$ as shown in reactions 2.6 and 2.7 (Arslan-Alaton et al., 2009; Ay et al., 2009).

4.3.2.2 Interactive Effect of Fe^{2+} and pH

Figure 4.5 (d) presented the 3D surface plot as an estimate of COD removal as a function of the two variables, ie., Fe^{2+} and pH. Increasing pH from 2 to 3.5 had a positive effect on COD removal. The increase in COD removal was also observed as Fe^{2+} increased from 0.72 to 1.79 mM. In addition, the maximum COD removal was occurred at the pH and Fe^{2+} concentration of 2 and 1.79 mM, respectively, which in accordance with the outcome from the model.

4.3.2.3 Interactive Effect of pH and H_2O_2

pH variation between 2 and 3.5 practically had no influence on COD removal. Increasing the initial H_2O_2 concentration had a positive effect on COD removal as shown in Figure 4.5 (f).

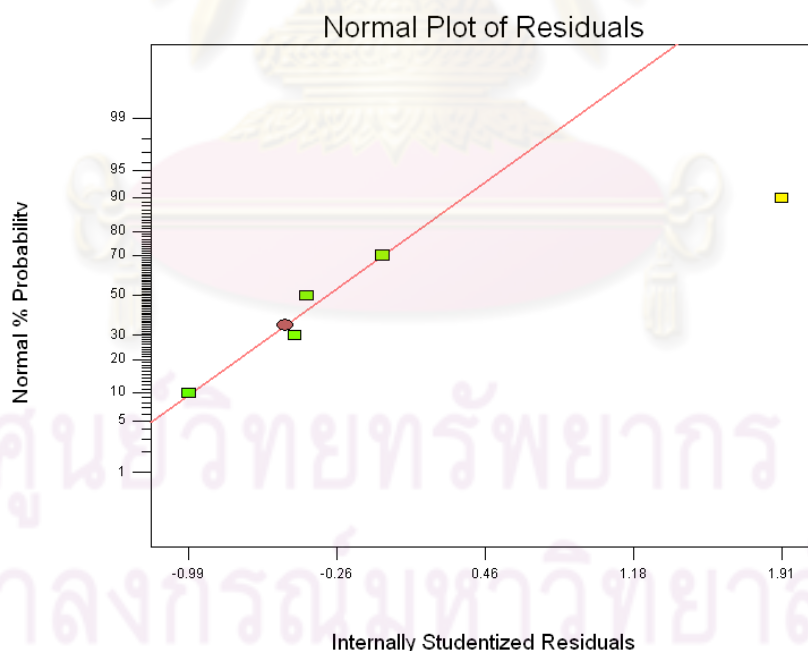


Figure 4.6 Normal probability plot of residual for aniline removal.

A statistical testing using F-test for ANOVA was also conducted for each response and found that the predictability of the model was better than 95% confidence level ($P < 0.05$). For these ANOVA results as shown Table 4.6, the model F-value of 9.41 implying that the model was significant as well. Value of "p" of 0.0037 which was less than 0.05 indicating that the model terms were significant. Furthermore, the coefficient of determination " R^2 " of the model was reasonably close to 1 (0.94), implying that 94% of the variability in the data could be explained by the model. Figure 4.5 shows the 3D response surface which was constructed to demonstrate the effects of H_2O_2 and Fe^{2+} . The non-significant lack of fit (more than 0.05) showed that quadratic model was valid in the present study. Non-significant lack of fit guaranteed the sufficiency for data fitness of the model. It was further shown that the main effect of H_2O_2 (X_1) and the two level interaction of X_1X_2 were significant model terms as observed from the high level of significance indicating the importance of these variables on the COD removal by electro-Fenton process. Other model terms were relatively less influencing on aniline removal as their confidence level were less than 95% ($P > 0.05$). Analyses on normal probability plot of the residual were shown in Figure 4.7 depicting nearly a straight line residual distribution, which denoting the errors were evenly distributed and therefore support adequacy of the least square fit.

4.3.3 Process Optimization

The main objective of this optimization was to determine the optimum set of variables which could provide the maximum removals for aniline and COD from electro-Fenton process by predicting from the real experimental data. The optimized conditions for aniline and COD removals were shown in Table 4.7. Under these conditions, aniline and COD removals were estimated to be 100 and 57.12%, respectively, which were consistency with experimental data as shown in Figure 4.8. The desirability function value was found to be 0.725 at these optimum conditions.

Table 4.6 ANOVA test for COD removal by Box-Behnken design.

Source	Sum of Squares	df	Mean Square	F Value	p-value Prob > F	
Model	1132.28	9	125.81	9.41	0.0037	significant
X_1 - H_2O_2	937.01	1	937.01	70.09	<0.0001	
X_2 - Fe^{2+}	33.83	1	33.83	2.53	0.1557	
X_3 -pH	1.40	1	1.40	0.10	0.754	
X_1X_2	80.46	1	80.46	6.02	0.0439	
X_1X_3	0.35	1	0.35	0.026	0.8754	
X_2X_3	6.38	1	6.38	0.48	0.5121	
X_1^2	61.34	1	61.34	4.59	0.0694	
X_2^2	3.00	1	3.00	0.22	0.6501	
X_3^2	9.93	1	9.93	0.74	0.4173	
Residual	93.57	7	13.37			
Lack of Fit	26.02	3	8.67	0.51	0.6946	not significant
Pure Error	67.55	4	16.89			
Cor Total	1225.85	16	R^2		0.94	

In this optimum study, 10 mM of aniline was removed with 72 mM of H_2O_2 by electro-Fenton process. Anotai et al. (2006) studied the removal of aniline by electro-Fenton process using an acrylic reactor with Ti/Pt or DSA anodes and stainless cathodes. They used 300 mM of H_2O_2 with 10 mM of aniline which were higher than in this study; however, the removals of aniline and COD were quite the same.

The H_2O_2 efficiency for aniline was also determined in the study and it was shown in Table 4.8. The H_2O_2 efficiency for aniline removal was calculated using the amount of H_2O_2 theoretically consumed for COD removal. The efficiency of H_2O_2 , η , is defined as follows (Huang et al., 2001; Kang and Hwang, 2000):

$$\eta (\%) = \left[\frac{\Delta COD}{\text{available } O_2} \right] \times 100 \quad (\text{equation 4.3})$$

$$= \left[\frac{COD_i - COD_t}{H_2O_2 \times 0.4706} \right] \times 100 \quad (\text{equation 4.4})$$

where

COD_i is the initial COD (mg/L);

COD_t is the COD (mg/L) at given time (t);

H_2O_2 is the dosage concentration of H_2O_2 (mg/L) at time (t)

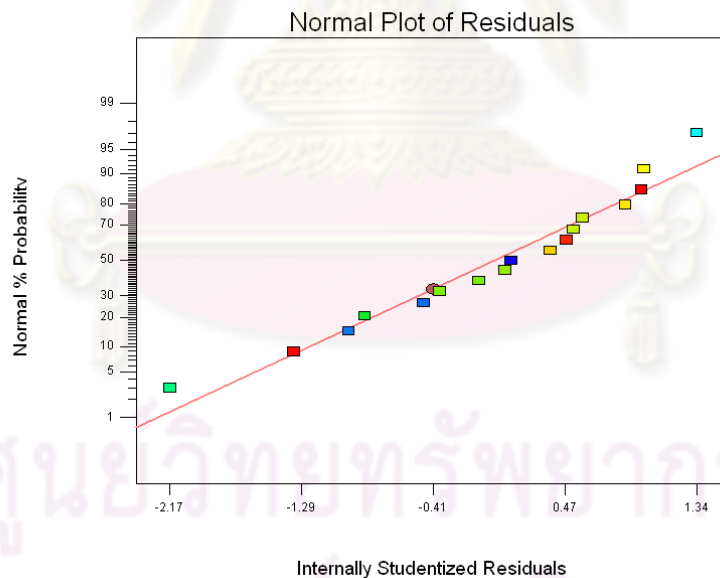


Figure 4.7 Normal probability plot of residual for COD removal.

Table 4.7 Results of optimum operational conditions for 10 mM of aniline and COD removal.

H_2O_2 - X_1 (mM)	Fe^{2+} - X_2 (mM)	pH- X_3	Percent removal	
			Aniline	COD
72	1.79	2	100	57.12

The H_2O_2 efficiency for COD removal decreased from 148.27% to 90.25% when increasing H_2O_2 concentration from 44 to 100 mM. Increased Fe^{2+} concentration from 0.72 to 1.79 mM had a negative effect on the system performance and the H_2O_2 efficiency decreased from 124.08% to 119.43%. pH also affected on H_2O_2 efficiency for COD removal, i.e., efficiency decreased from 124.08% to 109.96% when increasing pH from 2 to 3.5. The results showed that efficiency of H_2O_2 decreased with increased the Fenton's reagent dosage. The efficiency of H_2O_2 exceeding 100% was possible since the COD removal was not only attributed to Fenton's reaction (Zhang et al., 2007). In the electro-Fenton process, COD was removed by both oxidation and coagulation (Zhang et al., 2007; Zhang et al., 2006).

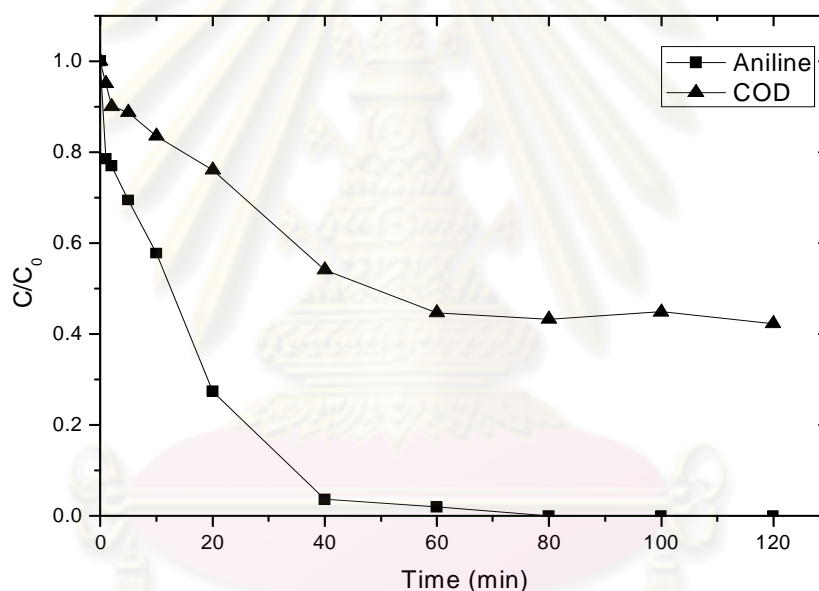


Figure 4.8 Aniline and COD removal by electro-Fenton process at the optimum condition.

Table 4.8 Efficiency and rate constant of aniline removal at 10 mM of aniline and current 2 A by electro-Fenton.

H_2O_2 (mM)	Fe^{2+} (mM)	pH	Efficiency			
			Aniline	COD	Current	H_2O_2
44	1.79	2	90.86	46.49	306.1	148.27
72	1.79	2	100	57.19	392.51	119.43
100	1.79	2	97.56	66.91	424.61	90.5
72	1.79	3.5	93.18	57.02	371.44	109.96
72	0.72	2	91.01	48.93	340.18	124.08
72	1.79	2	58.34	30.25	-	311.28

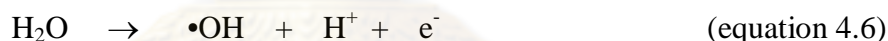
The performance of electro-Fenton process was generally evaluated by the current efficiency (η). Current efficiency, defined as the ratio of the electricity consumed by the electrode reaction of interest over the total electricity passed through the circuit which can be calculated by the following equation (Comminellis and Pulgarin, 1991; Panizza and Cerisola, 2001):

$$\eta (\%) = \left[\frac{(\text{COD}_i - \text{COD}_t) \times F \times V}{8000 \times I \times t} \right] \times 100 \quad (\text{equation 4.5})$$

where

- COD_i is the initial COD (mg/L);
- COD_t is the COD (mg/L) at given time (t);
- V is the volume of the electrolyte (L);
- F is the Faraday constant (96,487 C/mol);
- I is the current intensity (A);
- t is the time of operation (sec)

In this study, the efficacy of electro-Fenton process in term of COD was calculated. Current efficiency for H_2O_2 at the concentrations of 44, 72, 100 mM were 306.1%, 393.51% and 424.61%, respectively. Increasing Fe^{2+} concentration from 0.72 to 1.79 mM increased the current efficiency from 340.18% to 392.18%. pH also affected on current efficiency for COD removal, i.e., efficiency decreased from 392.188% to 340.18% when increasing pH from 2 to 3.5. Table 4.8 showed that the current efficiency could exceed 100%. This can be accounted for the fact that the determination of current efficiency only involves one electrochemical reaction. In electro-Fenton process, $\bullet\text{OH}$ radicals would be produced at the surface of a high-oxygen over-voltage anode from water oxidation:



$\bullet\text{OH}$ radicals would also be generated, according to reaction 2.1. Ferric ion from would be reduced to ferrous ion at the cathode as following reaction 2.15. This would induce Fenton chain reaction efficiently. It is noteworthy that theoretical current efficiencies as high as 200% are possible in principle in electro-Fenton since organics can be degraded by oxidants produced by the current supplied to both anode and cathode (Brillas and Casado, 2002; Fockedey and Lierde, 2002). In addition, the current also generates an oxidant H_2O_2 which also contributing to pollutant oxidation. However, Fe^{2+} regeneration is slow even at optimal current density, and both current density and current efficiency drop off precipitously above pH 2.5 (Qiang et al., 2002; Qiang et al., 2003). Electro-Fenton has a very good efficiency during the initial stage of electrolysis when easily oxidizable products were rapidly destroyed by $\bullet\text{OH}$. The decrease of current efficiency during the operation was due to the formation of hardly oxidizable products (Boye et al., 2003; Brillas et al., 2004).

4.3.4 Comparison of Fenton and Electro-Fenton Process

Figure 4.9 showed the comparative aniline degradation of electrolysis, Fenton and electro-Fenton process. In Fenton process, it can be seen that only 58.34% and 30.25% of aniline and COD were degraded within 120 minutes. This is due to the deficit of Fe^{2+} as a result from the fast reaction between Fe^{2+} and H_2O_2 to produce $\bullet\text{OH}$ radicals as shown in reaction 2.1. In contrast, electro-Fenton process could

completely degrade aniline in 80 minutes and 57.19% for COD removal due to the ability of electrochemical regeneration of Fe^{2+} from Fe^{3+} in the presence of current on the cathode side as shown in reaction 2.15. As a result, Fe^{2+} could continuously react with H_2O_2 to produce more $\bullet\text{OH}$ for aniline and COD degradation. Fe^{2+} remaining in electro-Fenton process was approximately 30% higher than Fenton process as showed in Figure 4.10.

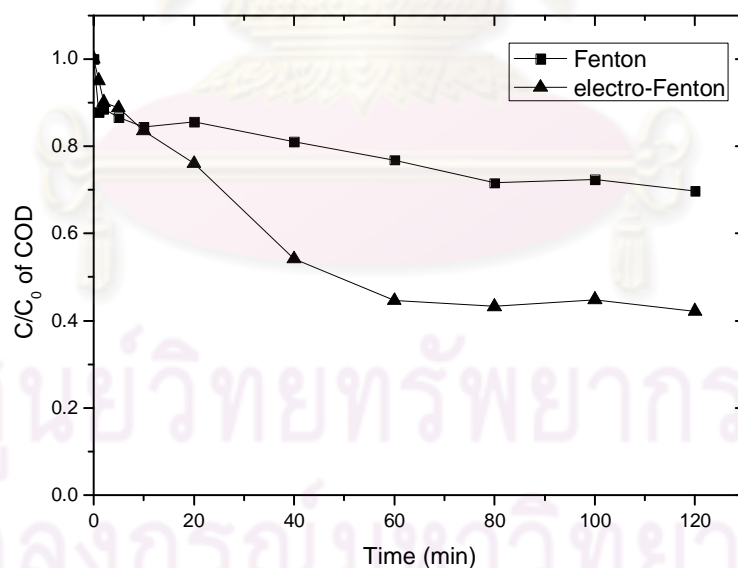
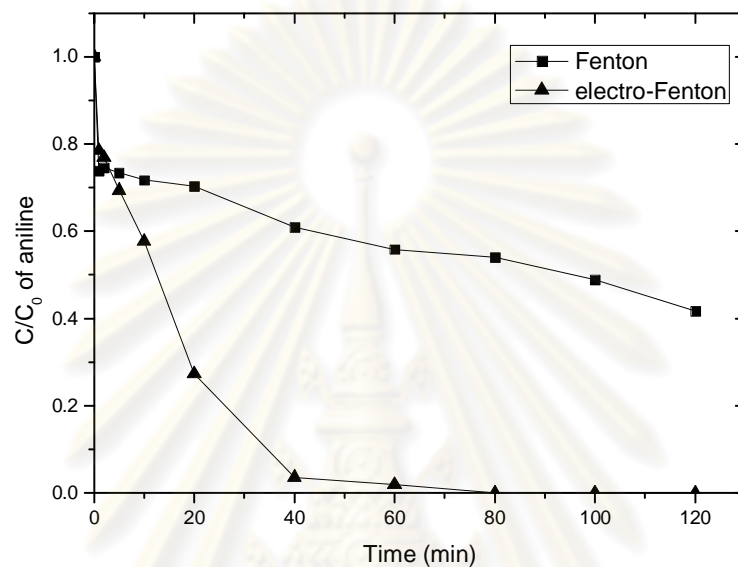


Figure 4.9 Comparison of aniline and COD removal by Fenton and electro-Fenton process at the optimum condition.

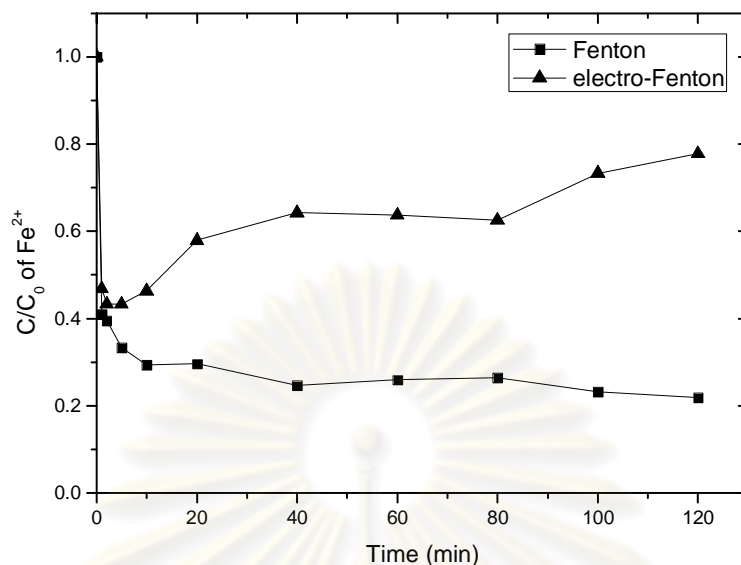


Figure 4.10 Fe^{2+} remaining in the experiments by Fenton and electro-Fenton processes at 2 A for 10 mM of aniline at pH 2, 1.79 mM of Fe^{2+} and 72 mM of H_2O_2 .

4.4 Improvement of Aniline Removal by Electro-Fenton Process

In this phase, the optimum condition obtained from Box-Behnken design (Table 4.7) was further tested for possible improvement by modifying the H_2O_2 addition and current supply patterns.

4.4.1 Effect of H_2O_2 Addition Pattern on Electro-Fenton Process

The stepwise and continuous addition patterns of H_2O_2 were also conducted in this study. H_2O_2 at constant total concentration of 0.72 mM was added in a single step (at 0 min), in a two-step manner (at 0 and 60 min), in three-step manner (at 0, 30, 60 min), and in a continuous mode for 60 min as demonstrated in Table 3.5. Total reaction time was kept at 120 min. The results from this operation are shown in Figure 4.11 indicating that the aniline removals were the same for all scenarios with the efficiency of 100%. The COD removal efficiencies increased with frequency of H_2O_2 addition and became highest in the continuous mode as shown in Table 4.9, i.e., increased from 55.17% for single dose to 61.27% for continuous addition. The addition of H_2O_2 one time at the beginning of the experiment resulted in a rapid and efficient production of $\bullet\text{OH}$; however, the remaining H_2O_2 would scavenge the $\bullet\text{OH}$ (in reaction 2.6) leading to low COD removal (Chu et al., 2007; Zhang et al., 2005). In the continuous mode, although the production of $\bullet\text{OH}$ was not as high as the single addition, H_2O_2 was kept at low concentration. As a result, the H_2O_2 scavenging effect was minimized.

Figures 4.12 and 4.13 showed profile of H_2O_2 and Fe^{2+} of this part. The addition of H_2O_2 all at once at the beginning of the experiment resulted in rapid decrease of H_2O_2 . 2-stepwise of H_2O_2 indicated that after added H_2O_2 into the process, Fe^{2+} quickly decreased because of $\bullet\text{OH}$ production from reaction 2.1; however, Fe^{2+} still maintained in the system implying that the regeneration and consumption rates of Fe^{2+} were not quite different. In 3-stepwise of H_2O_2 , lower H_2O_2 was added into the system at each time, as a result, Fe^{2+} was consumed at a lower rate than in previous experiments. For continuous addition, the concentration of Fe^{2+} reached the steady state after 60 minutes.

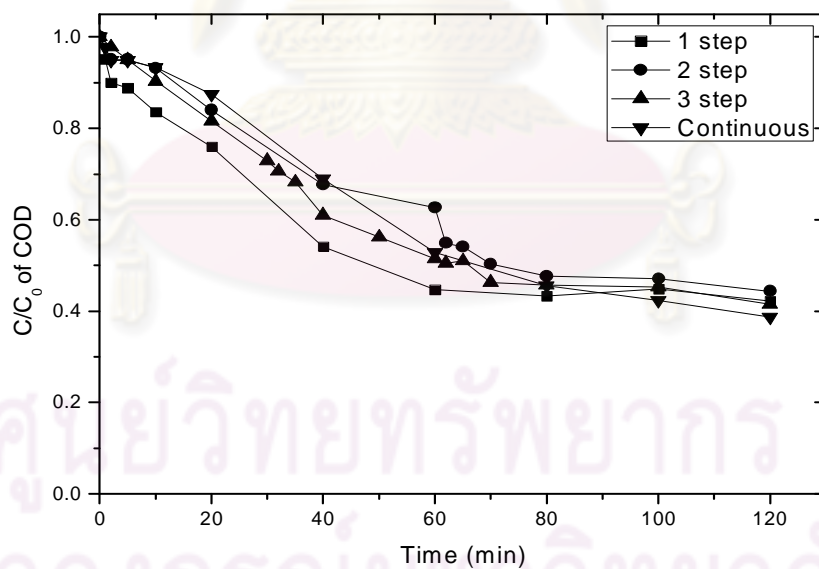
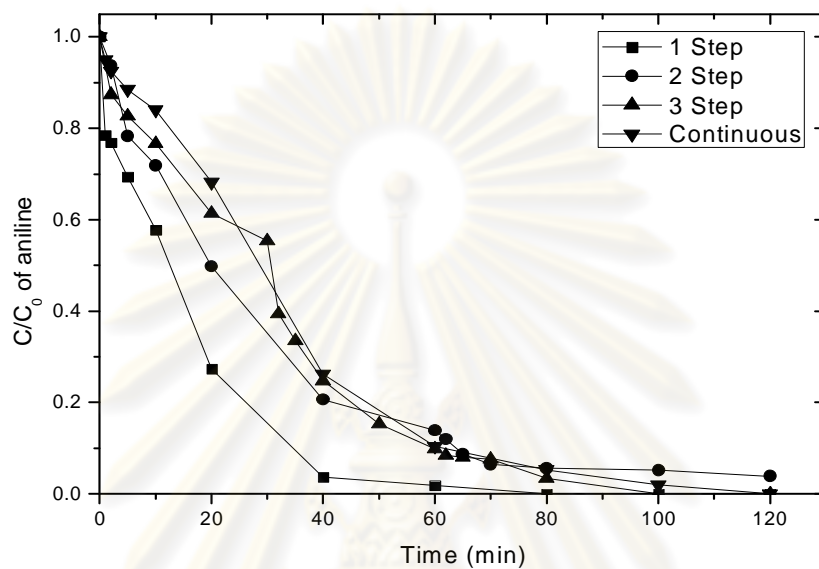


Figure 4.11 Effects of H_2O_2 of stepwise addition during electro-Fenton process at 10 mM of aniline, 1.25 mM of Fe^{2+} , 72 mM of H_2O_2 , pH 2 and current 2 A.

Table 4.9 COD removal efficiency versus number of feeding at 10 mM of aniline, 1.25 mM of Fe^{2+} , 72 mM of H_2O_2 , pH 2 and current 2 A.

Number of Feedings	COD removal efficiency (%)
1	55.17
2	55.61
3	58.52
Continuous	61.27

4.4.2 Effect of Current-Supply Delay on Electro-Fenton Process

Additional experiments were conducted by allowing the reaction to proceed through the ordinary Fenton process at the beginning stage for some certain periods of 20, 40, 60, 80 min before the electrical current was applied into the solution to initiate the electro-Fenton process as shown in Table 3.6. The results from this delay operation are shown in Figure 4.14. Aniline and COD were degraded much more rapidly when the power supply had been switched on. This enhancement was due to the acceleration in Fe^{2+} regeneration by electrochemical reduction in reaction 2.15. From aniline and COD profiles in Figure 4.14, it is possible to maintain the degradation efficiencies of aniline and COD with 20 minutes delay in current supply.. This current supply delay can reduce the power consumption and sequentially decrease the energy cost. Figure 4.15 showed that Fe^{2+} concentration increased and H_2O_2 decreased after switched on the current. This is because of Fe^{2+} regeneration by electrochemical reduction to produce the $\bullet\text{OH}$.

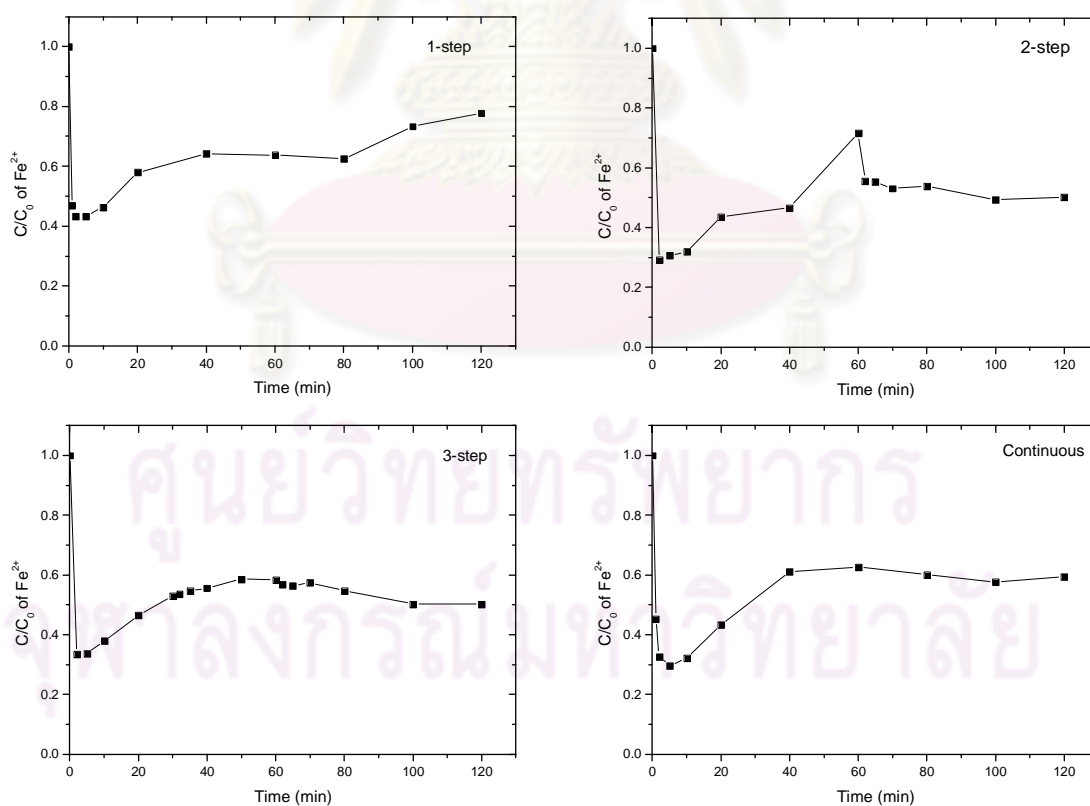


Figure 4.12 Profile of Fe^{2+} of H_2O_2 stepwise addition during electro-Fenton process at 10 mM of aniline, 1.25 mM of Fe^{2+} , 72 mM of H_2O_2 , pH 2 and current 2 A.

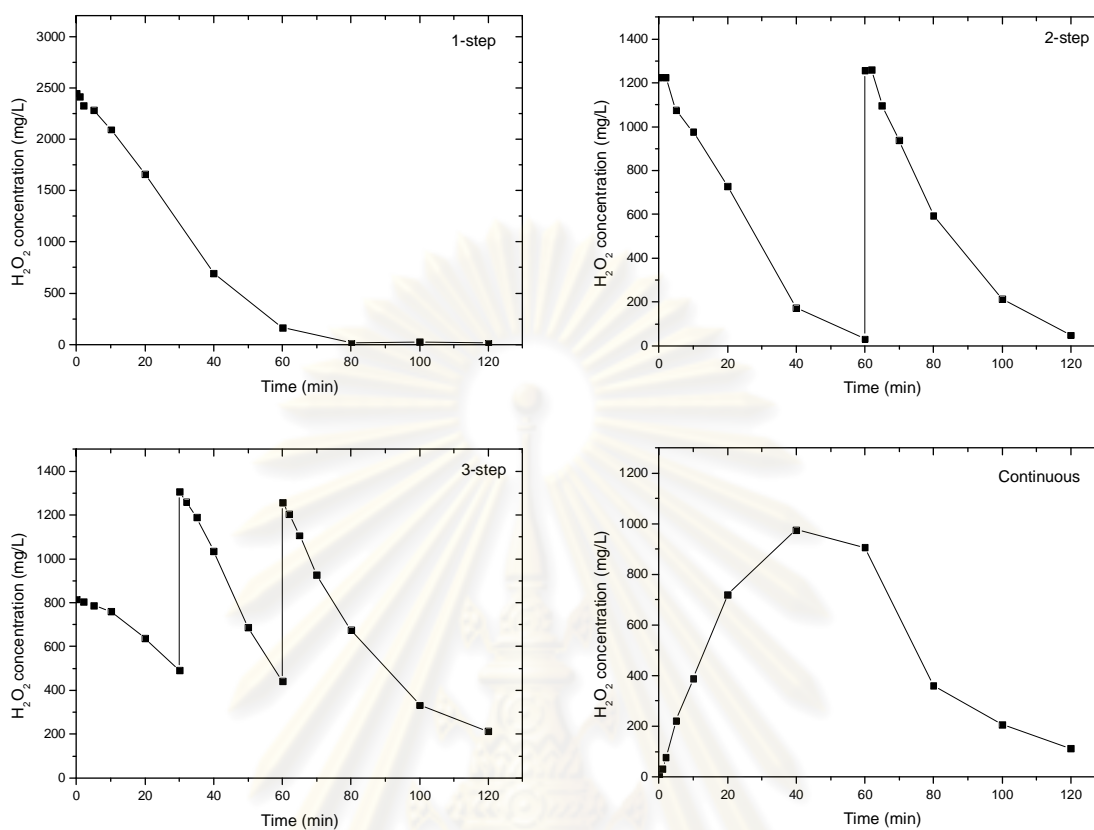


Figure 4.13 Profile of H_2O_2 of H_2O_2 stepwise addition during electro-Fenton process at 10 mM of aniline, 1.25 mM of Fe^{2+} , 72 mM of H_2O_2 , pH 2 and current 2 A.

ศูนย์วิทยทรัพยากร
จุฬาลงกรณ์มหาวิทยาลัย

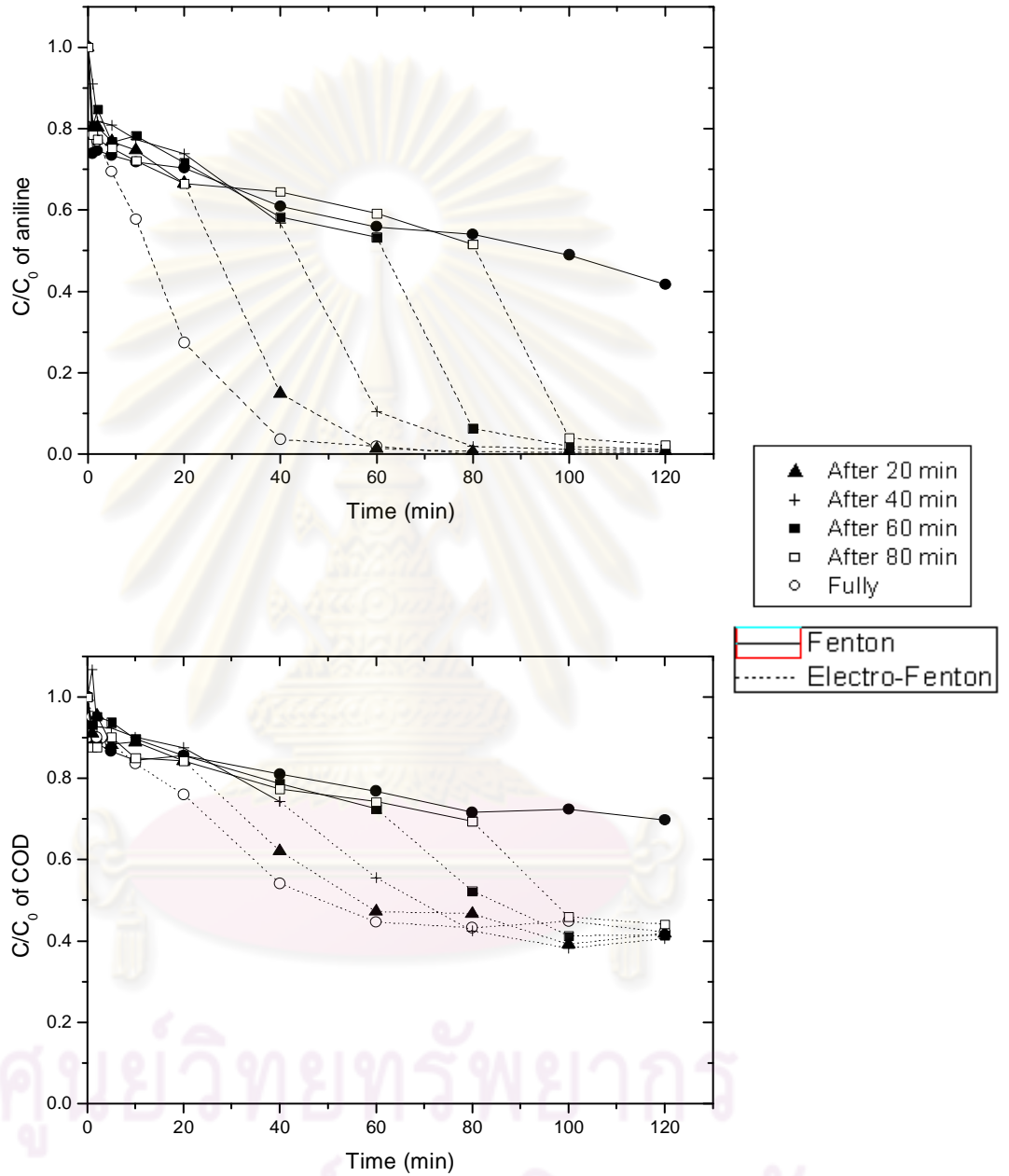


Figure 4.14 Effects of electrical discharging time at 10 mM of aniline, 1.25 mM of Fe^{2+} , 72 mM of H_2O_2 , pH 2 and current 2 A.

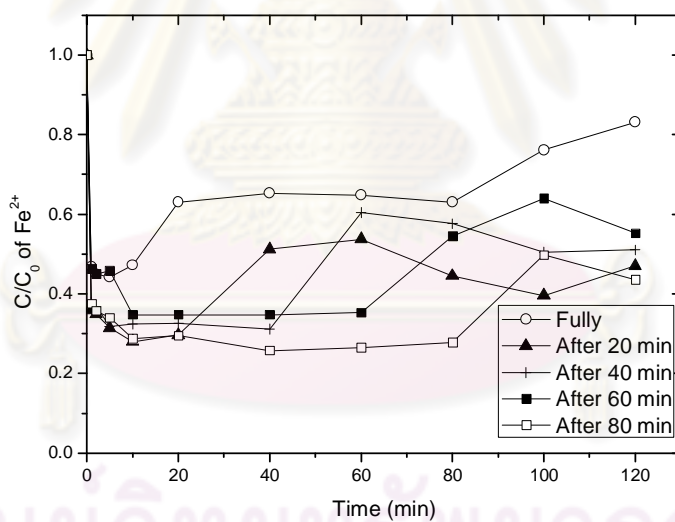
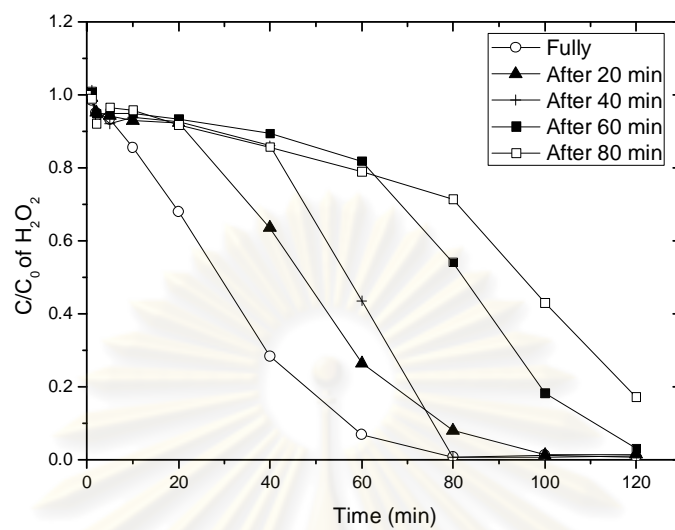


Figure 4.15 Profile of Fe²⁺ and H₂O₂ on effects of electrical discharging time at 10 mM of aniline, 1.25 mM of Fe²⁺, 72 mM of H₂O₂, pH 2 and current 2 A.

4.5 Pathway of aniline degradation

From the result of aniline and COD reductions by electro-Fenton process, it was observed that the COD removal efficiency was often lower than that of aniline degradation. Figure 4.16, as an example, shows only 60% removal of COD could be achieved whereas aniline was removed completely. In addition, little loss of TOC (30%) was noted during the electro-Fenton process indicating that aniline converted mainly to the intermediate products and complete mineralization did not occur. The degradation products of aniline included primary products (such as benzoquinonimine, benzoquinone, phenol, hydroquinone and nitrobenzene), more oxidized products (such as benzenetriol, maleic acid and oxalic acid), and the final product products (CO_2 and water) as shown in Figure 4.17 (Brillas et al., 1998; Sauleda and Brillas, 2001; Brillas and Casado, 2002). In this study, final samples were checked for some intermediates such as nitrobenzene, maleic acid and oxalic acid as shown in Figures 4.18 and 4.19. The results confirmed that aniline could not be completely oxidized to carbon dioxide and water during the reaction period but rather transformed to some intermediates which have similar or comparable COD as aniline itself. According to Figures 4.18 and 4.19, it indicates that the destruction of nitrobenzene from aniline degradation yielded maleic and oxalic acids.

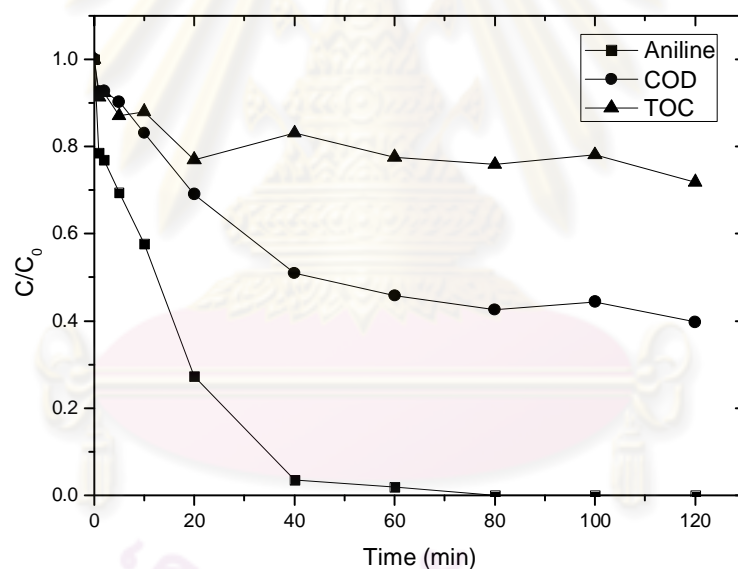


Figure 4.16 Aniline, COD and TOC removal by electro-Fenton process at the optimum condition.

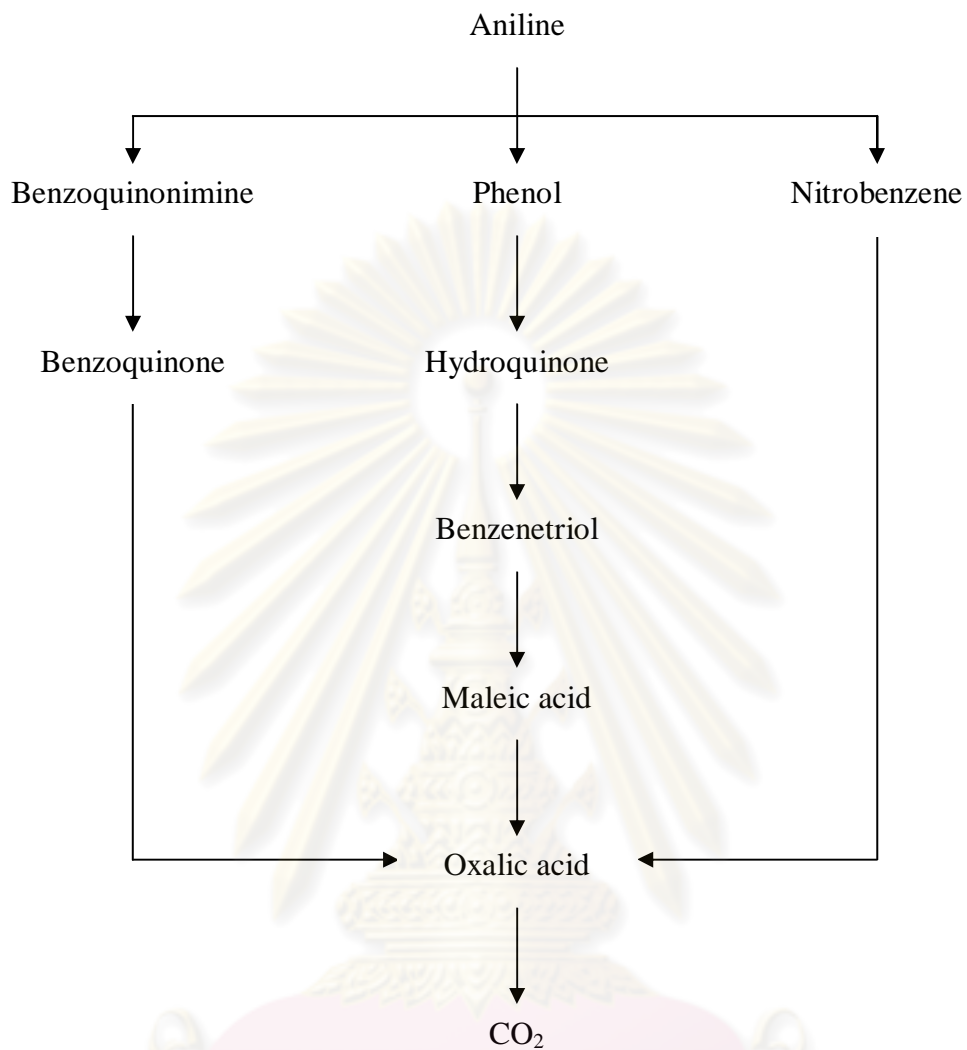


Figure 4.17 The degradation pathway of aniline by radical oxidation.

ศูนย์วิทยทรัพยากร
จุฬาลงกรณ์มหาวิทยาลัย

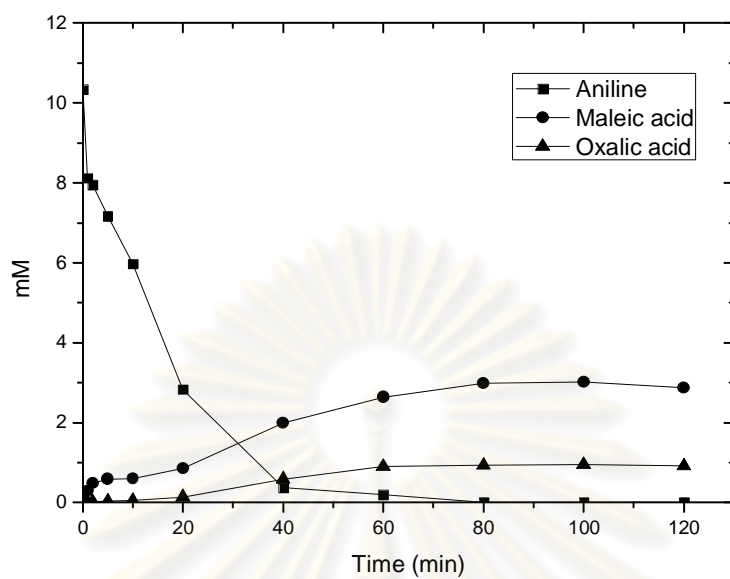


Figure 4.18 Formation of oxalic and maleic acids in electro-Fenton process at the optimum condition.

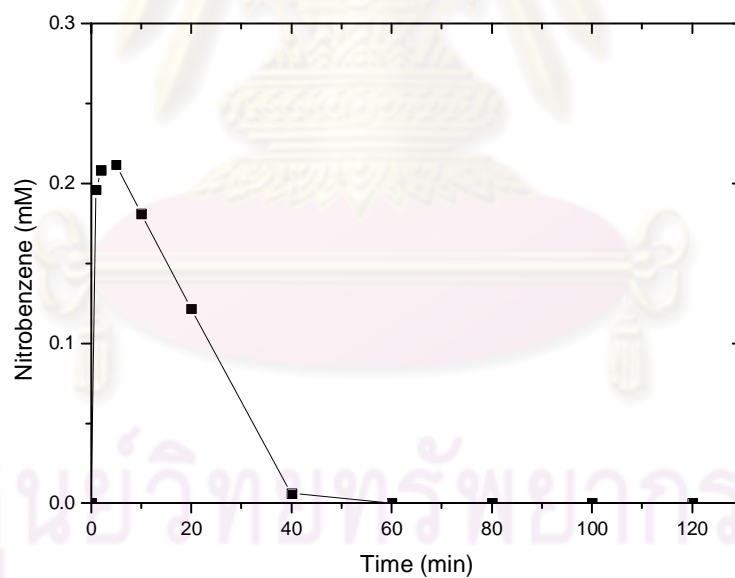


Figure 4.19 Formation of nitrobenzene in electro-Fenton process at the optimum condition.

4.6 Economic Considerations

According to the results, electro-Fenton process could remove 10 mM of aniline in 60 minutes whereas ordinary Fenton could only remove 60% in 120 minutes (electro-Fenton process required only 20 minutes to achieve 60% removal). This implies that the reactor for electro-Fenton can be 6 times smaller than that of ordinary Fenton process which will reduce the construction cost for the treatment unit. However, electrical devices are needed to install in electro-Fenton reactor to supply the current which will increase the capital cost of the process. In addition, the operating cost for electro-Fenton process will also be higher than the ordinary Fenton process. Therefore, it is important to compare the overall cost for these two processes before making the decision regarding on process selection. Furthermore, this study also proved that the delay of current supply could save energy consumption while maintain the system performance, e.g., one-third of the power could be reduced in this study. This suggests that modification of current supply time is a worth practice and should be taken into the account for electro-Fenton operation.



ศูนย์วิทยทรัพยากร
จุฬาลงกรณ์มหาวิทยาลัย

CHAPTER IV

CONCLUSIONS

5.1 Conclusions

The following conclusions were obtained from this study:

- Under similar chemical dosages, electro-Fenton process decomposed aniline and COD and its oxidation products much more rapidly and effectively than conventional Fenton and electrolysis due to the acceleration in Fe^{2+} regeneration at the cathode which promoted the $\bullet\text{OH}$ production rate.
- Two levels of factorial design and Box-Behnken design were effective tools to determine the significant parameters and predict the optimum conditions to maximize the process performance.
- Under the studied conditions, Fe^{2+} , H_2O_2 , and pH were found to be the key factors on the aniline and COD removals. Aniline and COD removals improved with increasing H_2O_2 , Fe^{2+} and pH.
- Optimum Fe^{2+} , H_2O_2 and pH for process performance were 1.79 mM, 72 mM and 2 for, respectively. Under these conditions, aniline and COD could be removed up to 100 and 57.12%, respectively.
- The empirical relationships between the aniline and COD removals and the independent variables could be estimated by cubic and quadratic polynomials, respectively, as shown in the following equations:

$$\begin{aligned} \text{Aniline removal} = & +95.80 + 3.19X_1 + 3.52X_2 - 2.43X_3 + \\ & 0.72 X_1X_2 + 0.095 X_1X_3 - 0.98 X_2X_3 - \\ & 0.93X_1^2 - 1.84X_2^2 - 0.89X_3^2 - 1.84X_1^2X_2 \\ & + 5.17X_1^2X_3 + 1.38 X_1X_2^2 \end{aligned}$$

$$\begin{aligned} \text{COD removal} = & +51.81 + 10.82X_1 + 2.06X_2 + 0.42X_3 + \\ & 4.48X_1X_2 - 0.29X_1X_3 - 1.26 X_2X_3 - \\ & 2.96X_1^2 + 0.015X_2^2 + 2.40X_3^2 \end{aligned}$$

Where: X_1 , X_2 , and X_3 are the concentrations of H_2O_2 and Fe^{2+} and pH, respectively.

- The initial delay in electrical current supply in electro-Fenton process could provide a possibility in reducing power consumption. This energy saving leads to the reduction in operating cost.
- Continuous and stepwise additions of H_2O_2 were sequentially more effective than one single step addition regarding on aniline and COD removals.

5.2 Future Works

- Investigate the effect of cathode and anode materials and surface area on the degradation of aniline and compare result on this study.
- Determine the effect of distance between electrodes in the degradation of aniline.
- Investigate into more details on the effect of feeding modes of Fe^{2+} and at the same time.



ศูนย์วิทยทรัพยากร
จุฬาลงกรณ์มหาวิทยาลัย

REFERENCES

- Abdessalem, A. K., Oturan, N., Bellakhal, N., Dachraoui, M., and Oturan, M. A. 2008. Experimental design methodology applied to electro-Fenton treatment for degradation of herbicide chlortoluron. Applied Catalysis B: Environmental **78**(3-4): 334-341.
- Anotai, J., Lu, M. C., and Chewprecha, P. 2006. Kinetics of aniline degradation by Fenton and electro-Fenton processes. Water Research **40**(9): 1841-7.
- Aoki, K., Shinke, R., and Nishira, H. 1983. Metabolism of Aniline by *Rhodococcus erythropolis* AN-13. Agricultural Biological Chemistry **47**(7): 1611-1616.
- APHA. 1992. Standard Methods for the Examination of Water and Wastewater. 18th Washington D.C.: American Public Health Association.
- Argun, M. E., Dursun, S., Karatas, M., and Gürü, M. 2008. Activation of pine cone using Fenton oxidation for Cd(II) and Pb(II) removal. Bioresource Technology **99**(18): 8691-8698.
- Arslan-Alaton, I., Tureli, G., and Olmez-Hanci, T. 2009. Treatment of azo dye production wastewaters using Photo-Fenton-like advanced oxidation processes: Optimization by response surface methodology. Journal of Photochemistry and Photobiology A: Chemistry **202**(2-3): 142-153.
- Atmaca, E. 2009. Treatment of landfill leachate by using electro-Fenton method. Journal of Hazardous Materials **163**(1): 109-114.
- Ay, F., Catalkaya, E. C., and Kargi, F. 2009. A statistical experiment design approach for advanced oxidation of Direct Red azo-dye by photo-Fenton treatment. Journal of Hazardous Materials **162**(1): 230-6.
- Badawy, M. I., Ghaly, M. Y., and Gad-Allah, T. A. 2006. Advanced oxidation processes for the removal of organophosphorus pesticides from wastewater. Desalination **194**(1-3): 166-175.
- Behnajady, M. A., Modirshahla, N., and Ghanbary, F. 2007. A kinetic model for the decolorization of C.I. Acid Yellow 23 by Fenton process. Journal of Hazardous Materials **148**(1-2): 98-102.
- Beltran, F. J., Encinar, J. M., and Alonso, M. A. 1998. Nitroaromatic hydrocarbon ozonation in water. 2. Combined ozonation with hydrogen peroxide or UV radiation. Industrial and Engineering Chemistry Research **37**: 32-40.
- Bezerra, M. A., Santelli, R. E., Oliveira, E. P., Villar, L. S., and Escalera, L. A. 2008. Response surface methodology (RSM) as a tool for optimization in analytical chemistry. Talanta **76**(5): 965-977.
- Boopathy, R. 2000. Factors limiting bioremediation technologies. Bioresource Technology **74**(1): 63-67.
- Boye, B., Dieng, M. M., and Brillas, E. 2003. Anodic oxidation, electro-Fenton and photoelectro-Fenton treatments of 2,4,5-trichlorophenoxyacetic acid. Journal of Electroanalytical Chemistry **557**: 135-146.
- Brillas, E., Baños, M. A., and Garrido, J. A. 2003. Mineralization of herbicide 3,6-dichloro-2-methoxybenzoic acid in aqueous medium by anodic oxidation, electro-Fenton and photoelectro-Fenton. Electrochimica Acta **48**(12): 1697-1705.
- Brillas, E., et al. 2007. Degradation of the herbicide 2,4-DP by anodic oxidation, electro-Fenton and photoelectro-Fenton using platinum and boron-doped diamond anodes. Chemosphere **68**(2): 199-209.

- Brillas, E., et al. 2004. Electrochemical destruction of chlorophenoxy herbicides by anodic oxidation and electro-Fenton using a boron-doped diamond electrode. Electrochimica Acta **49**(25): 4487-4496.
- Brillas, E., and Casado, J. 2002. Aniline degradation by Electro-Fenton^o and peroxi-coagulation processes using a flow reactor for wastewater treatment. Chemosphere **47**(3): 241-2148.
- Brillas, E., et al. 1998. Aniline mineralization by AOP's: anodic oxidation, photocatalysis, electro-Fenton and photoelectro-Fenton processes. Applied Catalysis B: Environmental **16**(1): 31-42.
- Celebi, N., Yildiz, N., Demair, A. S., and Calimli, A. 2008. Optimization of benzoin synthesis in supercritical carbon dioxide by response surface methodology (RSM). The Journal of Supercritical Fluids **47**(2): 227-232.
- Chen, S., Sun, D., and Chung, J. S. 2007. Anaerobic treatment of highly concentrated aniline wastewater using packed-bed biofilm reactor. Process Biochemistry **42**(12): 1666-1670.
- Chu, W., Chan, K. H., Kwan, C. Y., and Choi, K. Y. 2007. Degradation of atrazine by modified stepwise-Fenton's processes. Chemosphere **67**(4): 755-61.
- Cojocar, C., and Zakrzewska-Trznadel, G. 2007. Response surface modeling and optimization of copper removal from aqua solutions using polymer assisted ultrafiltration Journal of Membrane Science **20**(1-2): 56-70.
- Comninellis, C., and Pulgarin. 1991. Anodic oxidation of phenol for waste water treatment. Journal of Applied Electrochemistry **21**(8): 703-708.
- Daneshvar, N., Aber, S., Vatanpour, V., and Rasoulifard, M. H. 2008. Electro-Fenton treatment of dye solution containing Orange II: Influence of operational parameters. Journal of Electroanalytical Chemistry **615**(2): 165-174.
- Eisenberg, G. 1943. Colorimetric determination of hydrogen peroxide. Industrial and Engineering Chemistry, Analytical Edition **15**(5): 327-328.
- Faria, P. C., Orfao, J. J., and Pereira, M. F. 2007. Ozonation of aniline promoted by activated carbon. Chemosphere **67**(4): 809-15.
- Farre, M. J., Domenech, X., and Peral, J. 2006. Assessment of photo-Fenton and biological treatment coupling for Diuron and Linuron removal from water. Water Research **40**(13): 2533-40.
- Ferreira, S. L., et al. 2007. Box-Behnken design: an alternative for the optimization of analytical methods. Anal Chim Acta **597**(2): 179-86.
- Flox, C., et al. 2006. Electro-Fenton and photoelectro-Fenton degradation of indigo carmine in acidic aqueous medium. Applied Catalysis B: Environmental **67**(1-2): 93-104.
- Fockedey, E., and Lierde, A. V. 2002. Coupling of anodic and cathodic reactions for phenol electro-oxidation using three-dimensional electrodes. Water Research **36**(16): 4169-4175.
- Fukushima, M., Tatsumi, K., and Morimoto, K. 2000. The fate of aniline after a photo-Fenton reaction in an aqueous system containing iron(III), humic acid, and hydrogen peroxide. Environmental Science and Technology **34**(10): 2006-2013.
- Gözmen, B., Oturan, M. A., Oturan, N., and Erbatur, O. 2003. Indirect electrochemical treatment of bisphenol A in water via electrochemically generated Fenton's reagent. Environ Sci Technol **37**(16): 3716-23.

- Guinea, E., et al. 2008. Mineralization of salicylic acid in acidic aqueous medium by electrochemical advanced oxidation processes using platinum and boron-doped diamond as anode and cathodically generated hydrogen peroxide. Water Research **42**(1-2): 499-511.
- Güven, G., Perendeci, A., and Tanyolac, A. 2008. Electrochemical treatment of deproteinated whey wastewater and optimization of treatment conditions with response surface methodology. Journal of Hazardous Materials **157**(1): 69-78.
- Hanrahan, G., and Lu, K. 2006. Application of factorial and response surface methodology in modern experimental design and optimization. Critical Reviews in Analytical Chemistry **36**: 141-151.
- Huang, C.P., Dong, C., and Tang, Z. 1993. Advanced chemical oxidation: its present role and potential future in hazardous waste treatment. Waste Management **13** (5-7): 361-377.
- Huang, Y. H., Chen, C. C., Huang, G. H., and Chou, S. S. 2001. Comparison of a novel electro-Fenton method with Fenton's reagent in treating a highly contaminated wastewater. Water Sci Technol **43**(2): 17-24.
- Huang, Y. H., Huang, Y. F., Chang, P. S., and Chen, C. Y. 2008. Comparative study of oxidation of dye-Reactive Black B by different advanced oxidation processes: Fenton, electro-Fenton and photo-Fenton. Journal of Hazardous Materials **154**(1-3): 655-62.
- Irmak, S., Yavuz, H. I., and Erbatur, O. 2006. Degradation of 4-chloro-2-methylphenol in aqueous solution by electro-Fenton and photoelectro-Fenton processes. Applied Catalysis B: Environmental **63**(3-4): 243-248.
- Kang, N., Lee, D. S., and Yoon, J. 2002. Kinetic modeling of fenton oxidation of phenol and monochlorophenols. Chemosphere **47**(9): 915-24.
- Kang, Y. W., and Hwang, K. Y. 2000. Effects of reaction conditions on the oxidation efficiency in the Fenton process. Water Research **34**(10): 2786-2790.
- Karunakaran, C., Senthilvelan, S., and Karunathapandian, S. 2005. TiO₂ photocatalyzed oxidation of aniline. Journal of Photochemistry and Photobiology A: Chemistry **172**(2): 207-213.
- Khataee, A. R., Vatanpour, V., and Amani, A. R. 2009. Decolorization of C.I. Acid Blue 9 Solution by UV/Nano-TiO₂, Fenton, Fenton-like, Electro-Fenton and Electrocoagulation Processes: A Comparative Study. Journal of Hazardous Materials **161**(2-3): 1225-1233.
- Khattar, J. I. S., and Shailza. 2009. Optimization of Cd²⁺ removal by the cyanobacterium *Synechocystis pevalekii* using the response surface methodology. Process Biochemistry **44**(1): 118-121.
- Khayet, M., Cojocar, C., and Zakrzewska-Trznadel, G. 2008. Response surface modelling and optimization in pervaporation. Journal of Membrane Science **321**(2): 272-283.
- Lin, S. H., and Chang, C. C. 2000. Treatment of landfill leachate by combined electro-Fenton oxidation and sequencing batch reactor method. Water Research **34**(17): 4243-4249.
- Liou, M. J., and Lu, M. C. 2008. Catalytic degradation of explosives with goethite and hydrogen peroxide. Journal of Hazardous Materials **151**(2-3): 540-6.
- Liou, M. J., Lu, M. C., and Chen, J. N. 2004. Oxidation of TNT by photo-Fenton process. Chemosphere **57**(9): 1107-1114.

- Liu, H., et al. 2007. A novel electro-fenton process for water treatment: Reaction-controlled pH adjustment and performance assessment. Environ. Sci. Technol **41**(8): 2937-2942.
- Liu, Z., Yang, H., Huang, Z., Zhou, P., and Liu, S. J. 2002. Degradation of aniline by newly isolated, extremely aniline-tolerant *Delftia* sp. AN3. Appl Microbiol Biotechnol **58**(5): 679-82.
- Losito, I., Amorisco, A., and Palmisano, F. 2008. Electro-Fenton and photocatalytic oxidation of phenyl-urea herbicides: An insight by liquid chromatography electrospray ionization tandem mass spectrometry. Applied Catalysis B: Environmental **79**(3): 224-236.
- Lucas, M. S., and Peres, J. A. 2006. Decolorization of the azo dye Reactive Black 5 by Fenton and photo-Fenton oxidation. Dyes and Pigments **71**(3): 236-244.
- Mazellier, P., Rachel, A., and Mambo, V. 2004. Kinetics of benzenesulfonates elimination by UV and UV/H₂O₂. Journal of Photochemistry and Photobiology A: Chemistry **163**(3): 389-393.
- Myers, R. H., and Montgomery, D. C. 2002. Response surface methodology: Process and product optimization using designed experiments Series Editor. U.S.A.: John Wiley & Sons.
- Neyens, E., and Baeyens, J. 2003. A review of classic Fenton's peroxidation as an advanced oxidation technique. Journal of Hazardous Materials **98**(1-3).
- O'Neill, F. J., Bromley-Challenor, K. C. A., Greenwood, R. J., and Knapp, J. S. 2000. Bacterial growth on aniline: Implications for the biotreatment of industrial wastewater. Water Research **34**(18): 4397-4409.
- Oh, K., and Kim, Y. 1998. Degradation of explosive 2,4,6-trinitrotoluene by s-triazine degrading bacterium isolated from contaminated soil. Bull Environ Contam Toxicol **61**(6): 702-708.
- Ölmez, t. 2009. The optimization of Cr(VI) reduction and removal by electrocoagulation using response surface methodology. Journal of Hazardous Materials **162**(2-3): 1371-1378.
- Oturan, M. A. 2000. An ecologically effective water treatment technique using electrochemically generated hydroxyl radicals for in situ destruction of organic pollutants: Application to herbicide 2,4-D. Journal of Applied Electrochemistry **30**: 475-482.
- Oturan, M. A., Oturan, N., Lahitte, C., and Trevin, S. 2001. Production of hydroxyl radicals by electrochemically assisted Fenton's reagent Application to the mineralization of an organic micropollutant, pentachlorophenol. Journal of Electroanalytical Chemistry **507**(1-2): 96-102.
- Oturan, M. A., Peiroten, J., Chartrin, P., and Acher, A. J. 2000. Complete destruction of p-nitrophenol in aqueous medium by electro-Fenton method. Environmental Science and Technology **34**(16): 3474-3479.
- Ozcan, A., Sahin, Y., Kopal, A. S., and Oturan, M. A. 2008. Degradation of picloram by the electro-Fenton process. J Hazard Mater **153**(1-2): 718-27.
- Panizza, M., and Cerisola, G. 2001. Removal of organic pollutants from industrial wastewater by electrogenerated Fenton's reagent. Water Research **35**(16): 3987-92.
- Panizza, M., and Cerisola, G. 2009. Electro-Fenton degradation of synthetic dyes. Water Research **43**(2): 339-44.
- Pera-Titus, M., Garcia-Molina, V., Baños, M. Z., Giménez, J., and Esplugas, S. 2004. Degradation of chlorophenols by means of advanced oxidation

- processes: a general review. Applied Catalysis B: Environmental **47**(4): 219-256.
- Pozzo, A. D., Palma, L. D., Merli, C., and Petrucci, E. 2005. An experiment comparison of a graphite electrode and a gas diffusion electrode for the the cathodic production of hydrogen peroxide. Journal of Applied Electrochemistry **35**(4): 413-419.
- Prakash, O., Talat, M., and Hasan, S. H. 2009. Response surface design for the optimization of enzymatic detection of mercury in aqueous solution using immobilized urease from vegetable waste. Journal of Molecular Catalysis B: Enzymatic **56**(4): 265-271.
- Qiang, Z., Chang, J. H., and Huang, C. P. 2002. Electrochemical generation of hydrogen peroxide from dissolved oxygen in acidic solutions. Water Research **36**(1): 85-94.
- Qiang, Z., Chang, J. H., and Huang, C. P. 2003. Electrochemical regeneration of Fe^{2+} in Fenton oxidation processes. Water Research **37**(6): 1308-1319.
- Rahulan, R., Nampoothiri, K. M., Szakacs, G., Nagy, V., and Pandey, A. 2009. Statistical optimization of l-leucine amino peptidase production from *Streptomyces gedanensis* IFO 13427 under submerged fermentation using response surface methodology. Biochemical Engineering Journal **43**(1): 64-71.
- Romantschuk, M., et al. 2000. Means to improve the effect of in situ bioremediation of contaminated soil: an overview of novel approaches. Environ Pollut **107**(2): 179-85.
- Sánchez-Sánchez, C. M., Expósito, E., Casado, J., and montiel, V. 2007. Goethite as a more effective iron dosage source for mineralization of organic pollutants by electro-Fenton process. Electrochemistry Communications **9**(1): 19-24.
- Sánchez, L., Peral, J., and Domènech, X. 1998. Aniline degradation by combined photocatalysis and ozonation. Applied Catalysis B: Environmental **19**(1).
- Sarasa, J., Cortes, S., Ormad, P., Gracia, R., and Ovelleiro, J. L. 2002. Study of the aromatic by-products formed from ozonation of anilines in aqueous solution. Water Research **36**(12): 3035-44.
- Sauleda, R., and Brillas, E. 2001. Mineralization of aniline and 4-chlorophenol in acidic solution by ozonation catalyzed with Fe^{2+} and UVA light. Applied Catalysis B: Environmental **29**(2): 135-145.
- Secula, M. S., Suditu, G. D., Poullos, I., Cojocar, C., and Cretescu, I. 2008. Response surface optimization of the photocatalytic decolorization of a simulated dyestuff effluent. Chemical Engineering Journal **141**(1-3): 18-26.
- Segura, C., Zaror, C., Mansilla, H. D., and Mondaca, M. A. 2008. Imidacloprid oxidation by photo-Fenton reaction. Journal of Hazardous Materials **150**(3): 679-86.
- Sellers, R. M. 1980. Spectrophotometric determination of hydrogen peroxide using potassium titanium (IV) oxalate. The Analyst **105**(1255): 950-954.
- Shang, N. C., et al. 2007. Oxidation of methyl methacrylate from semiconductor wastewater by O_3 and O_3/UV processes. Journal of Hazardous Materials **147**(1-2): 307-12.
- Silva, M. R. A., Trovó, A. G., and Nogueira, R. F. P. 2007. Treatment of 1,10-phenanthroline laboratory wastewater using the solar photo-Fenton process. Journal of Hazardous Materials **146**(3): 508-513.

- Son, H. S., Lee, S. J., Cho, I. H., and Zoh, K. D. 2004. Kinetics and mechanism of TNT degradation in TiO₂ photocatalysis. Chemosphere **57**(4): 309-317.
- Sun, J. H., et al. 2008. Oxidative decomposition of p-nitroaniline in water by solar photo-Fenton advanced oxidation process. Journal of Hazardous Materials **153**(1-2): 187-93.
- Tavares, A. P., Cristovao, R. O., Loureiro, J. M., Boaventura, R. A., and Macedo, E. A. 2009. Application of statistical experimental methodology to optimize reactive dye decolourization by commercial laccase. Journal of Hazardous Materials **162**(2-3): 1255-60.
- Ting, W. P., Lu, M. C., and Huang, Y. H. 2008. The reactor design and comparison of Fenton, electro-Fenton and photoelectro-Fenton processes for mineralization of benzene sulfonic acid (BSA). Journal of Hazardous Materials **156**(1-3): 421-427.
- Ting, W. P., Lu, M. C., and Huang, Y. H. 2009. Kinetics of 2,6-dimethylaniline degradation by electro-Fenton process. Journal of Hazardous Materials **161**(2-3): 1484-1490.
- U.S.EPA. 1994. Aniline fact sheet: Support document (CAS No. 62-53-3)[Online]. Available from: <http://epa.gov/chemfact/anali-sd.pdf>[2008, August 10].
- Ventura, A., Jacquet, G., Bermond, A., and Camel, V. 2002. Electrochemical generation of the Fenton's reagent: application to atrazine degradation. Water Research **36**(14): 3517-22.
- Vidali, M. 2001. Bioremediation. An overview. Pure Appl. Chem. **73**(7): 1163-1172.
- Wang, A., Qu, J., Ru, J., Liu, H., and Ge, J. 2005. Mineralization of an azo dye Acid Red 14 by electro-Fenton's reagent using an activated carbon fiber cathode. Dyes and Pigments **65**(3): 227-233.
- Wang, C. T., Hu, J. L., Chou, W. L., and Kuo, Y. M. 2008. Removal of color from real dyeing wastewater by Electro-Fenton technology using a three-dimensional graphite cathode. Journal of Hazardous Materials **152**(2): 601-6.
- Wenhua, L., Hong, L., Sao'an, C., Jianqing, Z., and Chunan, C. 2000. Kinetics of photocatalytic degradation of aniline in water over TiO₂supported on porous nickel. Journal of Photochemistry and Photobiology A: Chemistry **131**(1-3): 125-132.
- Wu, Y., Zhao, C., and Wang, Q., and Ding, K. 2006. Integrated effects of selected ions on 2,4,6-trinitrotoluene-removal by O₃/H₂O₂. Journal of Hazardous Materials **132**(2-3): 232-236.
- Zhang, H., Choi, H. J., Canazo, P., and Huang, C. P. 2009. Multivariate approach to the Fenton process for the treatment of landfill leachate. Journal of Hazardous Materials **161**(2-3): 1306-12.
- Zhang, H., Choi, H. J., and Huang, C. P. 2005. Optimization of Fenton process for the treatment of landfill leachate. Journal of Hazardous Materials **125**(1-3): 166-74.
- Zhang, H., Fei, C., Zhang, D., and Tang, F. 2007. Degradation of 4-nitrophenol in aqueous medium by electro-Fenton method. Journal of Hazardous Materials **145**(1-2): 227-32.
- Zhang, H., Zhang, D., and Zhou, J. 2006. Removal of COD from landfill leachate by electro-Fenton method. Journal of Hazardous Materials **135**(1-3): 106-111.

- Zhou, M., Yu, Q., and Lei, L. 2008. The preparation and characterization of a graphite-PTFE cathode system for the decolorization of C.I. Acid Red 2. Dyes and Pigments **77**(1): 129-136.
- Zhou, M., Yu, Q., Lei, L., and Barton, G. 2007. Electro-Fenton method for the removal of methyl red in an efficient electrochemical system. Separation and Purification Technology **57**(2): 380-387.
- Zhuang, R., et al. 2007. Isolation and characterization of aniline-degrading *Rhodococcus* sp. strain AN5. J Environ Sci Health A Tox Hazard Subst Environ Eng **42**(13): 2009-16.
- Zoh, K. D., and Stenstrom, M. K. 2002. Fenton oxidation of hexahydro-1,3,5-trinitro-1,3,5-triazine (RDX) and octahydro-1,3,5,7-tetranitro-1,3,5,7-tetrazocine (HMX). Water Research **36**(5): 1331-1341.



ศูนย์วิทยทรัพยากร
จุฬาลงกรณ์มหาวิทยาลัย



APPENDICES

ศูนย์วิทยทรัพยากร
จุฬาลงกรณ์มหาวิทยาลัย



APPENDIX A

**Analytical Method for Aniline by GC
and
Analytical Method for Hydrogen Peroxide (H₂O₂)
(Potassium Titanium Oxalate/Spectrophotometric)**

ศูนย์วิทยทรัพยากร
จุฬาลงกรณ์มหาวิทยาลัย

**A.1 Analytical Method for Aniline by GC
Condition
(Oven Program)**

- Initial temperature: 85 °C
- Initial time: 1.60 min
- Flow rate 13.6-14.6 ml/min
- Sample volume 1 µl.

Table A1 GC condition of oven program

	Rate (°C/min)	Final temperature (°C)	Final time (min)
Level 1	65.0	200	1.00
Level 2 (A)	0.0	-	-
Level 3 (B)	-	-	-
			4.37

ศูนย์วิทยทรัพยากร
จุฬาลงกรณ์มหาวิทยาลัย

A.2 Analysis of Hydrogen Peroxide

Principle

Hydrogen peroxide reacted with potassium titanium oxalate in acid solution to form the yellow to orange pertitanic acid complex as $\text{TiO}_2 \cdot \text{H}_2\text{O}_2$, showing a true peroxide structure. The colored complex is measured spectrophotometrically at 400 nm. The reaction is usually written:



Scope of Application

This method is suitable for the determination of hydrogen peroxide in aqueous effluents and raw sewage in the range 0.1 - 50 mg/L as H_2O_2 .

Interferences

Formation of the peroxotitanium complex is specific to hydrogen peroxide. However, wastewaters possessing a strong yellow background color may affect accuracy. Normal background color can be reduced by filtering the sample, or compensated for by zeroing out a blank of unreacted sample. The method includes a flocculation pretreatment step to remove suspended matter – the AlCl_3 - NaOH pretreatment step may be omitted when analyzing clear waters.

Safety Precautions

Potassium titanium (IV) oxalate ($\text{K}_2\text{TiO}(\text{C}_2\text{O}_4)_2 \cdot 2\text{H}_2\text{O}$) is a toxic material and should be handled and disposed of in accordance with the MSDS. Neoprene gloves and monogoggles are recommended.

Concentrated sulfuric acid and sodium hydroxide are corrosive, hazardous materials and should be handled and disposed of in accordance with the MSDS. Neoprene gloves and monogoggles are recommended, as is working under a vacuum hood.

Sample bottles containing H_2O_2 should not be stopped, but rather vented or covered loosely with aluminum foil or parafin film.

Reagents

All reagents should be of analytical reagent grade unless otherwise stated.

Potassium titanium (IV) oxalate solution.

Mixed 272 ml of concentrated sulfuric acid with about 300 ml of dionized water (care should be taken and cooling is required). Dissolve in this mixture 35.4 g of potassium titanium (IV) oxalate, and make up to 1 l with dionized water.

CAUTION: POTASSIUM TITANIUM OXALATE IS TOXIC AND SOLUTIONS MUST BE HANDLED USING A SAFETY PIPETTE OR BURETTE. SAFETY GOGGLES MUST BE WORN WHEN HANDLING CONCENTRATED SULFURIC ACID.

Apparatus

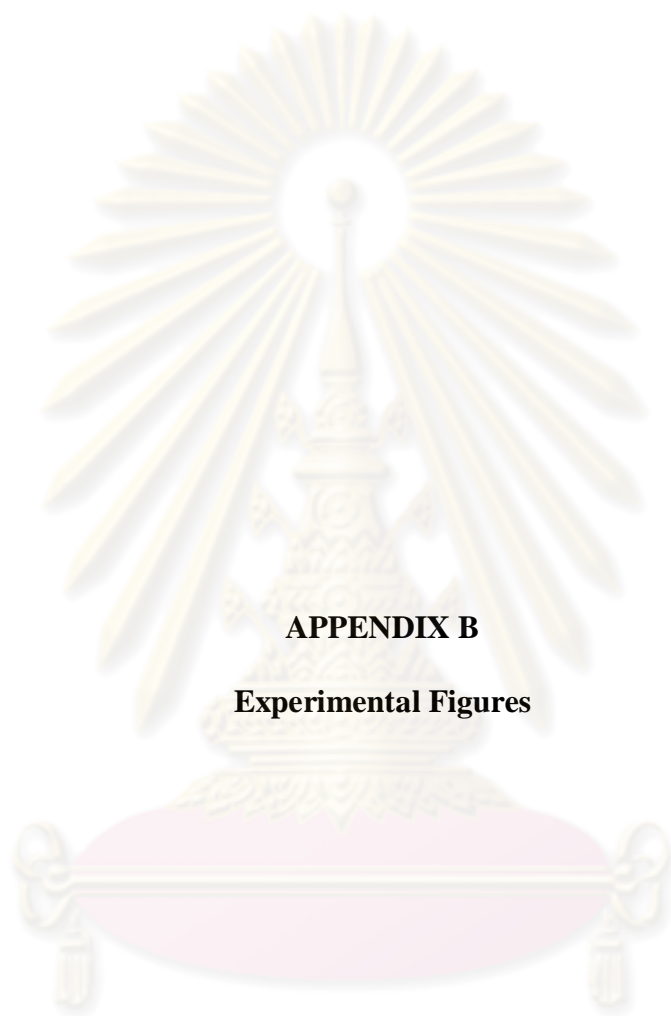
Spectrophotometer capable of measuring absorption at a wavelength of 400 nm and fitted with 10 mm and 40 mm pathlength glass cells.

Procedure

1. Add to volumetric flask 100 ml of deionized water, 5.0 ml of potassium titanium oxalate solution and 1.0 ml of sample.
2. Prepare a reagent blank solution, consisting of 5.0 ml of potassium titanium oxalate solution, 1.0 ml of sample without the hydrogen peroxide present and 1-2 drops of sulfuric acid.
3. Prepare a sample blank solution by adding deionized water, 1.0 ml of sample and 1-2 drops of sulfuric acid.
4. After that it had to stand for 10-30 min, color development was rapid in the presence of potassium titanium oxalate. Measure the absorption of the sample solution, the reagent blank and the sample blank solution as described. Subtract the absorption of the sample blank solution and the absorption of the reagent blank solution from that of the test solution.



ศูนย์วิทยทรัพยากร
จุฬาลงกรณ์มหาวิทยาลัย



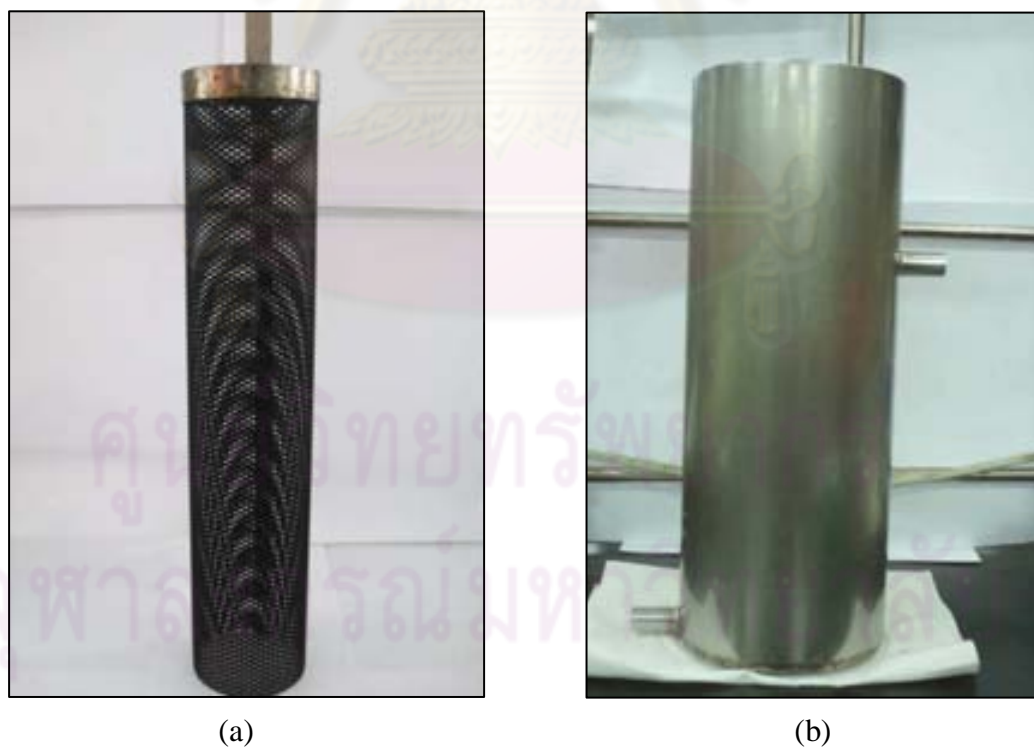
APPENDIX B

Experimental Figures

ศูนย์วิทยทรัพยากร
จุฬาลงกรณ์มหาวิทยาลัย



Figure B.1 Electro-Fenton reactor setup.



(a)

(b)

Figure B.2 Electrodes: (a) anode; and (b) cathode.



(a)



(b)



(c)



(d)

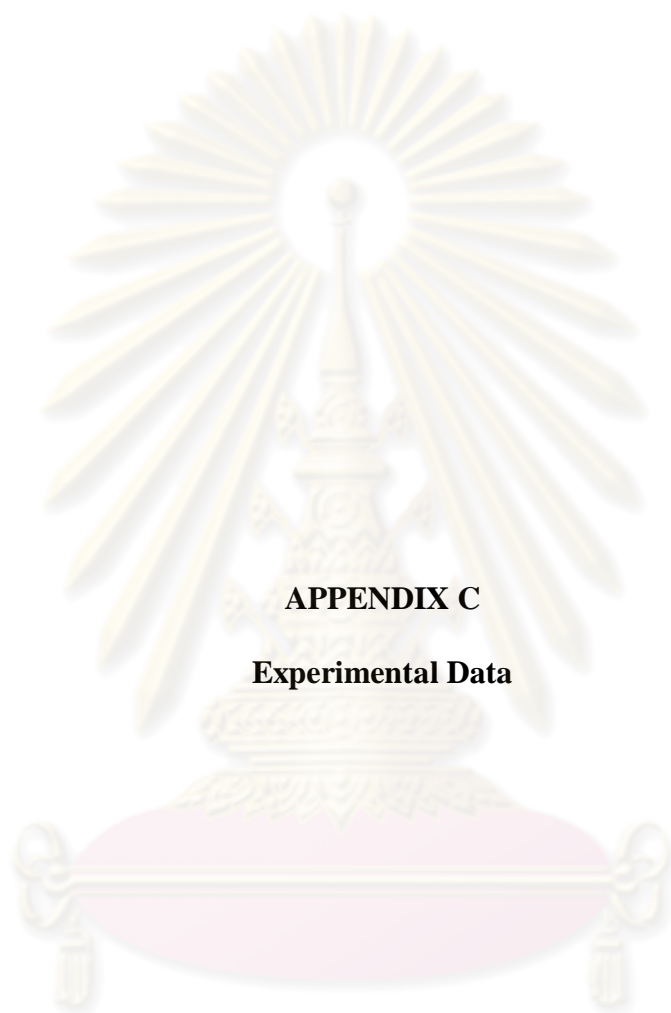


(e)



(f)

Figure B.3 Experimental instruments: (a) GC; (b) COD digestion during experiment; (c) TOC; (d) IC; (e) DC power supply; and (f) pump.



APPENDIX C

Experimental Data

ศูนย์วิทยทรัพยากร
จุฬาลงกรณ์มหาวิทยาลัย

C.1 Experimental data of control experiments

Table C.1.1 Experimental data of aniline by electrolysis, electrolysis with H₂O₂ and electrolysis with Fe²⁺

Time (min)	C/C ₀		
	Electrolysis	Electrolysis + H ₂ O ₂	Electrolysis + Fe ²⁺
0	1.00	1.00	1.00
1	1.00	1.00	1.02
2	1.00	0.99	1.00
5	1.00	0.99	0.96
10	1.00	0.99	0.98
20	0.99	0.99	0.95
40	0.99	0.98	0.96
60	0.99	0.97	0.97
80	0.98	0.97	0.94
100	0.98	0.97	0.93
120	0.98	0.97	0.92

Table C.1.2 Experimental data of COD by electrolysis, electrolysis with H₂O₂ and electrolysis with Fe²⁺

Time (min)	C/C ₀		
	Electrolysis	Electrolysis + H ₂ O ₂	Electrolysis + Fe ²⁺
0	1.00	1.00	1.00
1	0.98	1.01	1.01
2	0.97	0.97	0.97
5	1.00	0.98	0.98
10	1.00	0.98	0.98
20	1.00	0.99	0.96
40	0.97	0.97	0.94
60	0.97	0.96	0.94
80	0.97	0.96	0.94
100	0.97	0.97	0.94
120	0.97	0.97	0.94

ศูนย์วิจัยทรัพยากร
จุฬาลงกรณ์มหาวิทยาลัย

C.2 Experimental data two-level factorial design

Table C.2.1 Experimental data of run 1

Time (min)	C/C ₀			
	Aniline	COD	Fe ²⁺	H ₂ O ₂
0	1.00	1.00	1.00	1.00
1	0.27	0.77	0.66	0.80
2	0.19	0.75	0.62	0.72
5	0.12	0.62	0.46	0.16
10	0.07	0.64	0.48	0.11
20	0.08	0.60	0.50	0.06
40	0.07	0.63	0.54	0.05
60	0.06	0.63	0.53	0.06
80	0.06	0.65	0.50	0.07
100	0.05	0.57	0.46	0.05
120	0.05	0.62	0.44	0.07

Table C.2.2 Experimental data of run 2

Time (min)	C/C ₀			
	Aniline	COD	Fe ²⁺	H ₂ O ₂
0	1.00	1.00	1.00	1.00
1	0.32	0.81	0.71	0.79
2	0.20	0.70	0.65	0.67
5	0.10	0.67	0.58	0.09
10	0.09	0.65	0.56	0.01
20	0.07	0.62	0.59	0.01
40	0.07	0.65	0.56	0.01
60	0.07	0.63	0.55	0.02
80	0.05	0.66	0.50	0.00
100	0.05	0.62	0.44	0.01
120	0.05	0.61	0.46	0.00

Table C.2.3 Experimental data of run 3

Time (min)	C/C ₀			
	Aniline	COD	Fe ²⁺	H ₂ O ₂
0	1.00	1.00	1.00	1.00
1	0.77	0.91	0.66	0.86
2	0.77	0.91	0.67	0.82
5	0.67	0.87	0.66	0.82
10	0.57	0.83	0.69	0.77
20	0.24	0.72	0.84	0.63
40	0.05	0.43	0.81	0.22
60	0.04	0.44	0.72	0.06
80	0.03	0.37	0.70	0.01
100	0.03	0.34	0.84	0.00
120	0.02	0.33	0.84	0.00

Table C.2.4 Experimental data of run 4

Time (min)	C/C ₀			
	Aniline	COD	Fe ²⁺	H ₂ O ₂
0	1.00	1.00	1.00	1.00
1	0.92	0.90	0.95	1.02
2	0.88	0.92	0.83	0.99
5	0.83	0.88	0.81	0.94
10	0.77	0.86	0.78	0.85
20	0.76	0.82	0.87	0.66
40	0.53	0.78	0.88	0.26
60	0.36	0.68	0.80	0.03
80	0.37	0.65	0.70	0.00
100	0.36	0.63	0.66	0.02
120	0.36	0.65	0.65	0.01

Table C.2.5 Experimental data of run 5

Time (min)	C/C ₀			
	Aniline	COD	Fe ²⁺	H ₂ O ₂
0	1.00	1.00	1.00	1.00
1	0.60	0.83	0.77	0.99
2	0.43	0.94	0.71	0.96
5	0.33	0.78	0.53	0.80
10	0.19	0.70	0.21	0.70
20	0.13	0.62	0.15	0.60
40	0.10	0.59	0.33	0.45
60	0.06	0.52	0.58	0.28
80	0.05	0.51	0.65	0.16
100	0.03	0.51	0.76	0.07
120	0.03	0.53	0.78	0.01

Table C.2.6 Experimental data of run 6

Time (min)	C/C ₀			
	Aniline	COD	Fe ²⁺	H ₂ O ₂
0	1.00	1.00	1.00	1.00
1	0.56	0.79	0.60	0.99
2	0.40	0.79	0.27	0.96
5	0.25	0.63	0.15	0.82
10	0.23	0.59	0.08	0.67
20	0.19	0.56	0.14	0.50
40	0.18	0.49	0.11	0.26
60	0.14	0.51	0.08	0.19
80	0.14	0.43	0.13	0.14
100	0.13	0.45	0.14	0.14
120	0.11	0.50	0.13	0.15

Table C.2.7 Experimental data of run 7

Time (min)	C/C ₀			
	Aniline	COD	Fe ²⁺	H ₂ O ₂
0	1.00	1.00	1.00	1.00
1	0.26	1.04	0.40	0.87
2	0.13	0.95	0.43	0.67
5	0.06	0.97	0.46	0.55
10	0.03	0.88	0.64	0.33
20	0.00	0.81	0.72	0.09
40	0.00	0.59	0.54	0.00
60	0.00	0.59	0.50	0.00
80	0.00	0.56	0.45	0.00
100	0.00	0.53	0.38	0.00
120	0.00	0.54	0.34	0.00

Table C.2.8 Experimental data of run 8

Time (min)	C/C ₀			
	Aniline	COD	Fe ²⁺	H ₂ O ₂
0	1.00	1.00	1.00	1.00
1	0.63	0.96	0.77	0.95
2	0.51	0.92	0.21	0.95
5	0.33	0.75	0.15	0.92
10	0.27	1.05	0.15	0.81
20	0.24	0.78	0.11	0.65
40	0.21	0.61	0.10	0.44
60	0.15	0.64	0.11	0.30
80	0.15	0.57	0.09	0.20
100	0.13	0.79	0.12	0.16
120	0.13	0.66	0.09	0.15

Table C.2.9 Experimental data of run 9

Time (min)	C/C ₀			
	Aniline	COD	Fe ²⁺	H ₂ O ₂
0	1.00	1.00	1.00	1.00
1	0.25	0.67	0.42	0.84
2	0.18	0.63	0.42	0.62
5	0.09	0.56	0.46	0.53
10	0.04	0.51	0.61	0.37
20	0.00	0.39	0.75	0.14
40	0.00	0.35	0.54	0.00
60	0.00	0.35	0.54	0.00
80	0.00	0.31	0.53	0.00
100	0.00	0.31	0.52	0.00
120	0.00	0.34	0.45	0.00

Table C.2.10 Experimental data of run 10

Time (min)	C/C ₀			
	Aniline	COD	Fe ²⁺	H ₂ O ₂
0	1.00	1.00	1.00	1.00
1	0.80	0.97	0.47	0.86
2	0.78	0.95	0.49	0.82
5	0.69	0.90	0.48	0.77
10	0.50	0.85	0.62	0.70
20	0.12	0.60	0.82	0.47
40	0.00	0.43	0.67	0.09
60	0.00	0.38	0.56	0.02
80	0.00	0.35	0.69	0.01
100	0.00	0.33	0.66	0.01
120	0.00	0.31	0.49	0.01

Table C.2.11 Experimental data of run 11

Time (min)	C/C ₀			
	Aniline	COD	Fe ²⁺	H ₂ O ₂
0	1.00	1.00	1.00	1.00
1	0.87	0.91	0.70	0.99
2	0.86	0.97	0.70	1.00
5	0.81	0.93	0.67	0.99
10	0.72	0.92	0.67	0.73
20	0.39	0.76	0.85	0.39
40	0.13	0.57	0.83	0.03
60	0.12	0.65	0.82	0.01
80	0.11	0.63	0.79	0.00
100	0.10	0.55	0.83	0.00
120	0.10	0.57	0.76	0.00

Table C.2.12 Experimental data of run 12

Time (min)	C/C ₀			
	Aniline	COD	Fe ²⁺	H ₂ O ₂
0	1.00	1.00	1.00	1.00
1	0.83	0.93	0.80	0.97
2	0.81	0.94	0.82	0.93
5	0.81	0.90	0.82	0.94
10	0.75	0.91	0.76	0.90
20	0.59	0.76	0.80	0.82
40	0.36	0.70	0.69	0.72
60	0.20	0.60	0.67	0.54
80	0.12	0.52	0.70	0.41
100	0.07	0.47	0.71	0.29
120	0.06	0.47	0.76	0.20

Table C.2.13 Experimental data of run 13

Time (min)	C/C ₀			
	Aniline	COD	Fe ²⁺	H ₂ O ₂
0	1.00	1.00	1.00	1.00
1	0.80	0.94	0.84	0.98
2	0.76	0.91	0.74	0.92
5	0.74	0.90	0.77	0.90
10	0.72	0.88	0.71	0.88
20	0.62	0.83	0.79	0.77
40	0.33	0.74	0.68	0.55
60	0.14	0.56	0.68	0.31
80	0.08	0.53	0.70	0.10
100	0.05	0.50	0.70	0.00
120	0.05	0.51	0.71	0.00

Table C.2.14 Experimental data of run 14

Time (min)	C/C ₀			
	Aniline	COD	Fe ²⁺	H ₂ O ₂
0	1.00	1.00	1.00	1.00
1	0.58	0.79	0.00	0.97
2	0.48	0.75	0.04	0.84
5	0.31	0.73	0.17	0.79
10	0.23	0.63	0.21	0.70
20	0.17	0.54	0.26	0.58
40	0.12	0.51	0.50	0.42
60	0.05	0.47	0.61	0.10
80	0.03	0.42	0.59	0.01
100	0.02	0.39	0.56	0.01
120	0.02	0.44	0.56	0.01

Table C.2.15 Experimental data of run 15

Time (min)	C/C ₀			
	Aniline	COD	Fe ²⁺	H ₂ O ₂
0	1.00	1.00	1.00	1.00
1	0.81	1.04	0.64	1.04
2	0.75	0.95	0.62	1.05
5	0.68	0.97	0.59	1.04
10	0.64	0.88	0.58	0.96
20	0.55	0.81	0.70	0.86
40	0.20	0.59	0.79	0.27
60	0.09	0.59	0.79	0.00
80	0.09	0.56	0.86	0.00
100	0.09	0.53	0.85	0.00
120	0.09	0.54	0.88	0.00

Table C.2.16 Experimental data of run 16

Time (min)	C/C ₀			
	Aniline	COD	Fe ²⁺	H ₂ O ₂
0	1.00	1.00	1.00	1.00
1	0.91	0.87	0.80	1.03
2	0.91	0.90	0.73	1.00
5	0.87	0.88	0.78	0.94
10	0.77	0.80	0.69	0.90
20	0.68	0.81	0.75	0.79
40	0.64	0.76	0.91	0.58
60	0.40	0.72	0.88	0.32
80	0.28	0.63	0.75	0.10
100	0.28	0.63	0.70	0.01
120	0.27	0.60	0.37	0.02

C.3 Experimental data of Box-Behnken design

Table C.3.1 Experimental data of run 1

Time (min)	C/C ₀			
	Aniline	COD	Fe ²⁺	H ₂ O ₂
0	1.00	1.00	1.00	1.00
1	0.81	0.91	0.70	0.88
2	0.75	0.94	0.71	0.82
5	0.69	0.88	0.72	0.82
10	0.55	0.77	0.67	0.78
20	0.31	0.63	0.55	0.68
40	0.12	0.61	0.56	0.52
60	0.10	0.48	0.54	0.39
80	0.08	0.53	0.58	0.29
100	0.07	0.48	0.63	0.19
120	0.05	0.47	0.67	0.12

Table C.3.2 Experimental data of run 2

Time (min)	C/C ₀			
	Aniline	COD	Fe ²⁺	H ₂ O ₂
0	1.00	1.00	1.00	1.00
1	0.35	0.71	0.64	0.90
2	0.25	0.68	0.60	0.59
5	0.14	0.66	0.57	0.52
10	0.11	0.59	0.56	0.41
20	0.07	0.50	0.70	0.22
40	0.06	0.44	0.65	0.01
60	0.05	0.44	0.84	0.00
80	0.05	0.42	0.86	0.00
100	0.05	0.44	0.76	0.00
120	0.07	0.43	0.67	0.00

Table C.3.3 Experimental data of run 3

Time (min)	C/C ₀			
	Aniline	COD	Fe ²⁺	H ₂ O ₂
0	1.00	1.00	1.00	1.00
1	0.92	0.94	0.54	1.01
2	0.95	0.95	0.53	0.95
5	0.93	0.94	0.52	0.89
10	0.84	0.90	0.50	0.84
20	0.66	0.83	0.64	0.70
40	0.27	0.66	0.78	0.35
60	0.14	0.59	0.77	0.05
80	0.13	0.60	0.78	0.03
100	0.12	0.56	0.76	0.02
120	0.12	0.61	0.75	0.04

Table C.3.4 Experimental data of run 4

Time (min)	C/C ₀			
	Aniline	COD	Fe ²⁺	H ₂ O ₂
0	1.00	1.00	1.00	1.00
1	0.59	0.86	0.52	0.97
2	0.43	0.83	0.50	0.55
5	0.26	0.72	0.45	0.48
10	0.18	0.70	0.42	0.36
20	0.09	0.66	0.38	0.13
40	0.08	0.62	0.43	0.09
60	0.08	0.65	0.45	0.02
80	0.08	0.62	0.47	0.05
100	0.06	0.61	0.50	0.03
120	0.07	0.61	0.50	0.04

Table C.3.5 Experimental data of run 5

Time (min)	C/C ₀			
	Aniline	COD	Fe ²⁺	H ₂ O ₂
0	1.00	1.00	1.00	1.00
1	0.00	0.91	0.69	0.90
2	0.64	0.79	0.72	0.75
5	0.39	0.72	0.79	0.68
10	0.19	0.60	0.62	0.56
20	0.09	0.50	0.61	0.31
40	0.05	0.48	0.60	0.12
60	0.03	0.48	0.54	0.03
80	0.04	0.46	0.59	0.01
100	0.03	0.46	0.53	0.00
120	0.03	0.45	0.52	0.00

Table C.3.6 Experimental data of run 6

Time (min)	C/C ₀			
	Aniline	COD	Fe ²⁺	H ₂ O ₂
0	1.00	1.00	1.00	1.00
1	0.59	0.84	0.52	0.75
2	0.51	0.75	0.50	0.54
5	0.31	0.68	0.45	0.52
10	0.15	0.58	0.42	0.44
20	0.08	0.57	0.38	0.29
40	0.06	0.48	0.43	0.12
60	0.06	0.45	0.45	0.04
80	0.07	0.48	0.47	0.00
100	0.05	0.45	0.50	0.00
120	0.05	0.44	0.50	0.00

Table C.3.7 Experimental data of run 7

Time (min)	C/C ₀			
	Aniline	COD	Fe ²⁺	H ₂ O ₂
0	1.00	1.00	1.00	1.00
1	0.54	0.83	0.77	0.97
2	0.40	0.80	0.70	0.53
5	0.24	0.73	0.63	0.46
10	0.11	0.65	0.61	0.14
20	0.12	0.64	0.65	0.07
40	0.11	0.64	0.68	0.03
60	0.10	0.63	0.66	0.05
80	0.14	0.63	0.65	0.01
100	0.13	0.62	0.65	0.00
120	0.11	0.64	0.63	0.00

Table C.3.8 Experimental data of run 8

Time (min)	C/C ₀			
	Aniline	COD	Fe ²⁺	H ₂ O ₂
0	1.00	1.00	1.00	1.00
1	0.42	0.74	0.79	0.96
2	0.24	0.70	0.76	0.73
5	0.11	0.57	0.72	0.60
10	0.08	0.52	0.67	0.41
20	0.06	0.43	0.56	0.24
40	0.05	0.40	0.46	0.11
60	0.00	0.38	0.42	0.03
80	0.00	0.36	0.40	0.00
100	0.00	0.36	0.51	0.00
120	0.00	0.44	0.53	0.00

Table C.3.9 Experimental data of run 9

Time (min)	C/C ₀			
	Aniline	COD	Fe ²⁺	H ₂ O ₂
0	1.00	1.00	1.00	1.00
1	0.89	0.98	0.45	1.01
2	0.86	0.93	0.44	0.98
5	0.82	0.93	0.41	0.96
10	0.73	0.89	0.39	0.92
20	0.55	0.77	0.58	0.87
40	0.23	0.65	0.66	0.68
60	0.09	0.50	0.71	0.48
80	0.05	0.43	0.65	0.33
100	0.06	0.37	0.60	0.21
120	0.06	0.36	0.56	0.11

Table C.3.10 Experimental data of run 10

Time (min)	C/C ₀			
	Aniline	COD	Fe ²⁺	H ₂ O ₂
0	1.00	1.00	1.00	1.00
1	0.70	0.90	0.13	1.02
2	0.64	0.90	0.13	0.84
5	0.38	0.82	0.08	0.81
10	0.30	0.71	0.04	0.76
20	0.25	0.59	0.04	0.70
40	0.23	0.54	0.04	0.57
60	0.20	0.53	0.05	0.45
80	0.18	0.49	0.09	0.33
100	0.15	0.49	0.15	0.20
120	0.12	0.47	0.18	0.08

Table C.3.11 Experimental data of run 11

Time (min)	C/C ₀			
	Aniline	COD	Fe ²⁺	H ₂ O ₂
0	1.00	1.00	1.00	1.00
1	0.79	0.87	0.82	0.99
2	0.74	0.85	0.54	0.91
5	0.53	0.72	0.13	0.83
10	0.28	0.72	0.45	0.77
20	0.12	0.66	0.69	0.49
40	0.08	0.59	0.72	0.27
60	0.07	0.55	0.70	0.11
80	0.06	0.52	0.75	0.03
100	0.05	0.56	0.81	0.01
120	0.05	0.54	0.83	0.01

Table C.3.12 Experimental data of run 12

Time (min)	C/C ₀			
	Aniline	COD	Fe ²⁺	H ₂ O ₂
0	1.00	1.00	1.00	1.00
1	0.78	0.86	0.80	0.95
2	0.74	0.77	0.55	0.91
5	0.50	0.68	0.13	0.85
10	0.25	0.60	0.47	0.76
20	0.14	0.57	0.65	0.43
40	0.10	0.50	0.73	0.25
60	0.07	0.46	0.75	0.11
80	0.06	0.48	0.77	0.01
100	0.03	0.44	0.83	0.01
120	0.05	0.44	0.84	0.01

Table C.3.13 Experimental data of run 13

Time (min)	C/C ₀			
	Aniline	COD	Fe ²⁺	H ₂ O ₂
0	1.00	1.00	1.00	1.00
1	0.79	0.95	0.47	0.99
2	0.77	0.90	0.45	0.94
5	0.69	0.89	0.44	0.91
10	0.58	0.84	0.47	0.85
20	0.27	0.76	0.63	0.75
40	0.04	0.54	0.65	0.32
60	0.02	0.45	0.65	0.02
80	0.00	0.43	0.63	0.01
100	0.00	0.45	0.76	0.03
120	0.00	0.42	0.83	0.03

Table C.3.14 Experimental data of run 14

Time (min)	C/C ₀			
	Aniline	COD	Fe ²⁺	H ₂ O ₂
0	1.00	1.00	1.00	1.00
1	0.81	0.95	0.50	0.95
2	0.79	0.91	0.45	0.94
5	0.69	0.87	0.45	0.91
10	0.55	0.84	0.48	0.80
20	0.28	0.74	0.61	0.72
40	0.03	0.52	0.63	0.27
60	0.01	0.45	0.65	0.05
80	0.00	0.44	0.63	0.04
100	0.00	0.44	0.78	0.01
120	0.00	0.44	0.80	0.01

Table C.3.15 Experimental data of run 15

Time (min)	C/C ₀			
	Aniline	COD	Fe ²⁺	H ₂ O ₂
0	1.00	1.00	1.00	1.00
1	0.92	0.94	0.52	1.00
2	0.90	0.95	0.53	0.97
5	0.90	0.89	0.49	0.99
10	0.88	0.90	0.50	0.93
20	0.76	0.88	0.60	0.90
40	0.52	0.79	0.65	0.78
60	0.34	0.64	0.72	0.62
80	0.18	0.67	0.69	0.45
100	0.11	0.53	0.70	0.31
120	0.09	0.51	0.69	0.19

Table C.3.16 Experimental data of run 16

Time (min)	C/C ₀			
	Aniline	COD	Fe ²⁺	H ₂ O ₂
0	1.00	1.00	1.00	1.00
1	0.83	0.93	0.66	1.00
2	0.76	0.89	0.71	0.86
5	0.37	0.72	0.14	0.69
10	0.28	0.70	0.13	0.60
20	0.21	0.65	0.12	0.47
40	0.18	0.62	0.16	0.26
60	0.15	0.78	0.17	0.12
80	0.13	0.62	0.19	0.07
100	0.14	0.60	0.20	0.07
120	0.12	0.57	0.22	0.05

Table C.3.17 Experimental data of run 17

Time (min)	C/C ₀			
	Aniline	COD	Fe ²⁺	H ₂ O ₂
0	1.00	1.00	1.00	1.00
1	0.64	0.79	0.04	1.00
2	0.49	0.73	0.17	0.85
5	0.23	0.64	0.23	0.77
10	0.19	0.60	0.28	0.68
20	0.09	0.55	0.50	0.51
40	0.00	0.47	0.67	0.28
60	0.00	0.39	0.64	0.12
80	0.00	0.38	0.59	0.02
100	0.00	0.37	0.54	0.00
120	0.00	0.38	0.55	0.00

C.4 Experimental data on effects of electrical discharging time

Table C.4.1 Experimental data of aniline removal on effects of electrical discharging time at 10 mM of aniline, 1.25 mM of Fe^{2+} , 72 mM of H_2O_2 , pH 2 and current 2 A.

Time (min)	Current delay (C/C_0)					
	Fenton	Fully	After 20 min	After 40 min	After 60 min	After 80 min
0	1.00	1.00	1.00	1.00	1.00	1.00
1	0.74	0.79	0.80	0.91	0.81	0.78
2	0.75	0.77	0.80	0.82	0.85	0.77
5	0.73	0.69	0.77	0.81	0.77	0.75
10	0.72	0.58	0.75	0.77	0.78	0.72
20	0.70	0.27	0.67	0.74	0.72	0.66
40	0.61	0.04	0.15	0.57	0.58	0.64
60	0.56	0.02	0.01	0.11	0.53	0.59
80	0.54	0.00	0.01	0.02	0.06	0.52
100	0.49	0.00	0.00	0.01	0.02	0.04
120	0.42	0.00	0.01	0.01	0.01	0.02

Table C.4.2 Experimental data of COD removal on effects of electrical discharging time at 10 mM of aniline, 1.25 mM of Fe^{2+} , 72 mM of H_2O_2 , pH 2 and current 2 A.

Time (min)	Current delay (C/C_0)					
	Fenton	Fully	After 20 min	After 40 min	After 60 min	After 80 min
0	1.00	1.00	1.00	1.00	1.00	1.00
1	0.88	0.95	0.91	1.07	0.93	0.88
2	0.89	0.90	0.95	0.93	0.95	0.88
5	0.87	0.89	0.88	0.92	0.94	0.90
10	0.84	0.84	0.89	0.90	0.90	0.85
20	0.86	0.76	0.84	0.88	0.86	0.84
40	0.81	0.54	0.62	0.74	0.79	0.77
60	0.77	0.45	0.47	0.56	0.73	0.74
80	0.72	0.43	0.47	0.42	0.52	0.69
100	0.72	0.45	0.39	0.38	0.41	0.46
120	0.70	0.42	0.42	0.41	0.41	0.44

Table C.4.3 Experimental data of Fe^{2+} on effects of electrical discharging time at 10 mM of aniline, 1.25 mM of Fe^{2+} , 72 mM of H_2O_2 , pH 2 and current 2 A.

Current delay (C/C_0)						
Time (min)	Fenton	Fully	After 20 min	After 40 min	After 60 min	After 80 min
0	1.00	1.00	1.00	1.00	1.00	1.00
1	0.41	0.47	0.36	0.38	0.46	0.38
2	0.40	0.45	0.35	0.37	0.45	0.36
5	0.33	0.44	0.31	0.32	0.46	0.34
10	0.29	0.47	0.28	0.32	0.35	0.29
20	0.30	0.63	0.30	0.33	0.35	0.30
40	0.25	0.65	0.51	0.31	0.35	0.26
60	0.26	0.65	0.54	0.60	0.35	0.27
80	0.26	0.63	0.45	0.58	0.55	0.28
100	0.23	0.76	0.40	0.51	0.64	0.50
120	0.22	0.83	0.47	0.51	0.55	0.44

Table C.4.4 Experimental data of H_2O_2 on effects of electrical discharging time at 10 mM of aniline, 1.25 mM of Fe^{2+} , 72 mM of H_2O_2 , pH 2 and current 2 A.

Current delay (C/C_0)						
Time (min)	Fenton	Fully	After 20 min	After 40 min	After 60 min	After 80 min
0	1.00	1.00	1.00	1.00	1.00	1.00
1	1.00	0.99	0.99	1.01	1.01	0.99
2	0.96	0.95	0.95	0.95	0.95	0.92
5	0.95	0.93	0.94	0.92	0.95	0.97
10	0.95	0.86	0.93	0.94	0.95	0.96
20	0.96	0.68	0.92	0.93	0.93	0.92
40	0.94	0.28	0.64	0.86	0.89	0.86
60	0.92	0.07	0.26	0.44	0.82	0.79
80	0.90	0.01	0.08	0.01	0.54	0.71
100	0.87	0.01	0.01	0.01	0.18	0.43
120	0.80	0.01	0.01	0.01	0.03	0.17

C.5 Experimental data of H₂O₂ stepwise addition during electro-Fenton process

Table C.5.1 Experimental data of aniline removal of H₂O₂ stepwise addition during electro-Fenton process at 10 mM of aniline, 1.25 mM of Fe²⁺, 72 mM of H₂O₂, pH 2 and current 2 A.

Time (min)	Stepwise H ₂ O ₂ (C/C ₀)			Continuous
	1	2	3	
0	1.00	1.00	1.00	1.00
1	0.79	-	-	0.95
2	0.77	0.94	0.87	0.93
5	0.69	0.78	0.83	0.88
10	0.58	0.72	0.77	0.84
20	0.27	0.50	0.61	0.68
30	-	-	0.55	-
32	-	-	0.39	-
35	-	-	0.33	-
40	0.04	0.21	0.25	0.26
50	-	-	0.15	-
60	0.02	0.14	0.10	0.10
62	-	0.12	0.08	-
65	-	0.09	0.08	-
70	-	0.06	0.08	-
80	0.00	0.06	0.03	0.05
100	0.00	0.05	0.00	0.02
120	0.00	0.04	0.00	0.00

Table C.5.2 Experimental data of COD removal of H₂O₂ stepwise addition during electro-Fenton process at 10 mM of aniline, 1.25 mM of Fe²⁺, 72 mM of H₂O₂, pH 2 and current 2 A.

Time (min)	Stepwise H ₂ O ₂ (C/C ₀)			Continuous
	1	2	3	
100	0.45	0.47	0.45	0.42
120	0.42	0.41	0.41	0.39
0	1.00	1.00	1.00	1.00
1	0.95	-	-	0.98
2	0.90	0.95	0.98	0.95
5	0.89	0.95	0.95	0.95
10	0.84	0.93	0.90	0.93
20	0.76	0.84	0.82	0.87
30	-	-	0.73	-
32	-	-	0.71	-
35	-	-	0.68	-
40	0.54	0.68	0.61	0.69
50	-	-	0.56	-
60	0.45	0.63	0.52	0.53
62	-	0.55	0.51	-
65	-	0.54	0.51	-
70	-	0.50	0.46	-
80	0.43	0.48	0.46	0.46

Table C.5.3 Experimental data of Fe^{2+} of H_2O_2 stepwise addition during electro-Fenton process at 10 mM of aniline, 1.25 mM of Fe^{2+} , 72 mM of H_2O_2 , pH 2 and current 2 A.

Time (min)	Stepwise H_2O_2 (C/C ₀)			
	1	2	3	Continuous
0	1.00	1.00	1.00	1.00
1	0.47	-	-	0.45
2	0.43	0.29	0.33	0.33
5	0.43	0.31	0.34	0.30
10	0.46	0.32	0.38	0.32
20	0.58	0.44	0.47	0.43
30	-	-	0.53	-
32	-	-	0.54	-
35	-	-	0.55	-
40	0.64	0.47	0.56	0.61
50	-	-	0.59	-
60	0.64	0.72	0.58	0.63
62	-	0.56	0.57	-
65	-	0.55	0.56	-
70	-	0.53	0.57	-
80	0.62	0.54	0.55	0.60
100	0.73	0.49	0.50	0.58
120	0.78	0.50	0.50	0.59

Table C.5.4 Experimental data of H_2O_2 of H_2O_2 stepwise addition during electro-Fenton process at 10 mM of aniline, 1.25 mM of Fe^{2+} , 72 mM of H_2O_2 , pH 2 and current 2 A.

Time (min)	Stepwise H_2O_2 (mg/L)			
	1	2	3	Continuous
0	2448.72	1225.04	815.90	1.53
1	2412.65	-	-	31.52
2	2328.61	1225.58	805.38	77.04
5	2283.09	1075.01	787.88	220.61
10	2094.00	976.97	759.86	388.69
20	1663.29	728.35	637.30	721.34
30	-	-	490.23	-
30	-	-	1306.13	-
32	-	-	1260.60	-
35	-	-	1190.57	-
40	693.33	175.08	1036.49	976.97
50	-	-	686.33	-
60	164.58	31.52	441.21	906.93
60	164.58	1256.56	1257.11	906.93
62	-	1260.60	1204.57	-
65	-	1096.02	1106.53	-
70	-	938.45	927.94	-
80	17.51	595.28	675.82	360.67
100	28.01	213.60	332.66	206.60
120	17.51	49.02	213.60	112.05

BIOGRAPHY

Mr. Sermpong Sairiam was born on July 21st, 1984 in Chumphon, Thailand. He received his Bachelor's degree in Environmental Science from Department of General Science, Faculty of Science, Chulalongkorn University, Bangkok, Thailand in 2007. He pursued his Master's degree study in the National Center of Excellence for Environmental and Hazardous Waste Management, Inter-Department of Environmental Management, Graduate School, Chulalongkorn University, Bangkok, Thailand on May, 2007. He finished his Master's degree on March, 2009. He attained oral presentation in part of his works entitled "Enhancing Treatment Efficiency of Wastewater Containing Aniline by Electro-Fenton Process" in the 8th National Environmental Conference, March 25-27, 2009, Suranaree University of Technology, Nakhon Ratchasima, Thailand.



ศูนย์วิทยทรัพยากร
จุฬาลงกรณ์มหาวิทยาลัย